A Theoretical Method for Evaluating Stability of Openings in Rock

AD 736 047

FINAL REPORT
APRIL 12, 1972
BY CHIN-YUNG CHANG & KESHAVAN NAIR

U.S. BUREAU OF MINES
CONTRACT NUMBER H0210046

SPONSORED BY
ADVANCED RESEARCH PROJECTS AGENCY
ARPA ORDER NO. 1579, AMEND. 2
PROGRAM CODE 1F10

The views and conclusions contained in this document are those of the author and should not be interpreted as necessarily representing the official policies, either expressed or implied, of the Advanced Research Projects Agency or the U.S. Government.

AD 736 500

DDC
RETRIEVED
APR 21 1972
B

WOODWARD-LUNDGREN & ASSOCIATES
CONSULTING ENGINEERS AND GEOLOGISTS
AN AFFILIATE OF WOODWARD-CLYDE CONSULTANTS
2730 Adeline Street Oakland, Ca 94607

DISTRIBUTION STATEMENT A
Approved for public release;
Distribution Unlimited

Reproduced by
NATIONAL TECHNICAL
INFORMATION SERVICE
Springfield, Va 22151

BEST
AVAILABLE COPY

DOCUMENT CONTROL DATA - R & D

(Security classification of title, body of abstract and indexing annotation must be entered when the overall report is classified)

1. ORIGINATING ACTIVITY (Corporate author) Woodward-Lundgren & Associates	2a. REPORT SECURITY CLASSIFICATION Unclassified 2b. GROUP

3. REPORT TITLE

A Theoretical Method for Evaluating Stability of Openings in Rock

4. DESCRIPTIVE NOTES (Type of report and inclusive dates)
Final Report - March 12, 1971 - March 12, 1972

5. AUTHOR(S) (First name, middle initial, last name)

Chin-Yung Chang and Keshavan Nair

6. REPORT DATE April 12, 1972	7a. TOTAL NO. OF PAGES 144	7b. NO. OF REFS 31
8a. CONTRACT OR GRANT NO. H0210046 b. PROJECT NO. c. d.	9a. ORIGINATOR'S REPORT NUMBER(S) None 9b. OTHER REPORT NO(S) (Any other numbers that may be assigned this report) None	

10. DISTRIBUTION STATEMENT

Distribution of this document is unlimited.

11. SUPPLEMENTARY NOTES	12. SPONSORING MILITARY ACTIVITY Advanced Research Projects Agency, Washington, DC 20301

13. ABSTRACT

The purposes of this study are to evaluate the reliability of the available finite element techniques for the solution of plane problems to predict the stresses, strains, and deformations in a rock mass surrounding an excavation. The approach to this study is divided into two phases; (1) developing a general analytical procedure (i.e., a finite element computer program with wide capabilities) for determining the mechanical state in a rock mass, and (2) analysis of case histories to compare predicted and observed values. This report discusses essential features of finite element techniques for modelling rock behavior and describes the development and verification of a single general computer program which is capable of modelling joints, faults, bedding planes or other geologic discontinuities, "no tension" properties and elasto-plastic behavior of rock masses. Using the computational techniques developed in Phase 1, Morrow Point Underground Powerplant Excavation and a laboratory model of unlined openings in a rock-like material were analyzed. It was shown that the results of the analysis provided a good qualitative basis for predicting the performance of the model and the field study.

14. KEY WORDS	LINK A		LINK B		LINK C	
	ROLE	WT	ROLE	WT	ROLE	WT
Underground opening						
No tension analysis						
Joint perturbation analysis						
Elasto-plastic analysis						
Stress transfer technique						
Plane strain						
Morrow Point Underground Powerplant						
Model tests of unlined openings						

FINAL REPORT

MARCH 12, 1971 - MARCH 12, 1972

ARPA Order Number: 1579, Amend. 2

Program Code Number: 1F10

Name of Contractor:
Woodward-Lundgren & Associates

Effective Date of Contract:
March 12, 1971

Contract Expiration Date:
March 12, 1972

Amount of Contract:
$34,829

Contract Number: HO210046

Principal Investigator:
K. Nair

Telephone Number: (415) 444-1256

Project Scientist or Engineer:
C-Y Chang, K. Nair

Telephone Number: (415) 444-1256

Short Title of Work:
A Theoretical Method for Evaluating Stability of Openings in Rock

This research was supported by the Advanced Research Projects Agency of the Department of Defense and was monitored by Bureau of Mines under Contract Number HO210046.

FINAL REPORT SUMMARY

Contract Objectives

A major consideration in the design of excavations in rock is the evaluation of the structural stability of the opening. An essential step in this evaluation is the determination of the mechanical state in the rock mass in the vicinity of an opening through the formulation and solution of boundary value problems. The finite element method has proven to be a very powerful tool in the solution of boundary value problems. Within the general framework of the finite element method, procedures have been developed to model the response of certain classes of joints, cracks and fissures in the rock mass, the inability of rocks to withstand tension, localized yielding of rock due to stress concentrations and the time-dependent (creep) response of rock. While preliminary analysis has indicated that these procedures have the potential for predicting performance, their use in design will be limited unless their reliability is established. The objective of this contract is to evaluate the ability of certain available finite element techniques for the solution of plane problems to predict the stresses, strains and deformations in a rock mass surrounding an excavation.

General Approach and Technical Results

The approach to this study can be divided into two phases:

(1) Developing computational procedures which model the

essential features known to be present in a rock mass, for determining its mechanical state, pages 1 to 60, and (2) Analysis of case histories and comparison of predicted and measured performance, pages 61 to 102.

The essential features of the various finite element techniques to conduct the following analyses were reviewed: (I) "No-tension" Analysis, (II) Joint Perturbation Analysis, (III) Elastic-Plastic Analysis, and (IV) Time-dependent (Creep) Analysis. Because the time-dependent (creep) response of the great majority of rocks is not as significant as the time-independent response, and furthermore, since the computational procedures for time-independent and time-dependent problems are significantly different, it was decided that only time-independent analyses for plane problems would be considered in this study. It was found that different computational procedures were utilized to conduct the above-mentioned time-independent analyses. In order to develop a single computer program which could be used for conducting analyses which include the features in (I), (II), and (III), it was necessary to formulate a consistent computational procedure and develop a program on the basis of such a procedure. The "initial stress" (stress transfer) technique presented by Zienkiewicz and his co-workers was used and an operational finite element program with the capability of conducting a "no tension," joint perturbation and elastic-plastic analysis was developed. Various illustrative examples were solved using the combined program and the results

compared where possible with results published by other investigators.

A number of case history and laboratory studies were considered for analysis using the computational techniques developed in Phase I. One case history study (Morrow Point Power Plant) and one laboratory model were analyzed, and the results of the analysis provided a good qualitative basis for predicting the performance of the model and the field study. Quantitative estimates were of the right magnitude. The major difficulty was in idealizing the problem. Since there are always features in the actual problem which cannot be accurately modelled, it is necessary to introduce various approximations. In actual practice, more than one idealization of a problem will have to be considered. It is believed that the techniques of analysis provide the basis for identifying problems and suggest possible design solutions.

DOD Implications

The evaluation of the structural stability of underground openings, ground support structures, and other facilities is an essential step both in the design and in the survivability/vulnerability assessment of underground structures and the weapon systems. The computer code developed for this contract is a tool that can be utilized to evaluate the stability of unsupported tunnel openings sited in rock masses where the rock mass behavior is dominated by block slippage along discrete joint planes, or a global inability

of the rock mass to resist tensile stress, or elastic-plastic behavior of the rock mass, or any combination of the three rock mass physical characteristics. Under certain circumstances, simple ground support structures may be modeled as tunnel liners, although this feature of the computer program has not been exploited in this contract.

Considerations for Further Research

Further research should consider increasing the capability of the computational procedures to include construction sequence, rock reinforcement schemes, and commonly used steel supports. Computational techniques to predict and examine the influence of progressive failure should be developed. Efforts should be directed towards incorporating the work done by other investigators to extend the analytical capabilities developed under this contract.

Additional case studies should be investigated to further evaluate the capabilities of the computer program. Research in the determination of in-situ rock mass properties and conditions is necessary to fully utilize the capabilities of existing analytical techniques.

ACKNOWLEDGEMENTS

The research was supported by the Advanced Research Projects Agency of the Department of Defense and was monitored by the Bureau of Mines. The Project Officer for the Bureau of Mines was Dr. William J. Karwoski; his assistance and cooperation in conducting this study are acknowledged.

The assistance of the Woodward-Lundgren & Associates' typing, drafting and reproduction staff in preparing this report is appreciated.

TABLE OF CONTENTS

TABLE OF CONTENTS

LIST OF FIGURES

LIST OF TABLES

INTRODUCTION

The development of theoretically sound methods for designing excavations in rock is of significance because of the increased use of underground facilities for civilian and military purposes. A major consideration in the design of excavations in rock is the evaluation of the structural stability of the opening. If a mechanistic approach is taken for the evaluation of the structural stability, then an essential step in the evaluation is the determination of the mechanical state (i.e., stresses, strains, and deformation) in the rock mass in the vicinity of the excavation. In recent years, new technology has been developed which has the potential of predicting, with greater accuracy, than heretofore possible, the mechanical state in the rock mass. This would place the evaluation of the structural stability of an opening in rock on a theoretically sound basis. This new technology has been primarily in the area of numerical methods for the solution of boundary value problems. However, the application of these methods to practical design problems has been very limited. The primary reason for this is the designer's lack of confidence in the ability of theoretical methods to assist him in analyzing practical design problems.

Of the numerical methods developed, the finite element method has proven to be the most powerful for the solution of boundary value problems (Clough, 1960, Wilson, 1963, 1965, Zienkiewicz, 1967). The initial application of the finite element method to rock mechanics problems used techniques (computer programs) that

had been developed for the structural analysis of linear elastic continuous structures. When the results obtained from using these techniques were compared with field results, they were found to be inadequate for predicting the response of rock masses in the vicinity of an excavation. Typical results from such studies have been presented by Judd and Perloff (1971). It was recognized that one of the major reasons for the discrepancies between computed and observed behavior was the inability of the computational techniques utilized to include the natural geologic discontinuities that were usually prevalent in a rock mass. These discontinuities could exist in the rock formation prior to the excavation or could be a result of the induced stresses due to the excavation causing failure in the rock. Methods of analysis which have the capability of modelling joints and other forms of discontinuities that commonly exist in rock masses have been developed by Goodman, Taylor, and Brekke (1968), and Zienkiewicz, et al. (1970). Methods for stress analysis in a rock mass which cannot sustain tensions due to the presence of cracks and fissures have also been developed, Zienkiewicz, et al. (1968). In addition, methods for analyzing localized failure in a rock mass due to yielding have been presented by Reyes and Deere (1966). Approximate techniques for incorporating nonlinear time-dependent material properties have been developed by Nair and Boresi (1970). Preliminary analysis has indicated that these new methods of analysis using finite element techniques have the potential of predicting performance with improved accuracy. However, the

methods of analysis which account for a specific rock characteristic e.g., no tension or joints, are not adequate to study the general case where all these factors may be present. Furthermore, there has been very limited verification of these techniques on the basis of comparison with measured field performance. Without field verification, the use of these new techniques in the design of excavations in rock will remain limited. Therefore, to develop a theoretically sound method for designing excavations in rock, which will be used in practice, an essential step is to establish the reliability of the available methods of stress analysis in predicting the behavior of rock masses.

PURPOSE

The purpose of this study is to evaluate the ability of the available finite element techniques for the solution of plane problems to predict the stresses, strains, and deformations in a rock mass surrounding an excavation.

GENERAL APPROACH

The approach to this study can be divided into two phases: (1) Development of a general analytical procedure (i.e., a finite element computer program with wide capabilities) for determining the mechanical state in a rock mass, and (2) Analysis of case histories to compare predicted and observed values.

Phase I consisted of three steps:

a. Review of pertinent available finite element programs

b. Consolidation of the various programs into a single general program.

c. Use of examples to illustrate the use of the program.

Phase 2 consisted of analyzing selected case histories and comparing observed and predicted behavior.

ESSENTIAL FEATURES OF FINITE ELEMENT TECHNIQUES FOR MODELLING ROCK BEHAVIOR (Phase 1a)

Various techniques have been utilized in conjunction with the finite element method to include nonlinear and time-dependent properties, elasto-plastic yielding, and geologic discontinuities in the stress analysis of rock masses. These techniques were evaluated for the purpose of developing a general computer program for plane problems which can incorporate the significant features that exist in rock masses. The available techniques use different computational techniques within the general framework of the finite element method to develop solutions to boundary value problems. The basic concepts of the finite element method have been discussed extensively in the literature, e.g., Clough (1960), Wilson (1963, 1964) and Zienkiewicz (1967). These will not be repeated here. Those aspects which are considered special modifications for rock mechanics problems are discussed in general terms with respect to the computational techniques in the subsequent paragraphs. These are considered in four categories (1) "No Tension" analysis, (2) Joint Perturbation Analysis,

(3) Elasto-Plastic Analysis, and (4) Time Dependent Analysis. Detailed explanation of these techniques is provided in a subsequent section where the basis of the developed computer program is described.

1. "No Tension" Analysis

When numerous cracks and fissures are present in a rock mass, it has been assumed that the rock is incapable of withstanding tensile stresses. A procedure for modelling this nonlinear behavior has been presented by Zienkiewicz, et al. (1968). This method is called "no tension" or "stress transfer" analysis. This method is composed of the following four essential steps:

(a) A linear elastic solution to the problem is first obtained. The induced changes in stress are added to the initial stresses and the principal stresses computed.

(b) Those elements in which tensile stresses are present are identified. As the material is assumed incapable of sustaining them, the calculated tensile principal stresses are eliminated without permitting any point in the structure to displace. In order to maintain equilibrium, equivalent (balancing) nodal forces are calculated and temporarily applied to the structure.

(c) The elastic analysis is repeated (i.e., the equilibrium equations are satisfied) to remove the balancing nodal forces and the check for tensile stresses is repeated.

(d) If at the end of step (c) tensile stresses are still present, steps (b) and (c) are repeated until no appreciable difference in magnitude and distribution of stresses is obtained upon further iteration. It is important to recognize that the initial elastic stiffness matrix is used throughout the computation.

This type of analysis has been used by Zienkiewicz, et al. (1968) in the solution of plane strain problems in rock mechanics. Heuze, Goodman, and Bornstein (1971) have used the same technique to study the deformability of jointed rock in borehole jacking tests. The convergence of the solution has been found to be very slow. The number of iterations required for convergence ranged from 10 to 15 cycles. Zienkiewicz, et al. (1968) reported that faster convergence could be obtained if the elastic constants are modified by reducing the modulus in the direction of the principal tensile stress. With this modification, the stiffness matrix would have to be recomputed at every stage.

2. "Joint Perturbation" Analysis

A one-dimensional joint element was developed by Goodman, Taylor, and Brekke (1968) and applied to several rock mechanics problems. This technique is capable of modelling the behavior of joints,

bedding planes and other geologic discontinuities. The original version defined normal and shear stiffnesses, K_N and K_S, for joint elements and incorporated the stiffness of these elements into the stiffness of the overall structure. Fig. 1 shows a one-dimensional joint element with its local coordinate system and the sign convention on stresses and displacements. The joint element was assumed to have no thickness. The original version was only valid for a linear elastic analysis. In his study on the deformability of joints, Goodman (1969) has reported that there are four typical shear stress-deformation relationships for various weak surfaces as shown in Fig. 2. It is apparent that peak shear strength in most cases is greater than residual shear strength. After the peak shear strength is reached, shear stress drops to residual values and appreciable movement can take place without increase in shear stress. It is obvious that this type of stress-deformation behavior cannot be approximated by one single value of shear stiffness as used in the original analysis, Goodman et al. (1968). Heuze, Goodman and Bornstein (1971) modified the original version so that normal and tangential properties can be varied as a function of displacement. They used an iterative approach to solve this type of nonlinear problem. In their procedure, the same boundary value problem is analyzed repeatedly. For each analysis, a new set of normal and tangential stresses and displacements across a joint element is calculated and used together with joint properties and joint strength to modify the normal and shear stiffness for the next iteration. The iterative technique used by Heuze, Goodman and Bornstein (1971) is

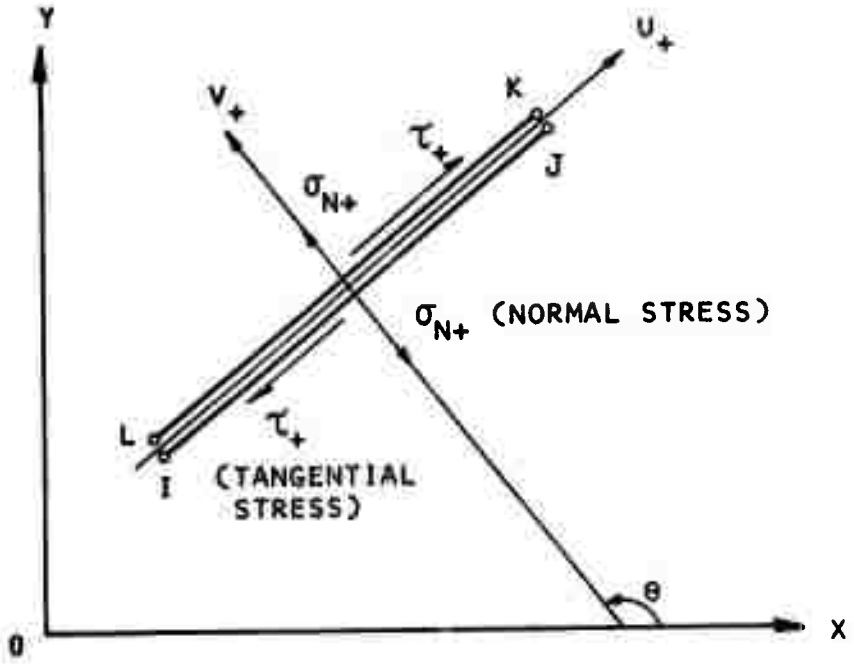

FIG. 1 - LINKAGE OR "JOINT" ELEMENT WITH ITS LOCAL COORDINATE SYSTEM (After Goodman, Taylor and Brekke, 1968)

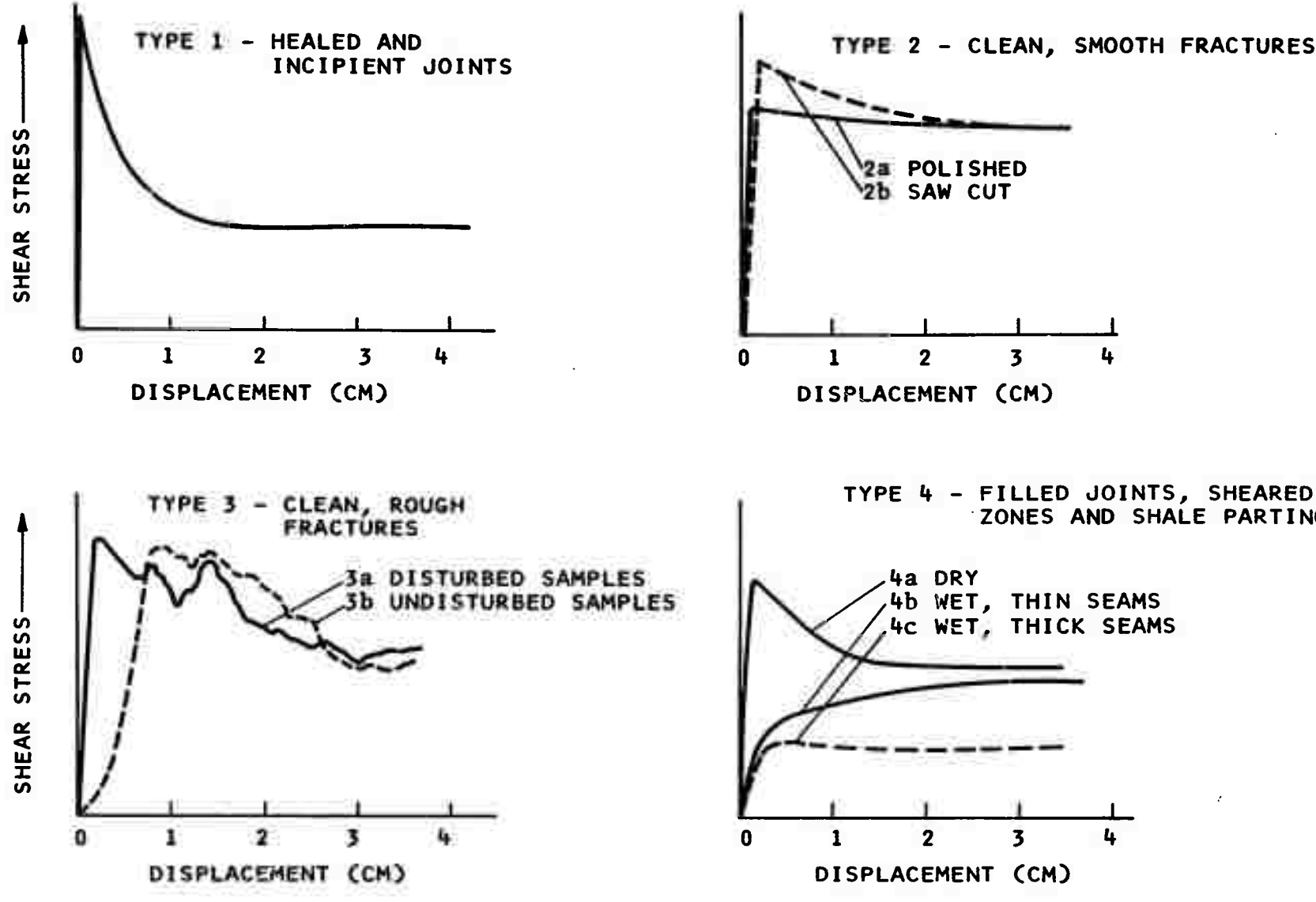

FIG. 2 - TYPICAL SHEAR STRESS - DEFORMATION RELATIONSHIPS FOR VARIOUS WEAKNESS SURFACES (AFTER GOODMAN, 1969)

illustrated in Fig. 3. In this approach, a new stiffness matrix has to be formulated and the same boundary value problem is solved for every iteration. This is a significant computational difference from the stress transfer technique used in the no tension analysis of Zienkiewicz et al. (1968) where the stiffness matrix is not changed with repeated iterations.

Zienkiewicz, et al. (1970) have shown that an iterative process similar to "stress transfer" analysis may be employed in the analysis of jointed rock systems.

3. Elasto-plastic Analysis

An elasto-plastic analysis has been suggested by various researchers to account for the possible yielding of rock due to the stress concentrations induced in the rock mass around an underground opening. Reyes and Deere (1966) developed a method based on the incremental theory of plasticity to study elasto-plastic behavior of underground openings. From the computational point of view, the process used by Reyes and Deere (1966) has the disadvantage in that, at each iteration the stiffness of the structure is changed, requiring a reformulation and computation of the stiffness matrix which will involve extra computer time. An alternative approach has been developed by Zienkiewicz, et al. (1969). This approach uses a technique referred to as the "initial stress" technique which is consistent with the "no tension" analysis. The solution obtained by the "initial stress" process involves a series of load increments. For each load increment,

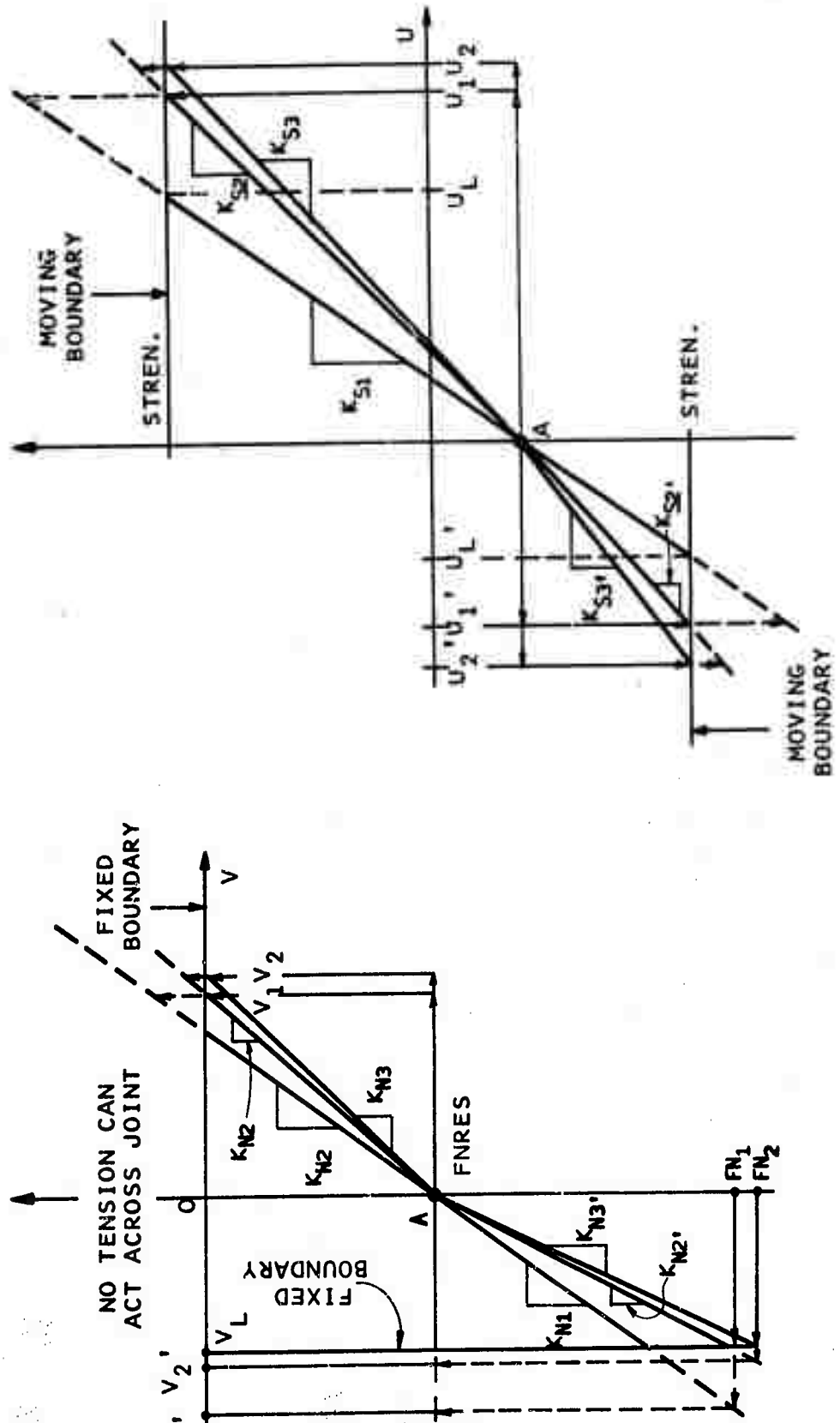

FIG. 3 - ITERATIVE TECHNIQUE FOR JOINT PERTURBATION ANALYSIS (AFTER HEUZE, GOODMAN AND BORNSTEIN, 1971)

the solution satisfying equilibrium and yield criteria is achieved by a series of approximations or iterations. Fig. 4 illustrates how the final solution may be achieved by a series of iterations. Baker, Sandhu, and Shieh (1969) have also developed a computational technique for the elasto-plastic analysis. The basic concept is quite similar to that used in the initial stress approach presented by Zienkiewicz, et al. (1969). To save computer execution time, both approaches use the initial (elastic) stiffness of the structure at each step of computation. Corrective body forces are calculated and applied to the structure during iterations to insure that the element is just on the yield surface. The only difference between the approaches of Zienkiewicz, et al. and Baker, et al. is that the latter employed a different method to insure the convergence of the final solution for each load increment.

4. Time-dependent Analysis

Time-dependent analysis for problems in rock mechanics can be considered in two categories. The first includes those cases where the boundary value problem changes with time. Such problems include consideration of the gradual (time-dependent) creation of the excavation or the installation of reinforcement (e.g., rock bolts) at various times during the construction of the opening or later during its performance. The second category includes those problems where the properties of the rock surrounding the excavation are time-dependent (creep). This

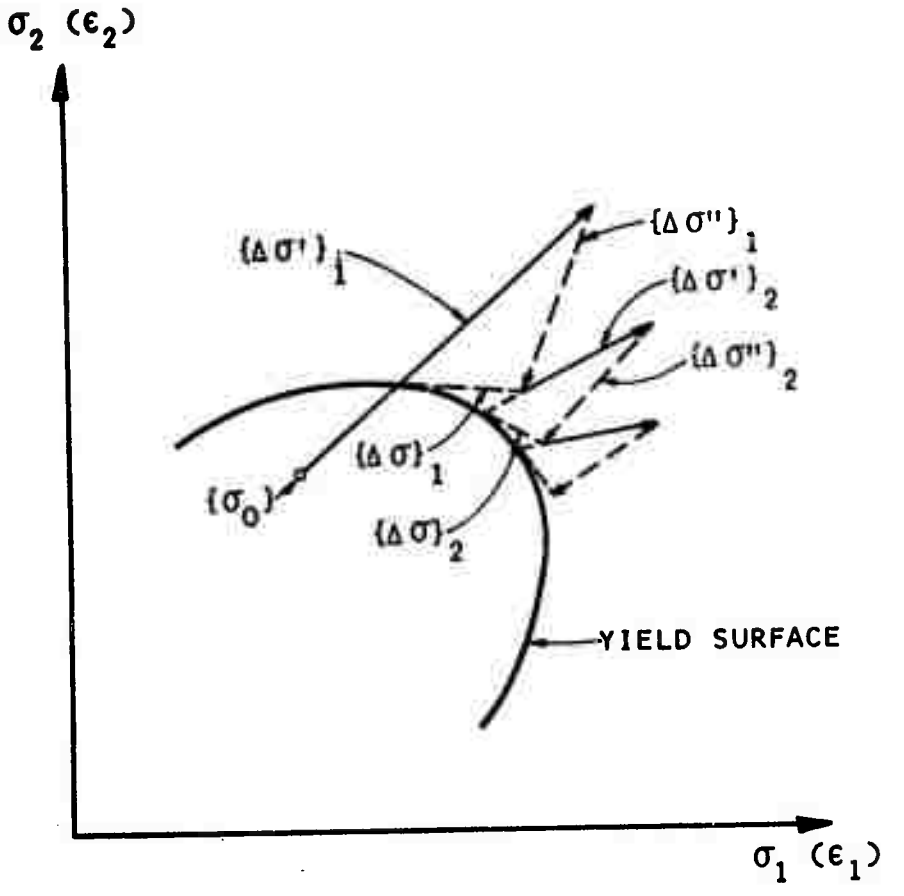

FIG. 4 - GRAPHICAL INTERPRETATION OF THE INITIAL STRESS PROCESS FOR ELASTO-PLASTIC ANALYSIS (AFTER ZIENKIEWICZ, ET AL 1969)

review was confined to problems in the second category, and in the subsequent discussions, time-dependent analyses refer only to time-dependent material properties.

Not much emphasis has been placed on developing time-dependent analyses for rock mechanics problems because the great majority of rocks do not exhibit significant time-dependent behavior. In structural analysis, two approaches have been taken in developing solutions for time-dependent problems. These depend on the complexity of material response. For linear problems, the theory of linear viscoelasticity has been utilized. For materials exhibiting nonlinear behavior, empirical stress-strain relations together with iterative solution techniques have been used. Excessive computer costs and difficulties associated with determining reliable material properties have limited the application of such analytical techniques to problems in rock mechanics.

Time-dependent analyses for nonlinear material properties have been developed by Deere and Boresi (1963), Nair (1967), Aiyer (1969), and Nair and Boresi (1970). All these analyses were developed for specialized problems and with the exception of Aiyer's work were confined to spherically symmetric or axisymmetric problems. However, at the time of this review, no published information was found on the availability of a plane finite element program which had been utilized to analyze problems in rock mechanics. The approach utilized by Nair and Boresi (1970) uses the finite element method and uses a computational technique which can be applied to the analysis of plane

problems. The basic concept used in this analysis is similar to that proposed by Greenbaum (1966). The method of incorporating the time-dependent behavior of the material is briefly described as follows: As a first step in the computation, an elastic stress distribution is computed; the effective stress is then computed. Based on the value of the effective stress, the effective strain rate is computed using the creep stress-strain time law. Taking a small time increment Δt, the incremental strains can now be computed. From these incremental strains, the incremental stresses are computed using the elastic stress-strain relations. These incremental stresses are then input into the program as initial stresses, converted into nodal point forces, and the problem is solved as an elastic problem and the new stresses and displacements are determined. These stresses are then used to develop the new incremental strains and the process repeated. In this manner, the variation of stress and displacement with time is determined.

Summary of Achievement for Phase 1a

A review of the available literature indicated that methods are available for modelling geologic discontinuities and failure characteristics that occur in rock masses. However, the computational techniques associated with the various methods are not identical. Consequently, the first step in the development of any general purpose computer program, which would include the capabilities of the individual programs, would be to make the various computational techniques consistent.

It was also found that time-dependent analyses were not developed to the level of sophistication of the time-independent analyses. Furthermore, the cost associated with a time-dependent analysis and the fact that relatively few rocks exhibit significant time-dependent behavior leads to the conclusion, at this time, that the development of a general purpose program for the time-independent plane problems be treated separately from the development of a program for time-dependent analyses. In this study, only the former has been considered.

DEVELOPMENT OF A GENERAL COMPUTER PROGRAM (Phase 1b)

In order to develop a single general computer program, it was necessary to develop a consistent computational technique to model the different aspects of rock behavior. On the basis of the review of the available techniques, it was concluded that the "initial stress" (stress transfer) technique presented by Zienkiewicz and his co-workers would provide a consistent approach in the development of a consolidated computer program, for the stress analysis of plane problems, which is capable of modelling joints and other geologic discontinuities, and elasto-plastic or time-dependent rock properties. The major reason for selecting this approach was the computational advantage that results from using the initial elastic stiffness at every stage of the solution process. The features incorporated in the combined computer program for time-independent plane problems are: (1) No Tension analysis, (2) Joint Perturbation analysis, and (3) Elasto-plastic analysis. In order to develop a single computer program using

the selected computational technique, it was necessary to formulate, write and debug programs for joint perturbation and elasto-plastic analysis. The essential concepts used to include the above listed rock characteristics are discussed in the subsequent paragraphs.

I. No Tension Analysis

The basic concept used in the combined computer program for the no tension analysis is similar to that developed by Zienkiewicz, et al. (1968). The major steps in the analysis used can be summarized as follows:

1. Assign initial stresses to the rock mass, and calculate the boundary loads required on the cavity face to simulate the creation of the opening and other structural loads applied to the system.

2. Analyze the problem as a linear elastic problem. Add the induced changes in stress to the initial stresses and compute the principal stresses.

3. Determine those elements in which tension exists. If the material is assumed incapable of sustaining tension, or if the tensile stress exceeds the tensile strength, it is necessary to eliminate the excess tensile stresses. This is done by applying nodal point forces calculated to eliminate the excess tensile stresses.

4. The elastic analysis is repeated for the calculated equivalent nodal point forces; stresses are determined in the elements. The check for tensile stresses is repeated.

5. If, at the end of step (4), principal tensile stresses are still present, steps (3) and (4) are repeated until there is no appreciable difference in magnitude and distribution of stresses with further iterations.

It has been reported by Nair and Chang (1971), and Sandhu, et al. (1971) that using the technique proposed by Zienkiewicz, et al. (1968), a large number of iterations is required to reduce tensile stresses to negligible values. Furthermore, the solution may not converge in some cases where one principal stress is tensile and the other compressive. The following modifications were made in the analysis to increase the rate of convergence.

In Step (3), when the linear elastic solution indicates that the rock is subjected to tensile stresses greater than the tensile strength, the rock is assumed fractured and incapable of transferring stresses between two orthogonal directions. In transferring tensile stresses, the Poisson's ratio for that element is reduced to zero. This technique has been employed by Nair and Chang (1971) in conjunction with an iterative process where the stiffness matrix was modified at each state. In the present study, since the same stiffness matrix is used in

all iterations, to consider the Poisson's effect a correction is made on the stress before the stress transfer process is performed. As shown in Fig. 5, where only the tensile stress in one direction (σ_x') is to be transferred, a stress state in accordance with the following equations has to be applied in order to eliminate Poisson's effect.

$$\sigma_x = \sigma_x' + \nu^2\sigma_x' + \ldots$$
$$\sigma_y = \nu\sigma_x' + \nu^3\sigma_x' + \ldots \quad (1)$$

In the case where both principal tensile stresses σ_x' and σ_y' are to be transferred, the state of stress

$$\sigma_x = (1 + \nu^2 + \ldots)\,\sigma_x'^2 + \nu\,(1 + \nu^2 + \ldots)\,\sigma_y'^2$$
$$\sigma_y = (1 + \nu^2 + \ldots)\,\sigma_y'^2 + \nu\,(1 + \nu^2 + \ldots)\,\sigma_x'^2 \quad (2)$$

is applied to the element. The rate of convergence is increased when this computational procedure is utilized.

II. Joint Perturbation Analysis

The stiffness matrix of one-dimensional joints is formulated according to the procedure developed by Goodman, Taylor, and Brekke (1968). The one-dimensional joint with its local coordinate system and the sign convention of its normal and shear stresses have been presented in Fig. 1. The approach used in this study for the nonlinear analysis of joint elements is similar to the stress transfer technique proposed by Zienkiewicz

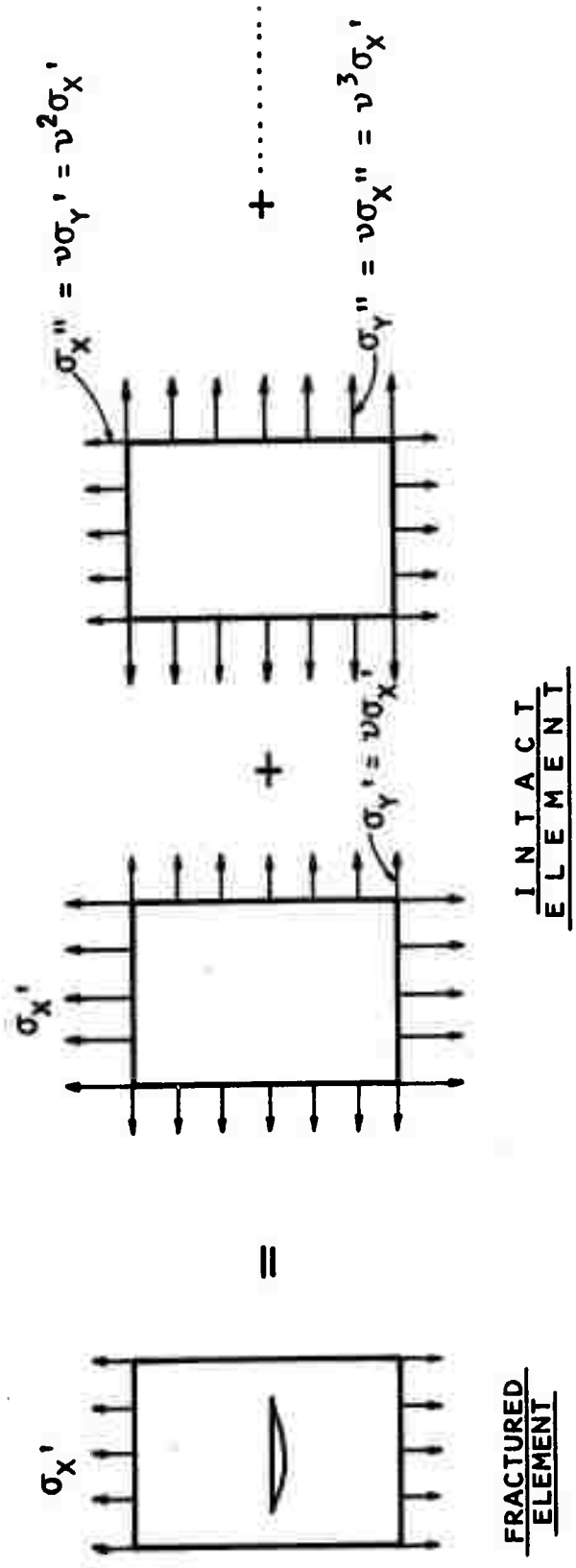

FIG. 5 - STRESS TRANSFER TECHNIQUE TO ELIMINATE POISSON'S EFFECT FOR ELEMENTS IN TENSION

and his co-workers. The shear strength of a joint element depends on the cohesion, c, the friction angle, ϕ, the joint roughness and the normal stress acting across the joint. Patton (1966) has shown that the influence of joint roughness on the shear strength along a rock surface can be taken into account by increasing the friction angle, ϕ, of the joint surface by an amount ϕ_r, which is the average angle between the undulations on the joint surface and the direction of sliding along the joint. Therefore, the effective friction angle ϕ_e of a rough joint surface is given by

$$\phi_e = \phi + \phi_r \tag{3}$$

and the shear strength of a joint may be expressed by

$$\tau_f = c + \sigma_N \tan \phi_e \tag{4}$$

where

τ_f = shear strength of the joint

c = cohesion along the joint

σ_N = normal stress across the joint

ϕ_e = effective friction angle of the joint surface.

If the normal stress across the joint is tensile, it is assumed that the joint is incapable of resisting any shear stress, i.e., it has no strength.

The procedure used to account for the nonlinear behavior of the joint elements is as follows:

1. Initial stresses are assigned to all elements, and the boundary loads required on the cavity face to simulate the creation of the opening and other loads applied to the system are calculated.

2. The problem is analyzed as a linear elastic problem. From the computed nodal point displacements, the normal and tangential displacements across the joint are calculated. These are used to compute the changes in normal and tangential stresses using the normal and shear stiffness of the joint. The induced changes in normal and tangential stresses are combined with the initial stresses.

3a. Since the joint is assumed incapable of sustaining any shear stress under a tensile normal stress, a check is made to see if a tensile normal stress exists across the joint. If a tensile normal stress is present, then both normal and tangential stresses are eliminated and the equivalent nodal point forces around the joint are calculated.

3b. If the normal stress is compressive, the shear strength of the joint is calculated by Equation (4). If the tangential stress is less than the calculated shear strength, the joint remains intact. The next step is to check closure as in step 3(c). If the tangential stress is greater

than the calculated shear strength, the joint is in yield. The excess tangential stress which is the difference between the tangential stress and shear strength is eliminated and replaced by equivalent nodal point forces.

3c. If the joint is in compression, and it undergoes excess closure beyond the allowable closure specified, the nodal point displacements around the joint are corrected to limit the displacement to the maximum allowable closure. Equivalent normal forces for the corrections in the nodal point displacements are computed.

4. The elastic analysis is repeated for the equivalent nodal point forces calculated in Step (3). The initial stiffness of the system is used throughout the computation. On the basis of the computed stresses and displacements, the checks described in Step (3) are repeated.

5. If, on repeated Step (3), corrective nodal point forces around the joints are still present, the analysis proceeds to Step (4). This iterative process is continued until the change in magnitude and distribution of stresses obtained upon iteration is negligible.

Fig. 6 illustrates schematically the stress transfer process for the nonlinear analysis of the joint systems described above.

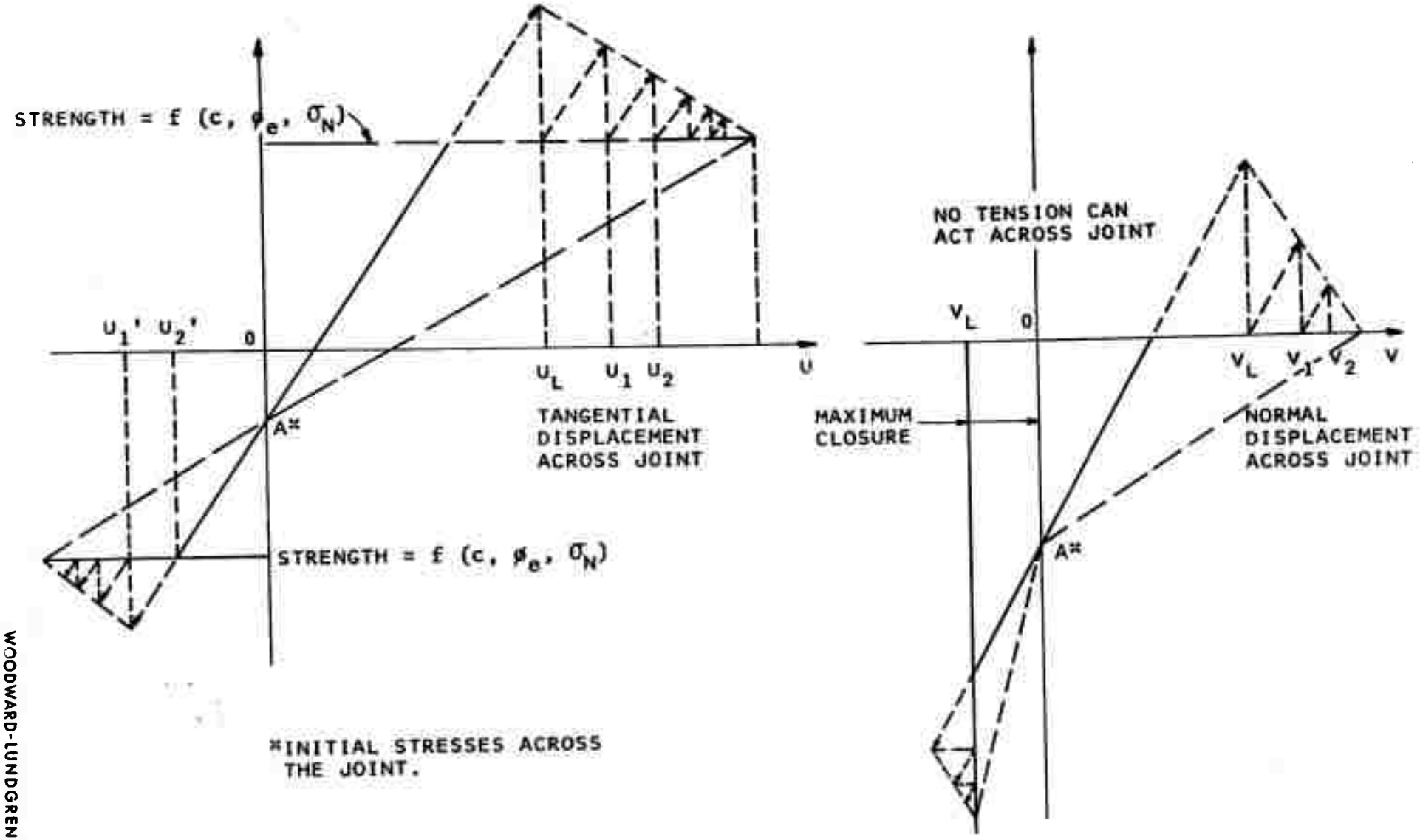

FIG. 6 - STRESS TRANSFER TECHNIQUE FOR JOINT PERTURBATION ANALYSIS

WOODWARD-LUNDGREN & ASSOCIATES

A flow diagram illustrating the stress transfer technique for joint perturbation analysis is shown in Fig. 7. It should be noted that in this technique, the joint stiffnesses are held constant while transferring excess stresses across joint elements. Heuze, Goodman and Bornstein (1971) use a different technique in conducting the joint perturbation analysis in that they employ an iterative process in which the joint stiffnesses are adjusted in each iteration.

III. Elasto-Plastic Analysis

In developing an elasto-plastic analysis, it is necessary to define a yield function and the stress-strain relations before and after yield. Prior to yield, it is assumed that linear elastic stress-strain relations are applicable.

Yield Function

In the present study, the yield function utilized is a generalization of the Mohr-Coulomb hypothesis suggested by Drucker and Prager (1952). The yield function is represented by the following equation:

$$f = \alpha J_1 + \sqrt{J_2} = k \qquad (5)$$

where:

α and k = material constants

J_1 = first stress invariant

J_2 = second invariant of stress deviation

The stress invariants may be expressed in terms of the stress components as follows:

$$J_1 = \sigma_x + \sigma_y + \sigma_z \qquad (6)$$

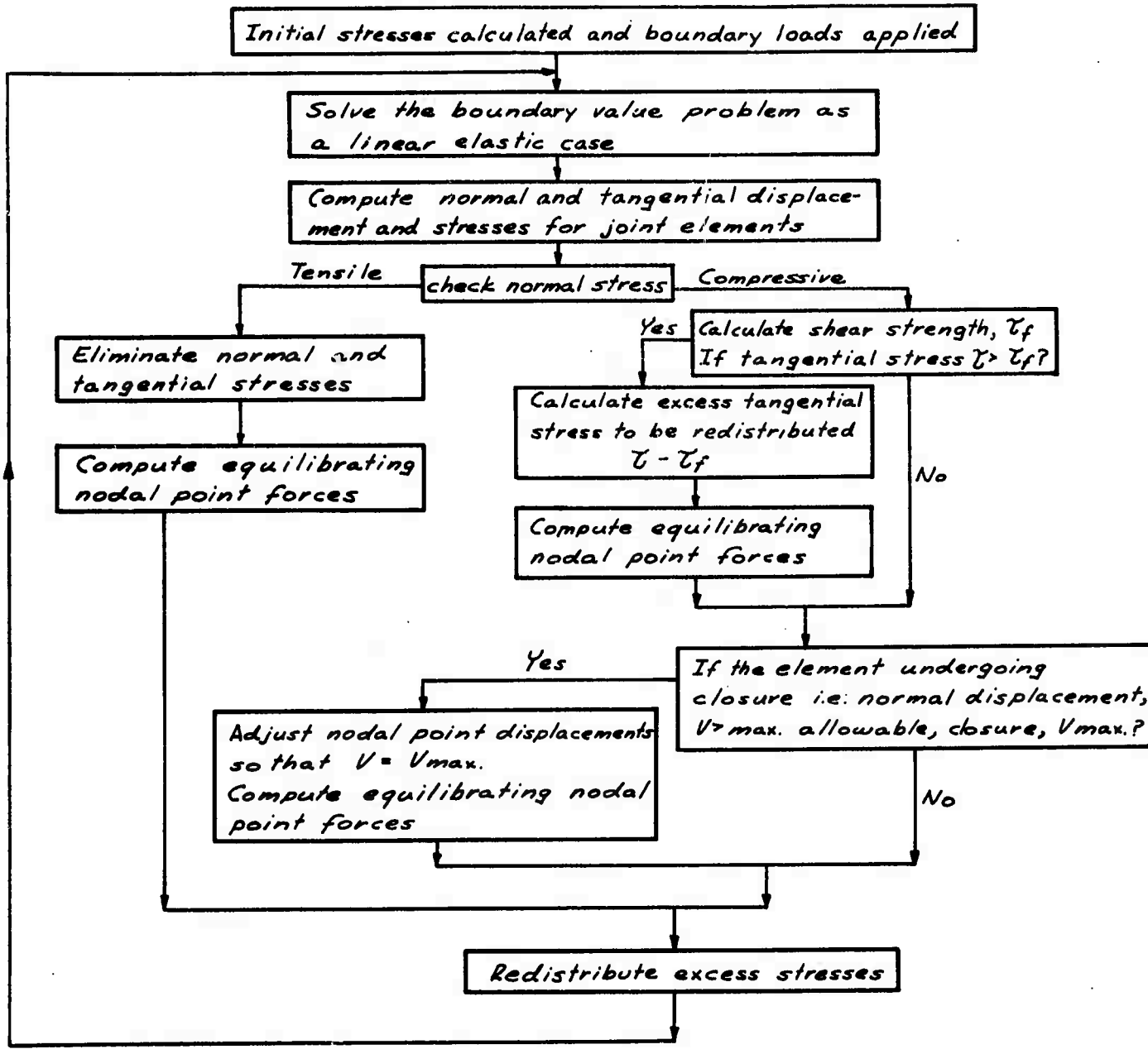

FIG. 7 -"STRESS TRANSFER" TECHNIQUE FOR JOINT PERTURBATION ANALYSIS

$$J_2 = \frac{1}{6}\left[(\sigma_x - \sigma_y)^2 + (\sigma_y - \sigma_z)^2 + (\sigma_z - \sigma_x)^2\right] + \tau_{xy}^2 + \tau_{yz}^2 + \tau_{zx}^2 \qquad (7)$$

The yield surface expressed by Equation (5) for $\alpha > 0$ is a right circular cone with its axis equally inclined to the coordinate axes. For $\alpha = 0$ equation (5) reduces to the Von Mises yield function; the yield surface is a right circular cylinder. These two yield surfaces are illustrated in Figure 8.

In the case of plane strain, Drucker and Prager (1952) have shown that

$$\alpha = \frac{\tan \phi}{(9 + 12 \tan^2 \phi)^{\frac{1}{2}}} \qquad (8)$$

and

$$k = \frac{3c}{(9 + 12 \tan^2 \phi)^{\frac{1}{2}}} \qquad (9)$$

where:

c = the cohesion of the material

ϕ = angle of internal friction of the material

Stress-Strain Relations

During an infinitesimal increment of stress, changes in strain are assumed to be composed of elastic and plastic parts if the element is in yield, i.e.

$$\{\Delta\varepsilon\} = \{\Delta\varepsilon\}_e + \{\Delta\varepsilon\}_p \qquad (10)$$

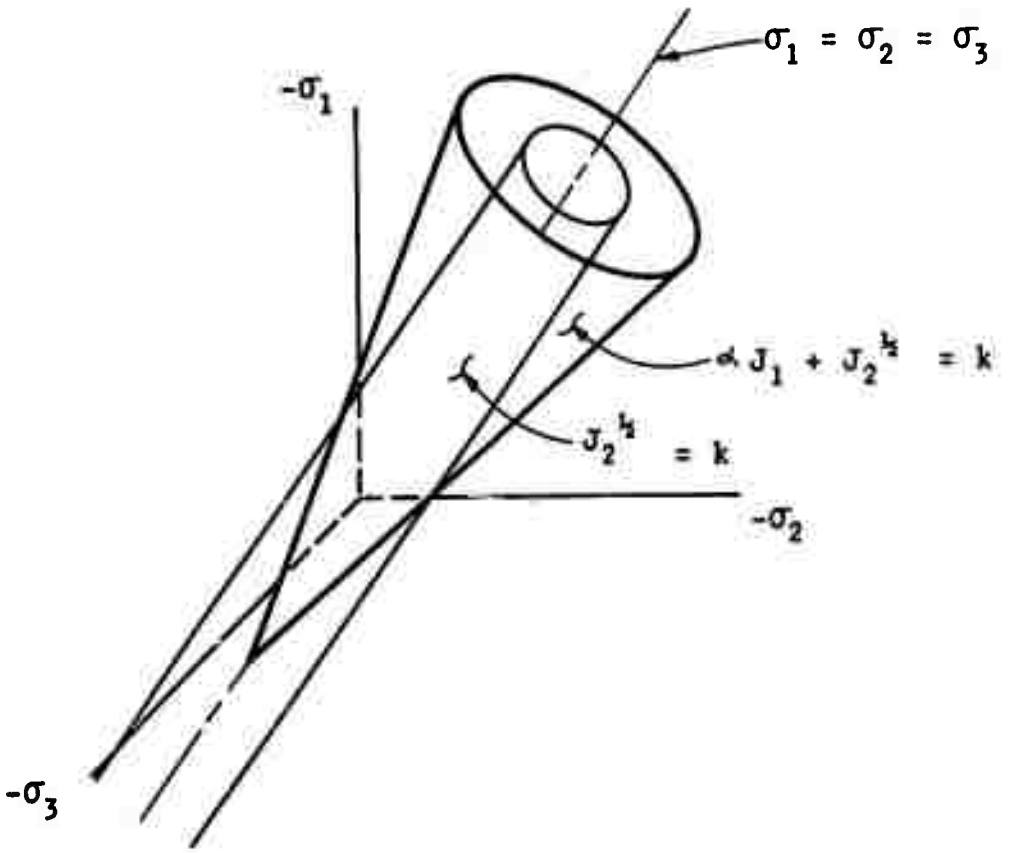

FIG. 8 - GENERALIZED MOHR-COULOMB YIELD SURFACE

The elastic strain increments are related to stress increments by the generalized Hooke's law as

$$\{\Delta\sigma\} = [D]\{\Delta\varepsilon\}_e \tag{11}$$

where the strain-stress matrix is

$$[D] = \frac{E}{(1+\nu)(1-2\nu)} \begin{bmatrix} (1-\nu) & \nu & o \\ \nu & (1-\nu) & o \\ o & o & \frac{(1-2\nu)}{2} \end{bmatrix} \tag{12}$$

and E is the elastic modulus and ν the Poisson's ratio for the linear isotropic elastic material.

Utilizing the Drucker Prager criteria (equation 5) Reyes (1966) developed elasto-plastic stress-strain relations. These relations can be expressed as follows:

$$\{\Delta\sigma\} = [D]_{e.p.}\{\Delta\varepsilon\}_p \tag{13}$$

where

$$[D]_{e.p.} = \begin{bmatrix} D_{11} & D_{12} & D_{13} \\ D_{21} & D_{22} & D_{23} \\ D_{31} & D_{32} & D_{33} \end{bmatrix}$$

$$D_{11} = 2G(1 - h_2 - 2h_1 \sigma_x - h_3 \sigma_x^2)$$

$$D_{22} = 2G(1 - h_2 - 2h_1 \sigma_y - h_3 \sigma_y^2)$$

$$D_{33} = 2G(\tfrac{1}{2} - h_3 \tau_{xy}^2) \qquad (14)$$

$$D_{12} = D_{21} = -2G\,[h_2 + h_1 (\sigma_x + \sigma_y) + h_3 \sigma_x \sigma_y]$$

$$D_{13} = D_{31} = -2G(h_1 \tau_{xy} + h_3 \sigma_x \tau_{xy})$$

$$D_{23} = D_{32} = -2G(h_1 \tau_{xy} + h_3 \sigma_y \tau_{xy})$$

where:

$$G \text{ (shear modulus)} = \frac{E}{2(1 + \nu)}$$

$$h_1 = \left[\frac{3K\alpha}{2G} - \frac{J_1}{6 J_2^{\frac{1}{2}}}\right] \Bigg/ \left[J_2^{\frac{1}{2}} (1 + 9\alpha^2 \frac{K}{G})\right] \qquad (15)$$

$$h_2 = \frac{\left[\alpha - \frac{J_1}{6 J_2^{\frac{1}{2}}}\right]\left[\frac{3K\alpha}{G} - \frac{J_1}{3 J_2^{\frac{1}{2}}}\right]}{(1 + 9\alpha^2 \frac{K}{G})} - \frac{3 \nu K k}{E J_2^{\frac{1}{2}} (1 + 9\alpha^2 \frac{K}{G})}$$

$$h_3 = \frac{1}{2 J_2 (1 + 9\alpha^2 \frac{K}{G})}$$

$$K \text{ (bulk modulus)} = \frac{E}{3(1 - 2\nu)}$$

Since the elasto-plastic stress-strain relation is a function of the elastic constants, the yield parameters (α, k) and the stress

state, it is necessary to keep a record of the axial stress σ_z. For the plane strain case the change in stress, $\Delta\sigma_z$, is related to the changes in stress in x - y plane in the elastic range by

$$\Delta\sigma_z = \nu(\Delta\sigma_1 + \Delta\sigma_2) \tag{16}$$

where $\Delta\sigma_1$ and $\Delta\sigma_2$ are changes in stress in two principal stress directions in x - y plane. In the plastic range, Drucker and Prager (1952) have shown that the change in axial stress is given by

$$\Delta\sigma_z = \frac{1}{2}(\Delta\sigma_1 + \Delta\sigma_2) - \frac{1}{2}(\Delta\sigma_1 - \Delta\sigma_2)\ \text{Sin}\ \phi \tag{17}$$

Computational Procedure

To conduct an incremental elasto-plastic analysis the initial stress approach developed by Zienkiewicz, et al (1969) is utilized. This approach is consistent with that described previously for the no tension and joint perturbation analyses. The load is applied in a series of increments. The initial stress process approaches the solution of a nonlinear problem by a series of approximations.

The procedure for conducting the elasto-plastic analysis during a typical load increment can be summarized as follows:

1. For the applied load increment, the elastic increments of stress $\{\Delta\sigma'\}_1$ and corresponding strain $\{\Delta\varepsilon'\}_1$ are determined.

2. Add $\{\Delta\sigma'\}_1$ to the stresses existing at the end of the last increment $\{\sigma_o\}$ to obtain $\{\sigma'\}$. The corresponding change in axial stress $\Delta\sigma_z'$ is calculated according to one of the following two conditions.

(a) If $f(\sigma_o) - k \geq 0$ i.e., the element was in yield at the start of increment

$$\Delta\sigma_z' = \frac{1}{2}(\Delta\sigma_1 + \Delta\sigma_2) - \frac{1}{2}(\Delta\sigma_1 - \Delta\sigma_2)\sin\phi \qquad (18)$$

(b) If $f(\sigma_o) - k < 0$ i.e., the element was in the elastic range at the start of increment

$$\Delta\sigma_z' = \nu(\Delta\sigma_1 + \Delta\sigma_2) \qquad (19)$$

and the current axial stress is obtained by

$$\sigma_z' = (\sigma_z)_o + \Delta\sigma_z' \qquad (20)$$

Calculate $[f(\sigma') - k]$ using equations (5) through (9). If $f(\sigma_o) - k < 0$ and $f(\sigma') - k < 0$, only changes in elastic strain occur (i.e., there is no yield). No further computations are required. If $f(\sigma_o) - k \geq 0$ and $f(\sigma') - k < 0$, this implies that no further yielding occurred during the applied load increment. The corresponding change in axial stress is corrected using equation (19) and σ_z' recalculated by equation (20).

3. If $f(\sigma') - k \geq 0$ and $f(\sigma_o) - k = 0$ i.e., the element was in yield at the start of increment, calculate $\{\Delta\sigma\}_1$, using the following relation:

$$\{\Delta\sigma\}_1 = [D]_{e.p.}\{\Delta\varepsilon'\}_1 \tag{21}$$

where $[D]_{e.p.}$ is the elasto-plastic stress-strain relation expressed by equation (14).

The excess stresses which have to be redistributed are calculated as follows:

$$\{\Delta\sigma''\}_1 = \{\Delta\sigma'\}_1 - \{\Delta\sigma\}_1 \tag{22}$$

whereas $(\Delta\sigma_z'')_1$ is computed in accordance with the following equation:

$$(\Delta\sigma_z'')_1 = \frac{1}{2}(\Delta\sigma_1'' + \Delta\sigma_2'') - \frac{1}{2}(\Delta\sigma_1'' - \Delta\sigma_2'') \sin\phi \tag{23}$$

The current stresses, which are stored, are computed as follows:

$$\{\sigma\} = \{\sigma'\} - \{\Delta\sigma''\}_1 \tag{24}$$

and current strains

$$\{\varepsilon\} = \{\varepsilon_o\} + \{\Delta\varepsilon'\}_1 \tag{25}$$

4. If $f(\sigma') - k > 0$ but $f(\sigma_o) - k < 0$ i.e., the element goes from the elastic to the plastic range, and it is necessary to find the intermediate stress value at which yielding commences. This is done by the following interpolation procedure:

$$\Delta f = f(\{\Delta\sigma'\}_1) \tag{26}$$

$$\{\Delta\sigma'\}_{1\ e.p.} = A\{\Delta\sigma'\}_1 \tag{27}$$

where

$$A = \frac{f(\sigma') - k}{\Delta f}$$

$$\{\sigma'\}_{e.p.} = \{\sigma'\} - \{\Delta\sigma'\}_{1\ e.p.} \tag{28}$$

Use $\{\sigma'\}_{e.p.}$ to compute $[D]_{e.p.}$ and equation (21) to calculate $\{\Delta\sigma\}_1$. Then proceed as in step (3).

5. Considering $\{\Delta\sigma''\}_1$ as initial stresses, the corresponding equilibrating nodal point forces $\{P\}^e_1$ are computed.

6. The system is solved for the loads $\{P\}^e_1$ and $\{\Delta\sigma'\}_2$ and $\{\Delta\varepsilon'\}_2$ are determined.

7. Steps 2 to 6 are repeated until the nodal forces $\{P\}^e$ reach sufficiently small values.

A flow diagram showing the stress transfer technique for elasto-plastic analysis is illustrated in Figure 9.

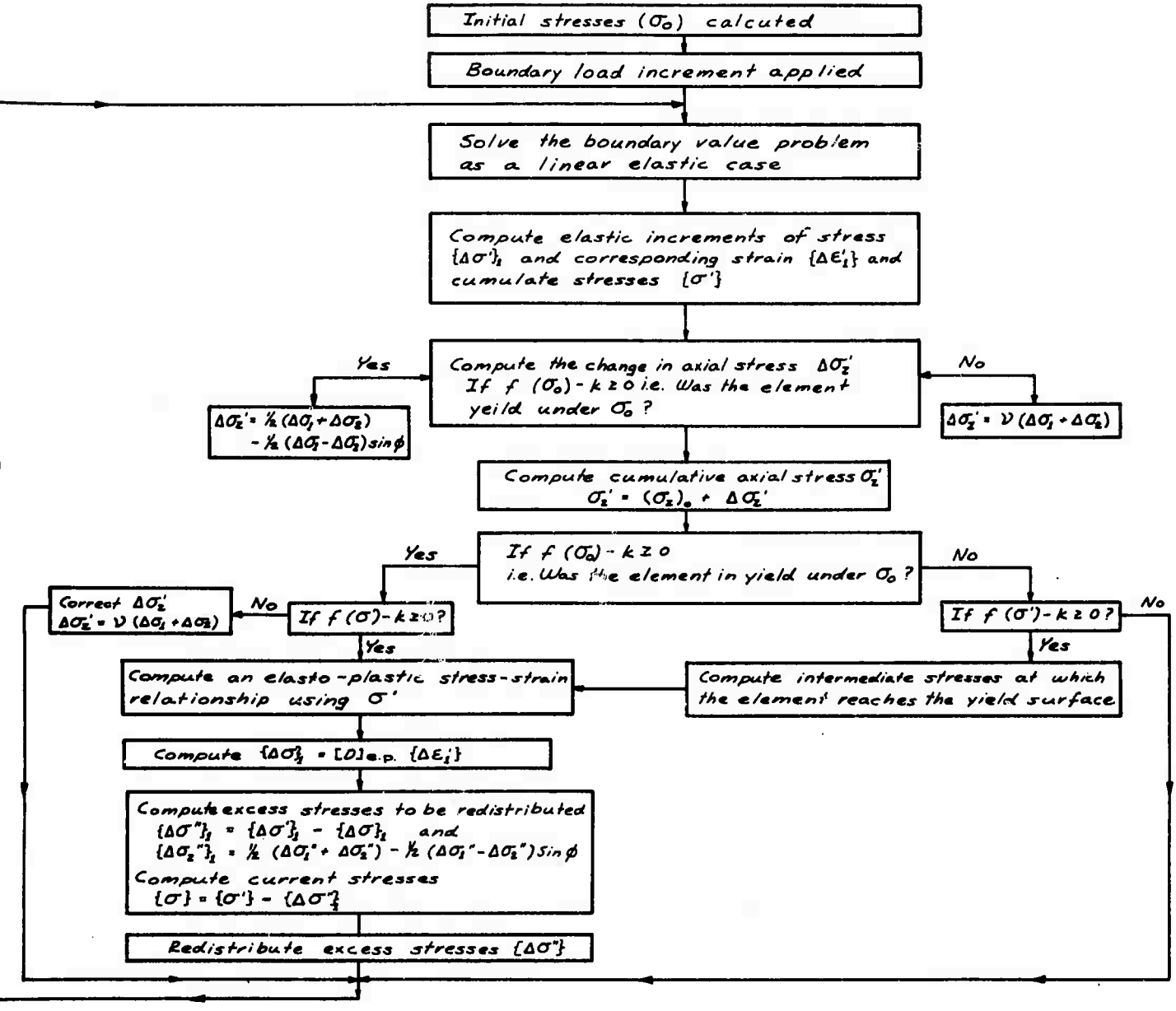

FIG. 9 - "STRESS TRANSFER" TECHNIQUE FOR ELASTO-PLASTIC ANALYSIS

Experience from a limited number of solutions performed indicated that the rate of solution convergence would depend on the stress state and the yield constants α and k given. In general, it was found that if the Von Mises yield criterion is used i.e., $\alpha = 0$ or $\phi = 0$, the solution convergence is rapid, three to six iterations being necessary in any increment. However, when ϕ is non-zero the solution converges considerably slower. This convergence problem was also noted by Baker, Sandhu and Shieh (1969). In some cases, it may be found necessary to use various numerical schemes to accelerate convergence.

Summary of Achievement for Phase 1b

A computational procedure using the initial stress (stress transfer) approach developed by Zienkiewicz and his co-workers was formulated for modelling certain classes of joints, no tension characteristics in the rock mass and elasto-plastic behavior. This procedure was used to develop a computer program which could determine the mechanical state in a rock mass with the above-mentioned characteristics in the vicinity of an excavation. Because available programs did not use a single computational technique, it was necessary to write new programs.

ILLUSTRATIVE PROBLEMS (Phase 1c)

Definition of Problems

The following examples were analyzed using the combined finite element computer program developed in this study for the purpose of verifying and demonstrating the use of the program.

I. Elasto-plastic analysis of a thick-walled circular tube with the Von Mises yield criterion. A closed form solution is available for this case for verification.

II. Elasto-plastic analysis of a circular opening with the generalized Mohr-Coulomb yield criterion. The results are compared with those obtained by Reyes (1966) and Baker, et al (1969).

III. Combined no tension, joint perturbation and elasto-plastic analysis of a rectangular underground opening to demonstrate the usage of the combined computer program.

Results

I. Elasto-Plastic Analysis of a Thick-walled Circular Tube with the Von Mises Yield Criterion Subject to Internal Pressure

Prager and Hodge (1951) have presented a closed form solution of the above problem. The material is assumed to obey the Von Mises yield criterion, a special case of the Mohr-Coulomb criterion expressed by Eq. (5) in which $\phi = 0$ or $\alpha = 0$ and $k = c$. The dimensions of the tube, the material properties and the finite element idealization of the problem are shown in Figure 10.

The circular tube was subjected to internal pressure up to $p = 1.39\ k$ in five unequal increments. The results of the analysis indicated that the interior surface reached the yield surface after the first increment of loading ($p > 0.75k$).

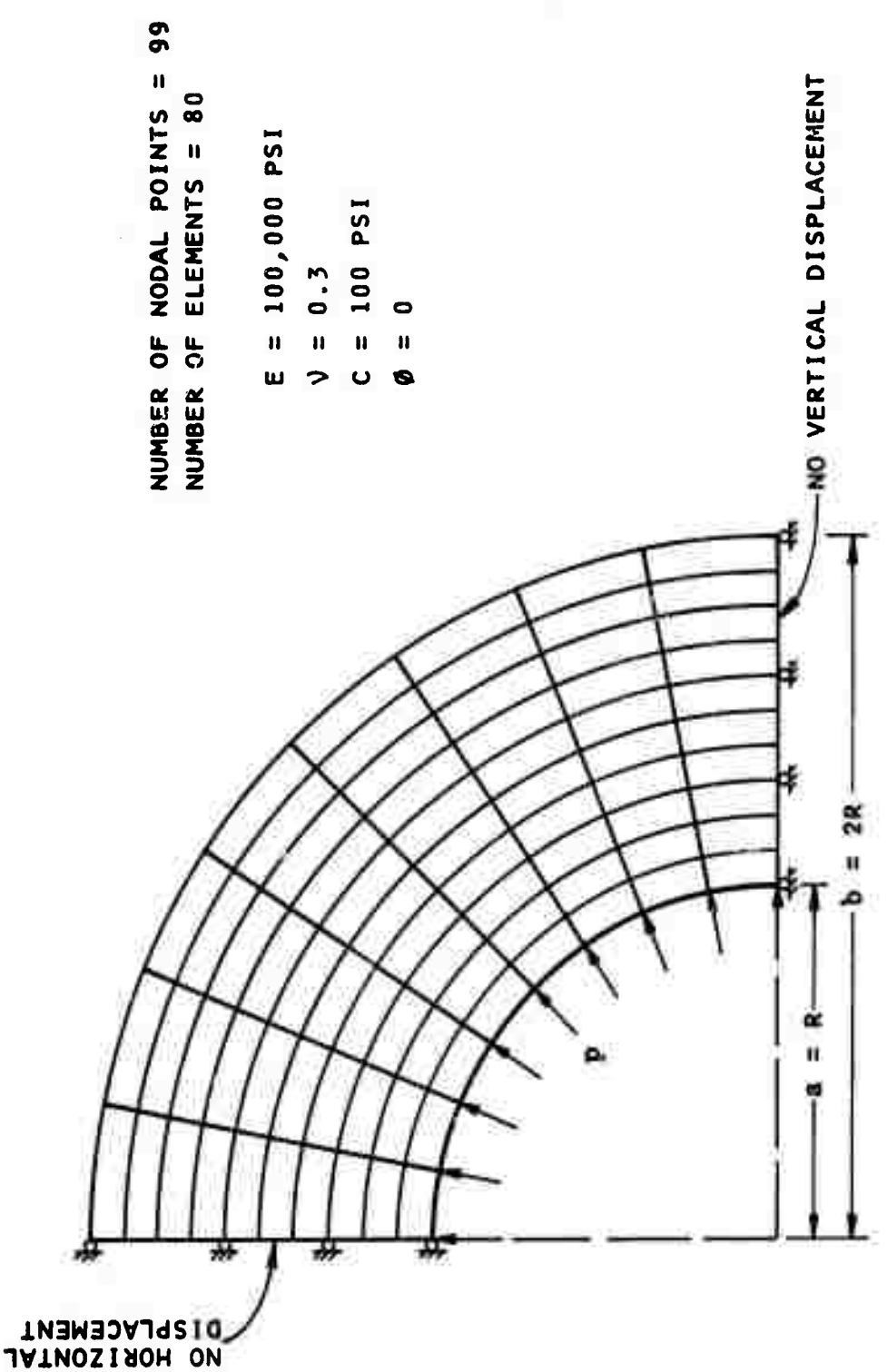

FIG. 10 - FINITE ELEMENT MESH FOR AN ELASTO-PLASTIC ANALYSIS OF A THICK-WALLED CIRCULAR TUBE (b = 2a)

Subsequent increase in pressure caused the material near the interior surface to undergo elasto-plastic behavior. For each subsequent pressure increment, six cycles of stress redistribution were required for solution convergence, except for the second increment for which only three cycles were required. The results of the analysis, together with the closed form solution are shown in the form of stresses and displacements in Figs. 11 through 14. Fig. 11 presents the distribution of circumferential stress for the various pressure increments. The apexes of these computed curves indicate the boundary of the plastic zone. It should be recognized that the values of stress are plotted at the centroid of the element. From Fig. 11, the ratio of the radius of the plastic zone boundary to the internal radius (ρ/a) is computed for each pressure increment.

Figs. 12 and 13 present the distribution of radial and axial stress for all pressure increments. Also shown on these figures is the ρ/a corresponding to the distribution. The results can be compared with the closed form solution for the corresponding ρ/a. The results are in excellent agreement. Fig. 14 shows the radial displacements on the interior surface as functions of the radius ρ of the elastic-plastic boundary. Comparison between the results obtained from the finite element analysis and those from the closed form solution indicates good agreement.

II. Elasto-plastic Analysis of a Circular Opening with the Generalized Mohr-Coulomb Yield Criterion

For purposes of demonstrating an elasto-plastic analysis for a material with the generalized Mohr-Coulomb yield criterion, a

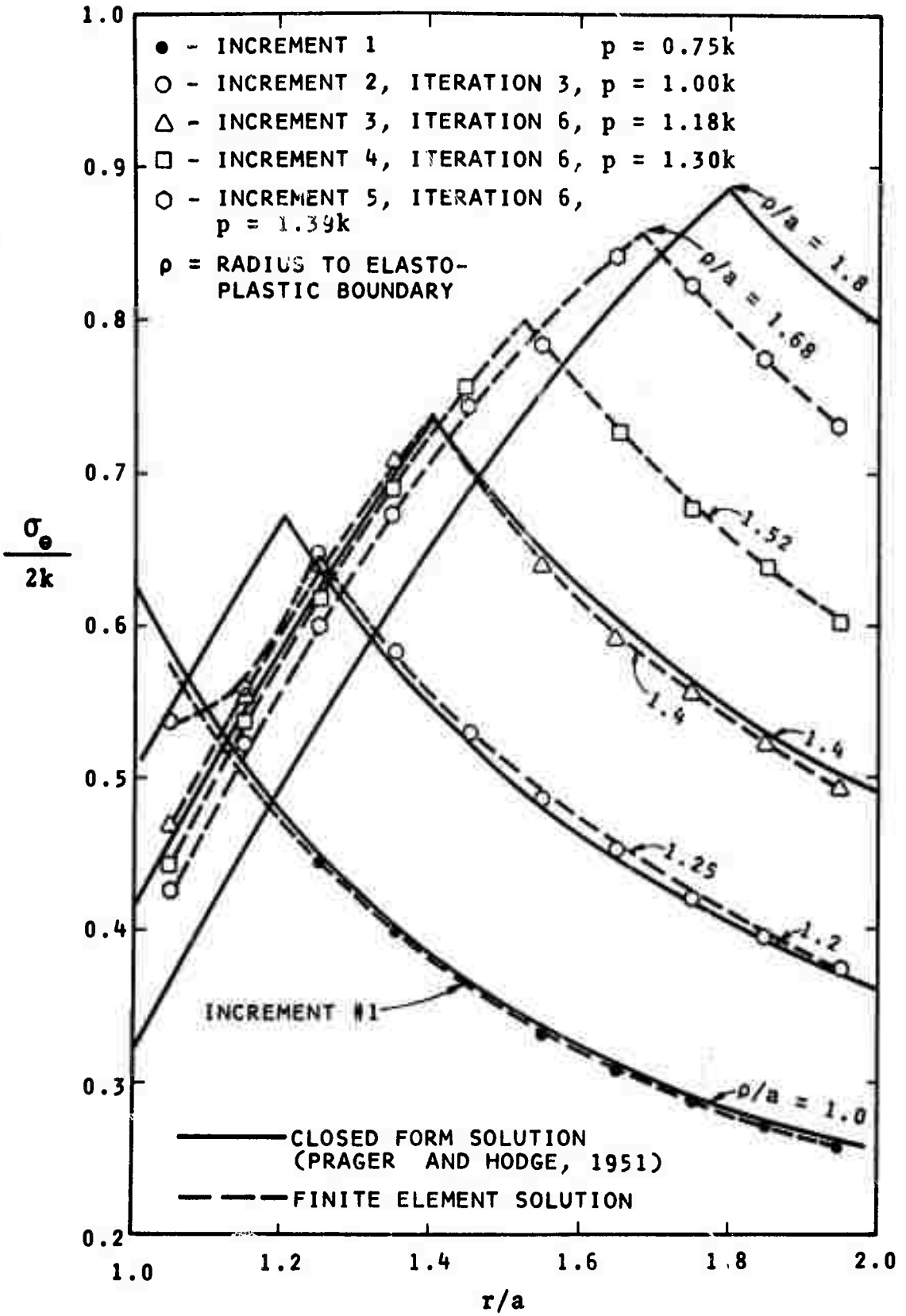

NOTE: THE APEX OF THE CURVES REPRESENTS THE BOUNDARY BETWEEN THE PLASTIC AND ELASTIC REGIONS. IN COMPARING CURVES IT IS NECESSARY TO EXAMINE CURVES WITH THE SAME ρ/a.

FIG. 11 - DISTRIBUTION OF CIRCUMFERENTIAL STRESS FOR A THICK-WALLED CIRCULAR TUBE

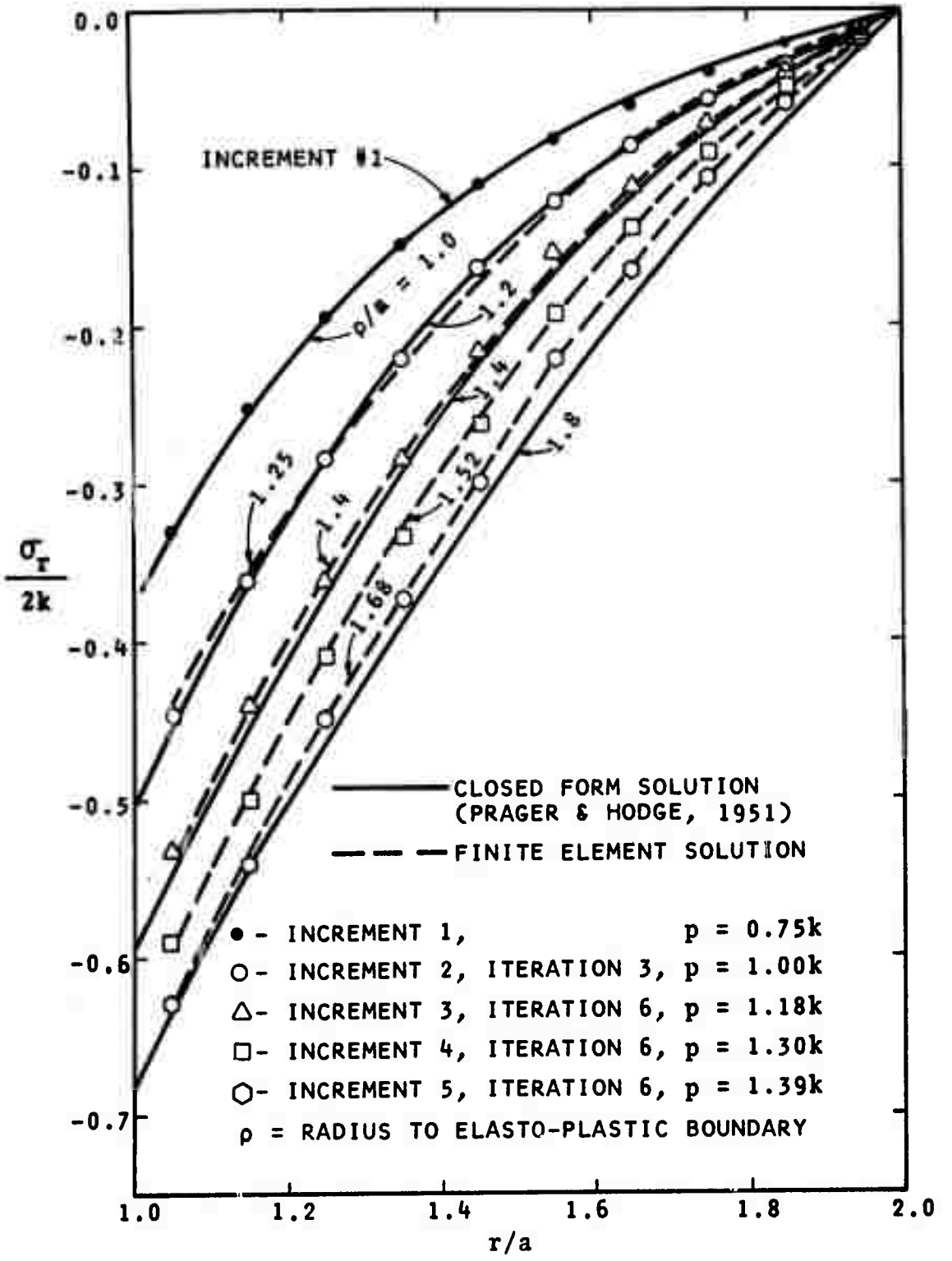

FIG. 12 - DISTRIBUTION OF RADIAL STRESS FOR A THICK-WALLED CIRCULAR TUBE

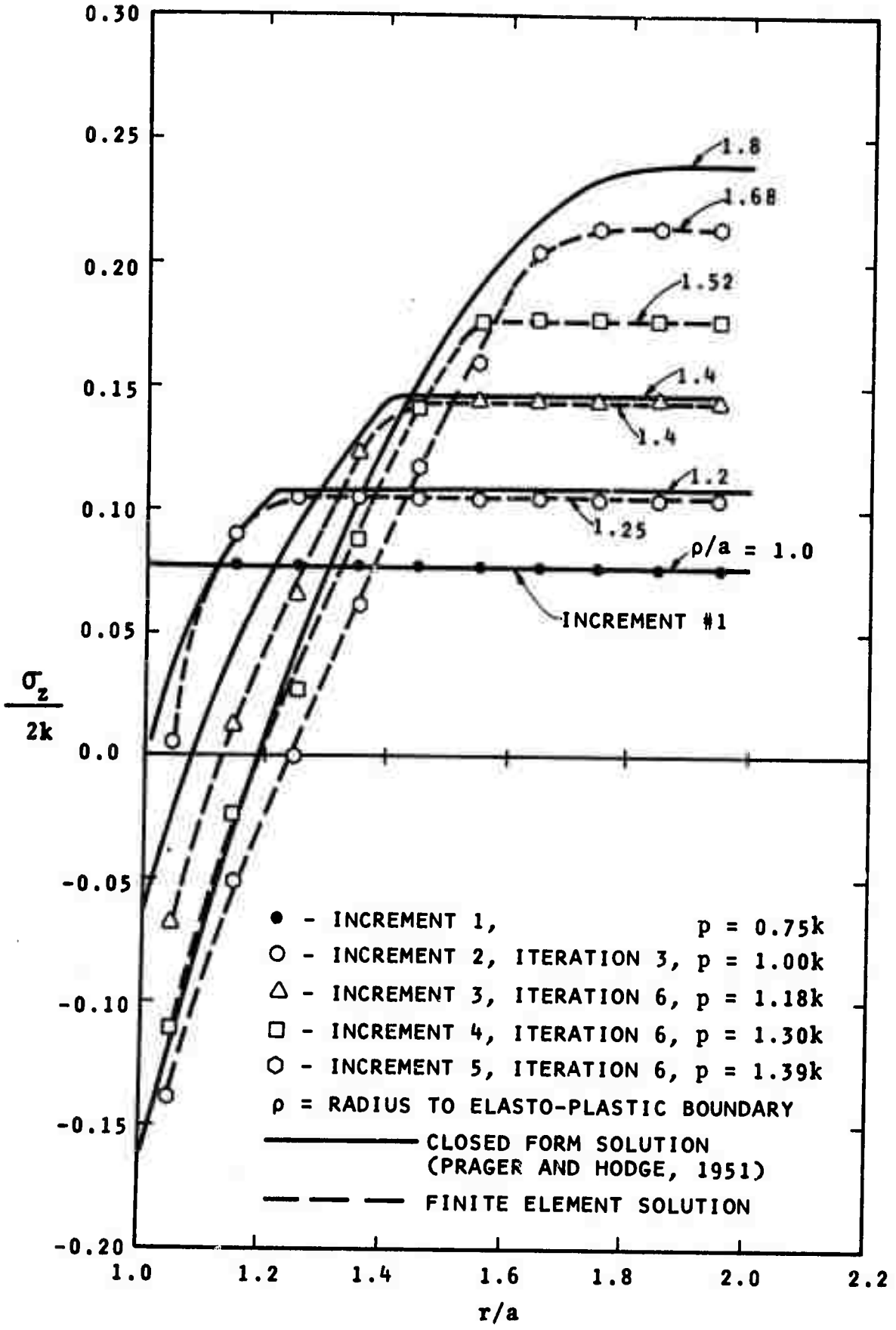

FIG. 13 - DISTRIBUTION OF AXIAL STRESS FOR A THICK-WALLED CIRCULAR TUBE

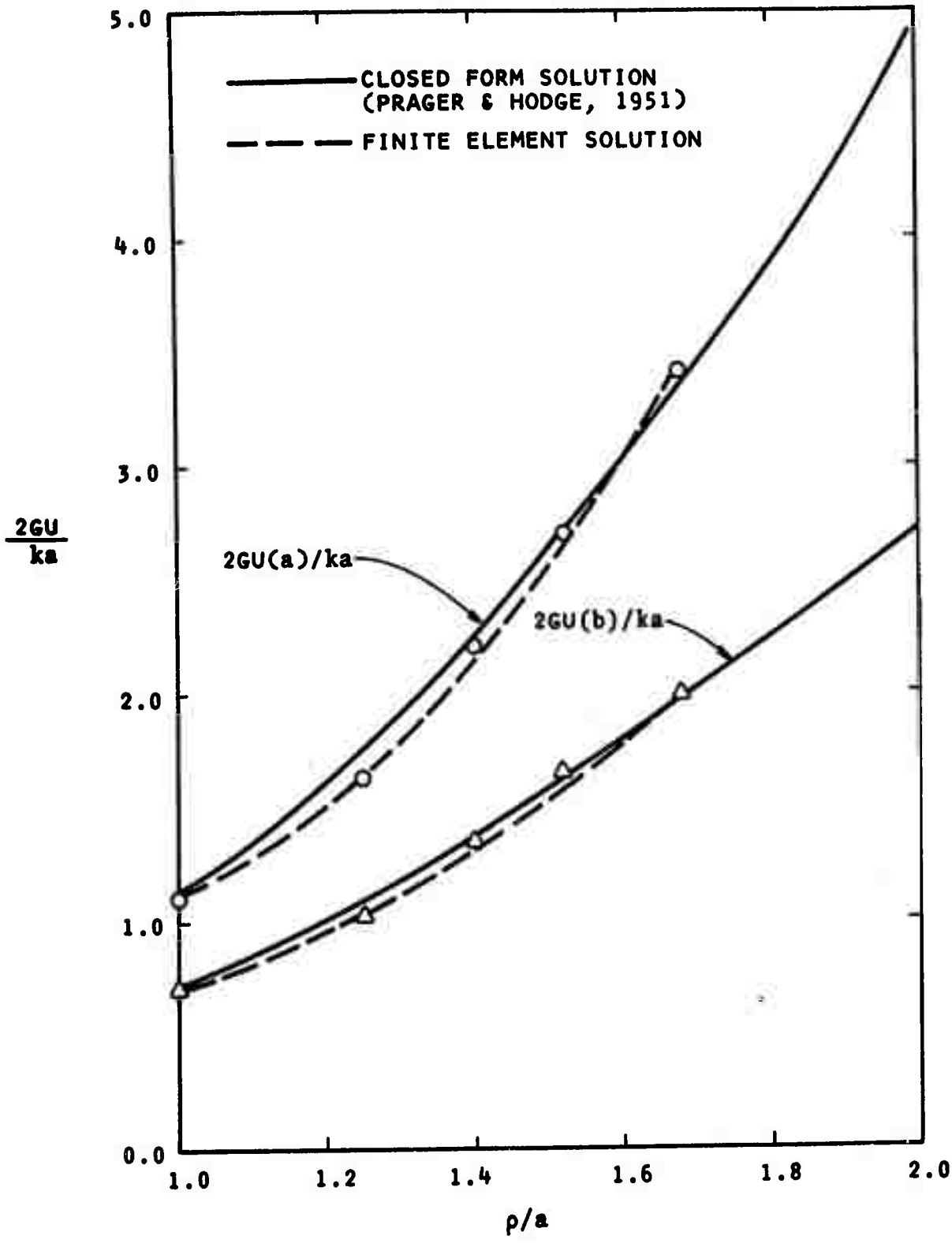

FIG. 14 - RADIAL DISPLACEMENT U (a), U (b) VS. RADIUS ρ OF ELASTIC-PLASTIC BOUNDARY FOR A THICK-WALLED CIRCULAR TUBE

circular opening shown in Fig. 15 was analyzed. The definition of the problem and the finite element idealization are shown in Fig. 15. The analysis was conducted by applying pressures on the outer boundary.* The boundary pressures which have vertical and horizontal components were applied in 14 increments. The percentage of the total boundary pressure applied for each increment is tabulated in Fig. 15.

It was experienced that the solution convergence was slow as compared with the case for the thick-walled circular tube described above. This convergence problem was also noted by Baker, et al. (1969). For the purpose of speeding convergence, the following over-relaxation technique was adopted.

For every iteration, the excess stresses $\{\Delta\sigma''\}$ as computed by Eq. (22), which are to be balanced by a set of body forces, are multiplied by an over-relaxation factor to bring the element to the point below the yield surface. The over-relaxation factor, Ro (ρ), which will ensure convergence of the solution, was found to be in the range between 1.0 and 1.5. Its value was selected in accordance with the following procedure.

---

* In the semi-annual technical report, this problem was analyzed with different loading conditions. A comparison of the results is presented in the Appendix D.

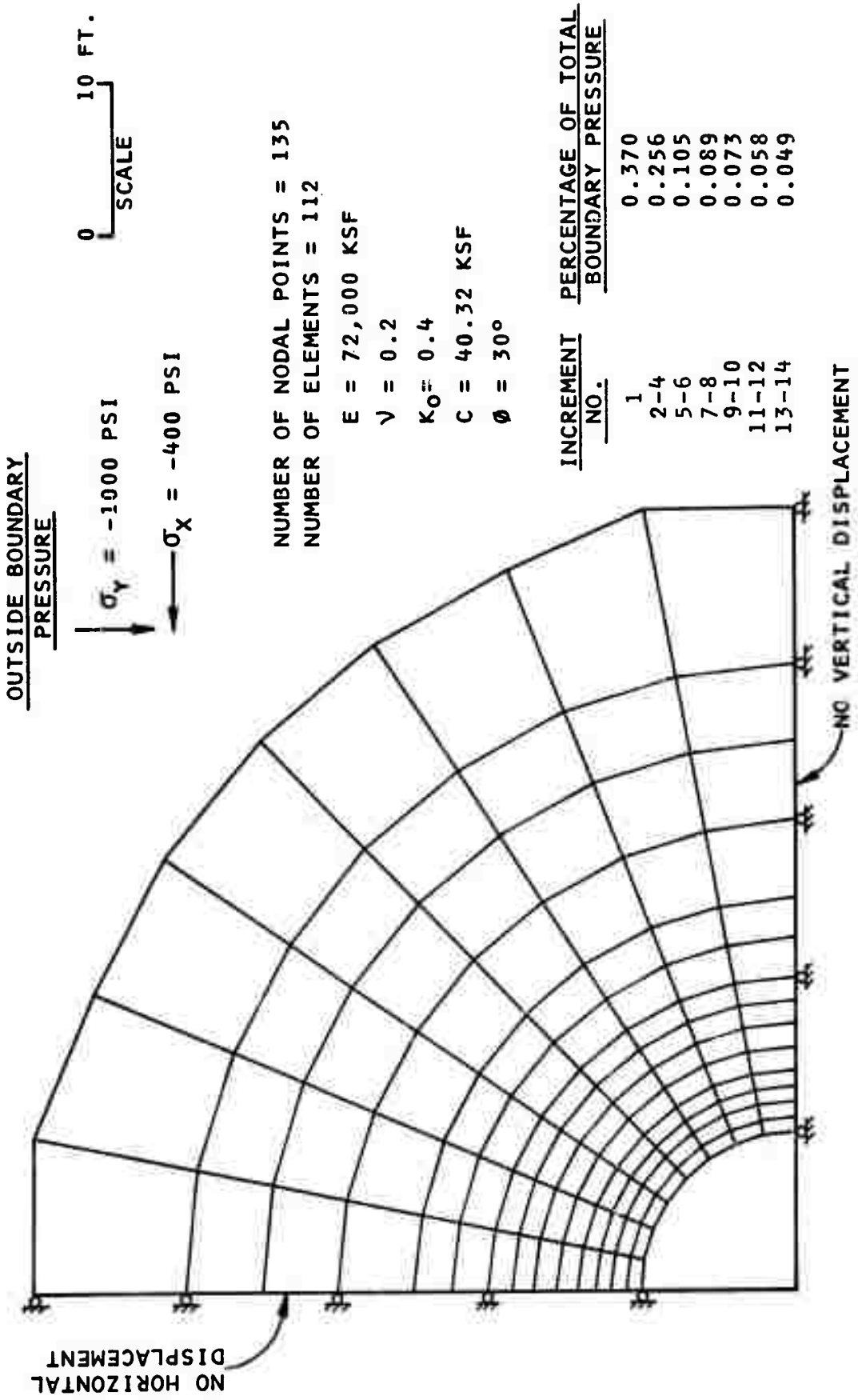

FIG. 15 - FINITE ELEMENT MESH FOR AN ELASTO-PLASTIC ANALYSIS OF A CIRCULAR OPENING

(1) For every iteration f_r, which is an index showing where the element was situated outside the yield surface, is calculated according to

$$f_r = [f(\sigma') - k] / (k - \alpha J_1) \quad (27)$$

(2) Define the current state of stress by the following equation

$$\{\sigma\} = \{\sigma'\} - \{\Delta\sigma''\}_1 \cdot \rho \quad (28)$$

ρ is to be determined. Express $[f(\sigma) - k]$ in terms of ρ.

(3)(a) If $f_r \geq 15\%$, determine ρ on the basis of the following equation:

$$[f(\sigma) - k] = [k - f(\sigma')] \quad (29)$$

(b) If $15\% < f_r \leq 10\%$, a value of ρ was selected such that

$$f(\sigma) - k < 0.75 [k - f(\sigma')] \quad (30)$$

(c) If $f_r < 10\%$, a value of ρ was selected such that

$$f(\sigma) - k < 0.5 [k - f(\sigma')] \quad (31)$$

Using this technique for increasing the rate of convergence, six to eight iterations were still needed for a loading increment. The results of the analysis together with those presented by Reyes (1966) and Baker, et al (1969) are shown in Figures 16 and 17. Figure 16 shows vertical (tangential) and horizontal (radial) stresses along a horizontal section through the opening. All three methods of analysis give the same

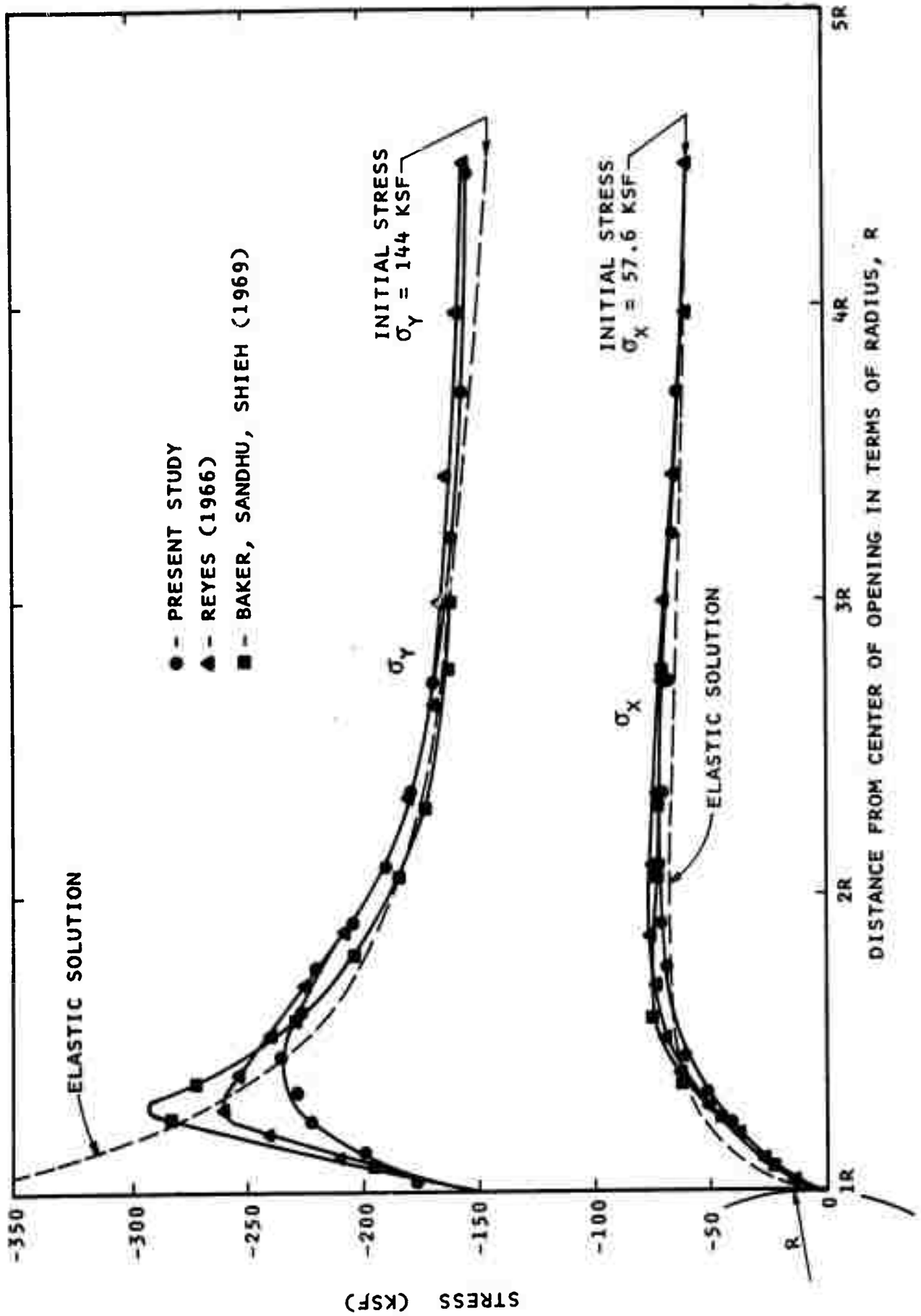

FIG. 16 - VERTICAL AND HORIZONTAL STRESSES ALONG HORIZONTAL

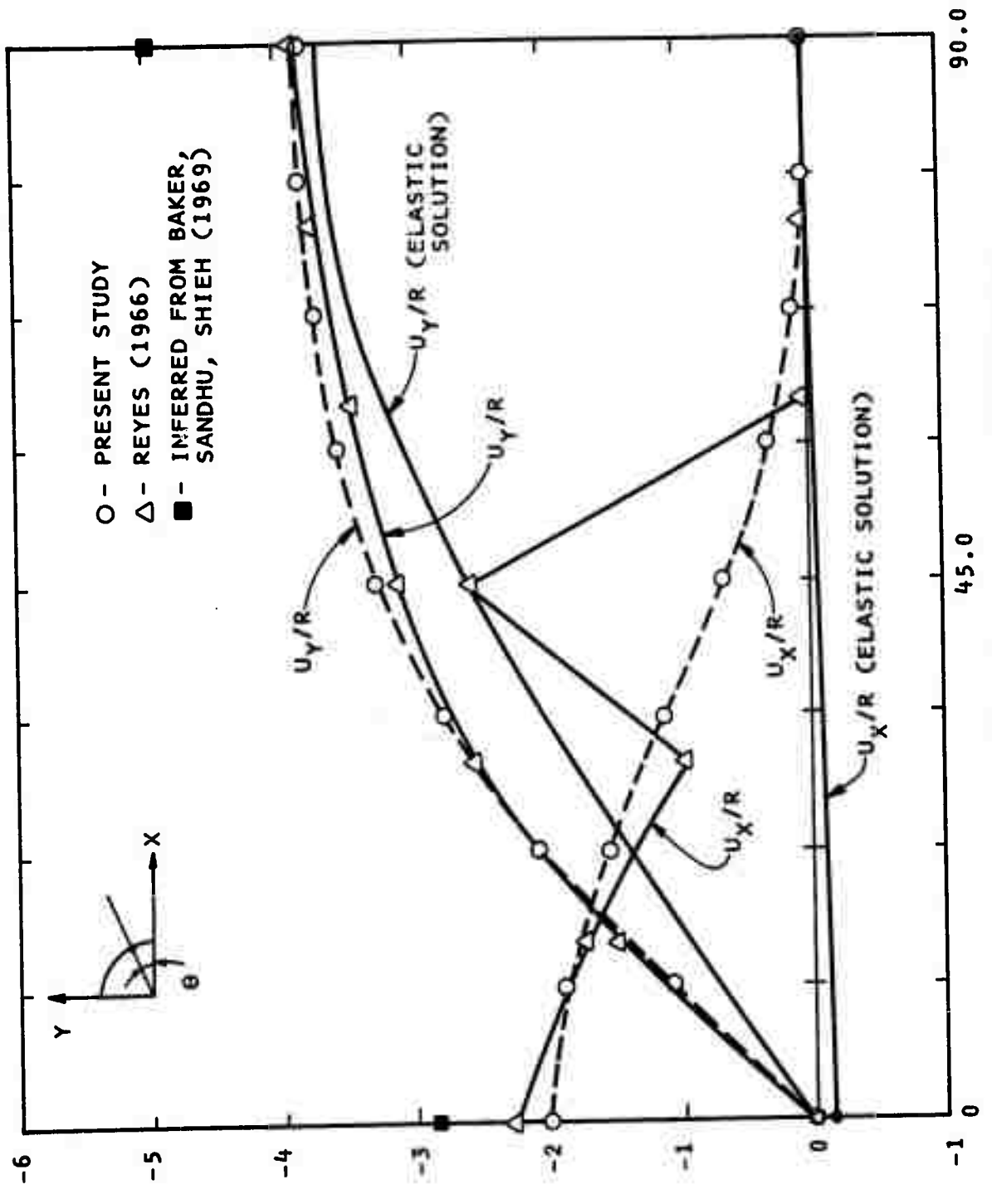

FIG. 17 - DEFORMATION ALONG CAVITY FACE OF A CIRCULAR OPENING AS COMPUTED BY ELASTIC AND ELASTIC-PLASTIC ANALYSIS

distribution of the horizontal stress. The tangential stress distribution indicates that the three methods of analysis predict approximately the same extent of the yield zone. The peak tangential stress, however, differs by approximately 25%. This difference is thought to be due to two causes: (i) differences in the degree of convergence obtained, and (ii) different methods of computing the axial stress. As discussed earlier, the yield criterion is assumed to be a function of the sum of three normal stresses and the second invariant of the stress deviation. Therefore, different values of the axial stress result in different yield surfaces. The differences in the methods utilized by Reyes (1966), Baker, et al. (1969) and that utilized in this study to calculate the axial stress are briefly discussed in the following paragraphs.

Baker, et al. (1969) used the following equation to compute the axial stress, σ_z.

In the elastic range, the axial stress is given by

$$\sigma_z = \nu \, (\sigma_1 + \sigma_3) \tag{32}$$

where σ_1 and σ_3 are major and minor principal stress, respectively, in the x-y plane, and ν = Poisson's ratio.

In the plastic range, the axial stress is expressed by

$$\sigma_z = \frac{1}{2} \, (\sigma_1 + \sigma_3) - \frac{1}{2} \, (\sigma_1 - \sigma_3) \, \text{Sin} \, \phi \tag{33}$$

where ϕ = the angle of internal friction.

Comparison of equation (32) and (33) shows that the values of σ_z computed by the two equations will not be the same for the cases in which $\nu \neq \frac{1}{2}$ and $\phi \neq 0$ indicating that there will be an abrupt change on the value of σ_z as the element undergoes from the elastic state to the plastic state. The total stress is used at each computation. A different method was used by Reyes (1966) to calculate σ_z. For every increment of loading, σ_z was first calculated using the equation similar to equation (16) assuming that the element was in the elastic range.

$$\sigma_z^{(r)} = \sigma_z^{(r-1)} + \nu \, (\Delta\sigma_x^{(r)} + \Delta\sigma_y^{(r)}) \tag{34}$$

If the yield function was exceeded and the element was in yield in the previous load increment, the new state of stress was computed by

$$\sigma_{ij}^{(r)} = \sigma_{ij}^{(r-1)} + 2G(\Delta\varepsilon_{ij} - a\delta_{ij} - b\sigma_{ij}^{(r)}) \tag{35}$$

where σ_{ij} are stress components, G is shear modulus, $\Delta\varepsilon_{ij}$ are the computed strain increments, δ_{ij} is the Kronecker delta, and a, b are constants to be determined, Equation 35 represents a set of equations for each stress component. These equations were solved for the constants a and b, and the new state of stress $\sigma_{ij}^{(r)}$ by successive substitutions.

The present study used a different approach to evaluate σ_z. The loading is applied incrementally, and for each load increment

the change in axial stress $\Delta\sigma_z$ is calculated in accordance with equations 16 or 17 depending upon whether the element is in the elastic or plastic range.

The vertical and horizontal components of the deflection at the face of the opening are presented in Fig. 17. It may be seen that the elasto-plastic solution indicates an increase in both vertical and horizontal deflections toward the opening as compared with the elastic solution. The horizontal deflection for the solution obtained by Reyes (1966) does not appear to be reliable. The comparison of the vertical deflections indicates excellent agreement between the results obtained by Reyes (1966) and the present study.

III. Analysis of a Rectangular Underground Opening

To demonstrate the usage of the combined computer program developed in which all three types of analysis - no tension, joint perturbation and elasto-plastic analysis are considered, a hypothetical rectangular opening located at the depth of 1000 ft was analyzed. The finite element idealization is shown in Fig. 18. A horizontal joint is assumed to exist 50 ft above the crown of the opening. Initial stresses were assumed to increase with depth in accordance with the gravity stress field. The vertical stress is assumed equal to depth times unit weight of the rock (144 pcf assumed) and the horizontal stress equal to $\nu/(1-\nu)$ times the vertical stress. The problem is defined in Fig. 18. The excavation for the opening was simulated by applying the boundary pressures in four increments as shown in Fig. 18.

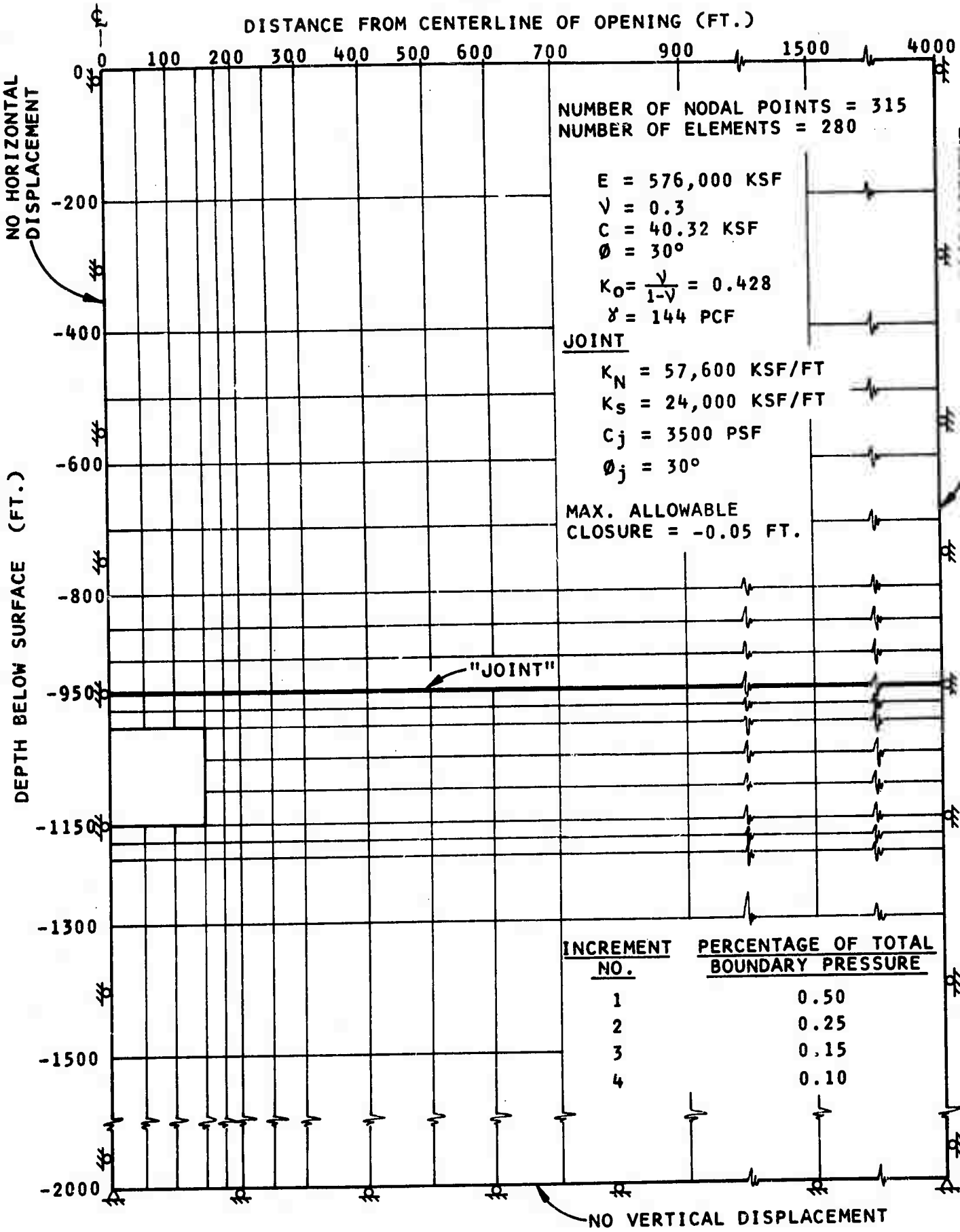

FIG. 18 - FINITE ELEMENT MESH FOR ANALYSIS OF A RECTANGULAR OPENING

The results of the analysis are presented in Figs. 19 through 25. Figs. 19 and 20 show, respectively, the distribution of the normal and tangential stress along the horizontal joint for both elastic and combined solution. Some readjustment of stresses may be noted near the centerline of the opening resulting from the yielding of the joint elements. It should, however, be recognized that only a few joint elements have yielded and there are no large movements along the joint since the joint is intact over the majority of its length. Figs. 21 and 22 show, respectively, the distribution of the major principal stress in the vicinity of the opening obtained from the elastic and combined solution; Figs 23 and 24 are for the distribution of the minor principal stress obtained from the elastic and combined solution. It may be noted, by comparing with the elastic solution, that some readjustment of stresses occurs in the vicinity of the opening. The magnitude and region of tensile stresses have been reduced by the stress transfer process to simulate the no tension rock characteristic. Fig. 25 indicates the development of the plastic zone in the vicinity of the opening.

Summary of Achievement for Phase 1c

The combined computer program developed in Phase 1b was used to analyze certain illustrative problems. Satisfactory agreement was obtained when the results of these analyses were compared with closed form solutions and the solutions obtained by other researchers. Using this combined computer program, complex geometries and heterogeneous rock conditions and properties can be accounted for.

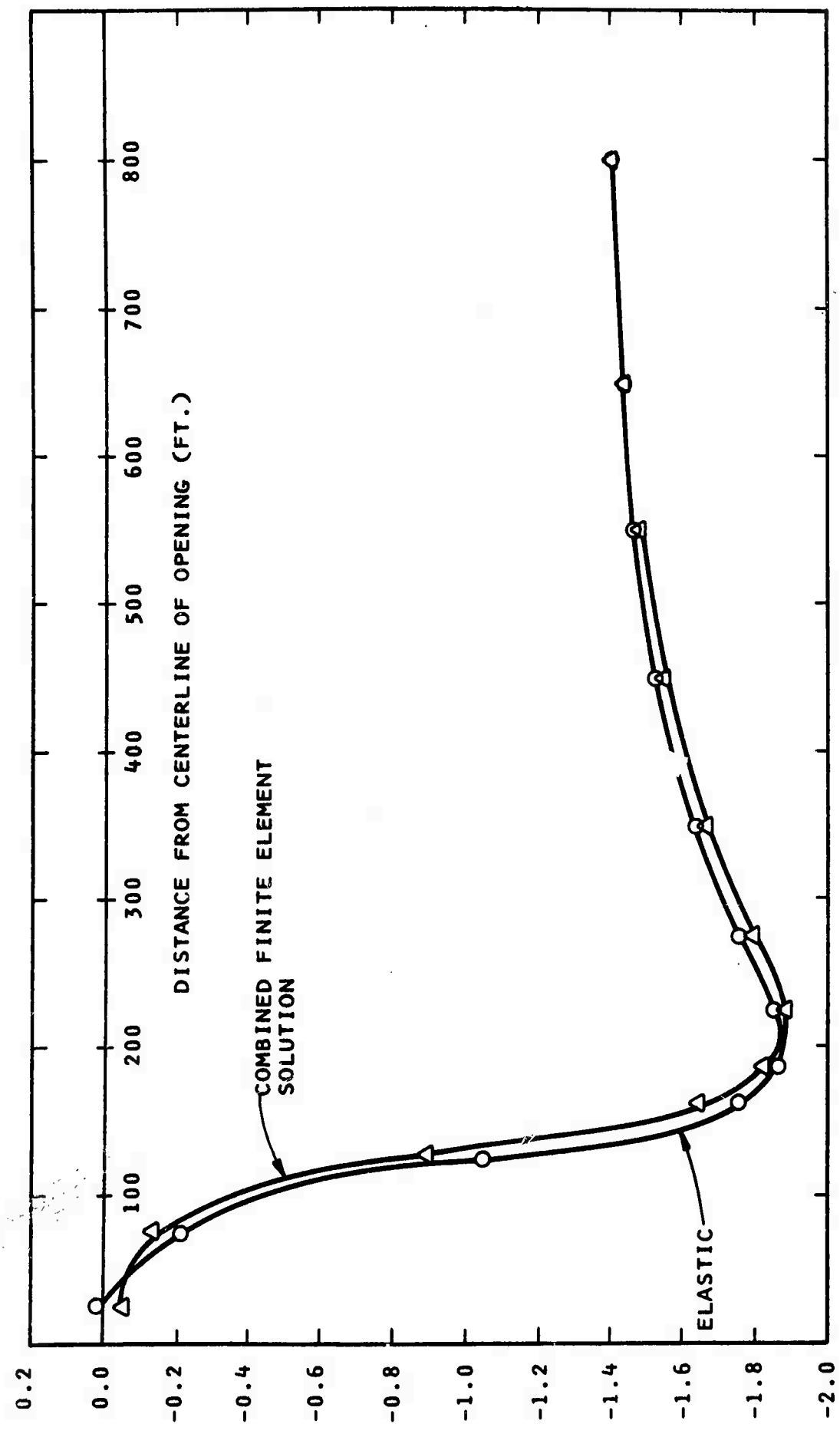

FIG. 19 - DISTRIBUTION OF NORMAL STRESS ALONG HORIZONTAL JOINT

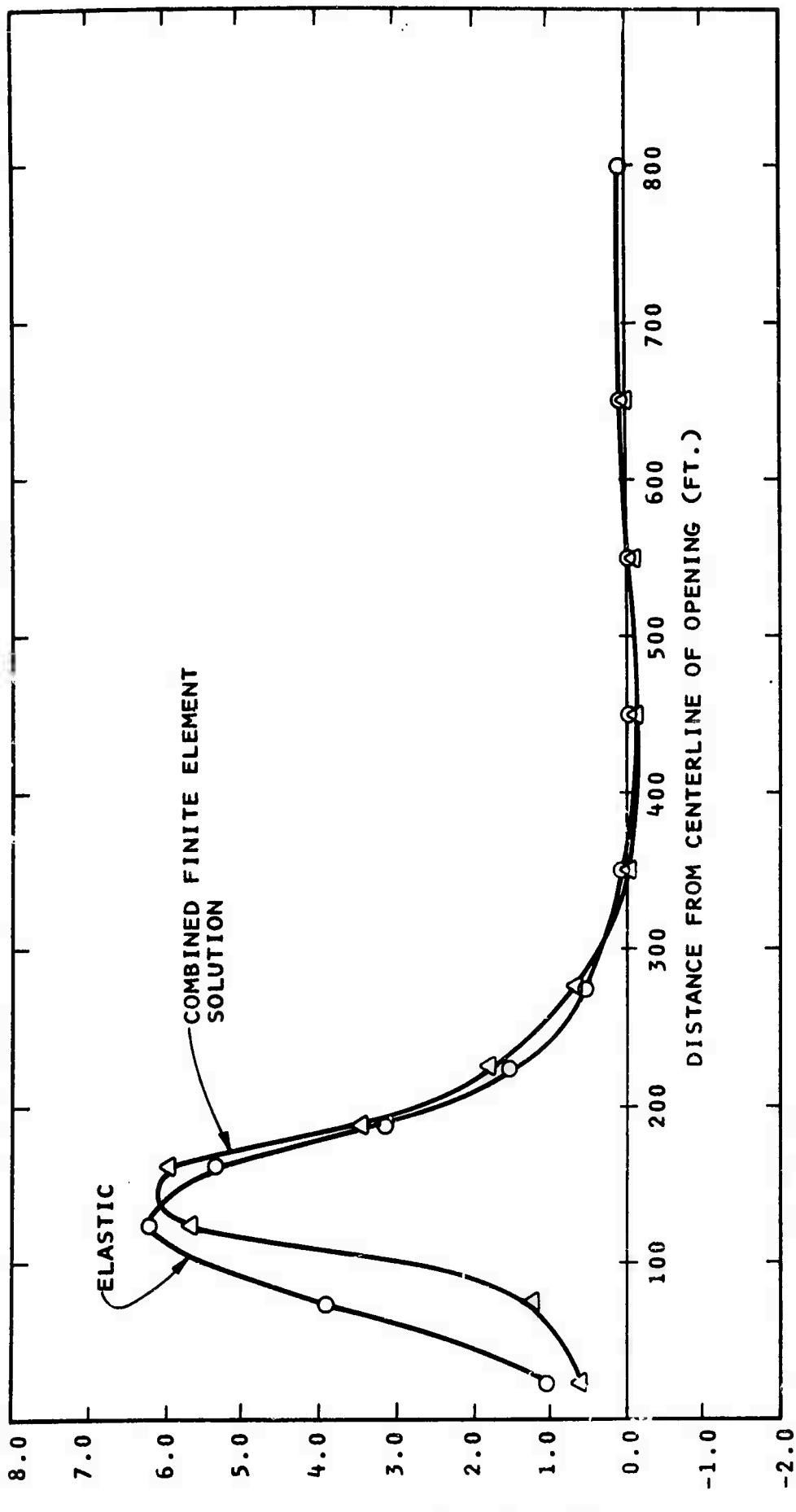

FIG. 20 - DISTRIBUTION OF TANGENTIAL STRESS ALONG HORIZONTAL JOINT

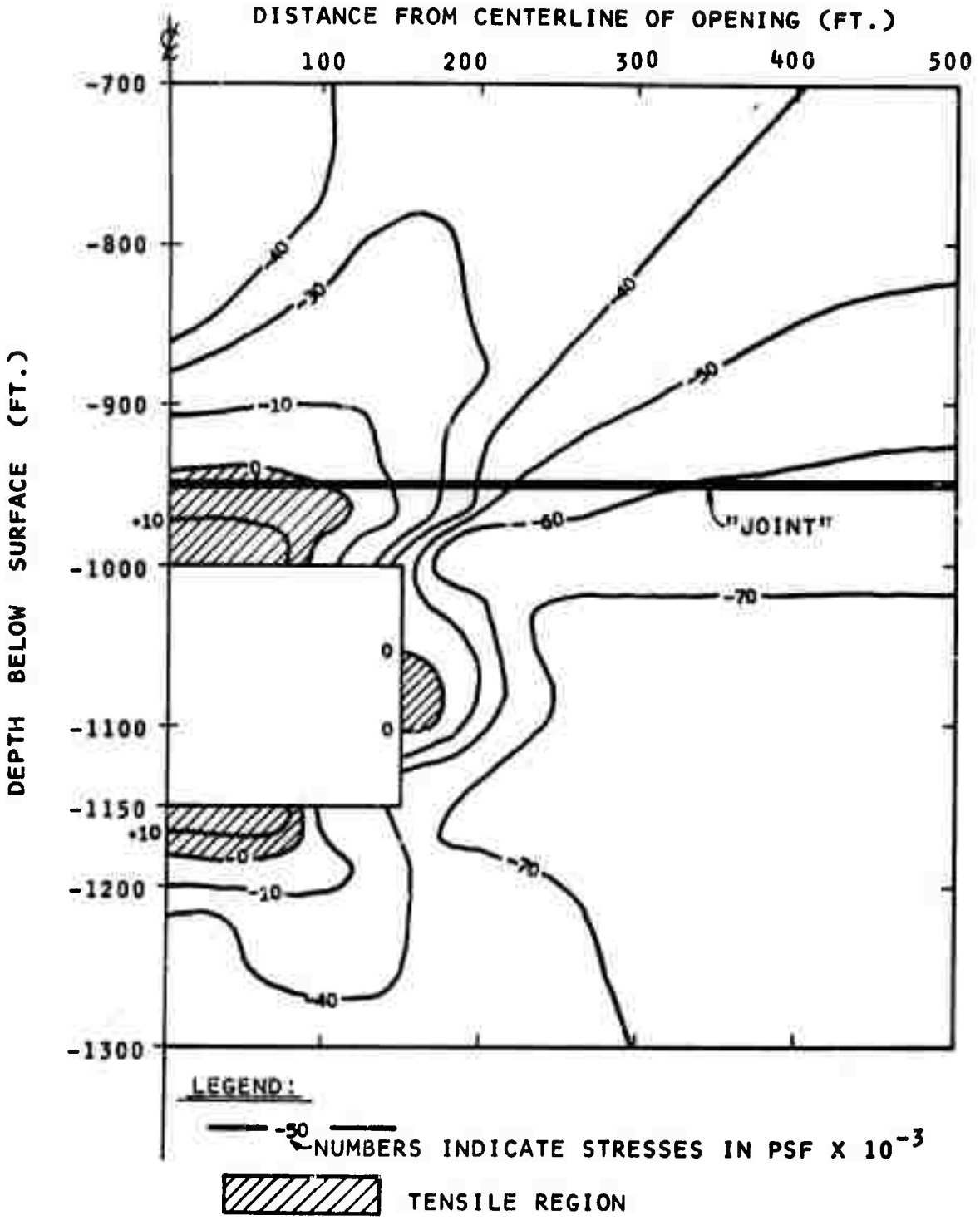

FIG. 21 - DISTRIBUTION OF MAJOR PRINCIPAL STRESS AROUND A RECTANGULAR OPENING (ELASTIC CASE)

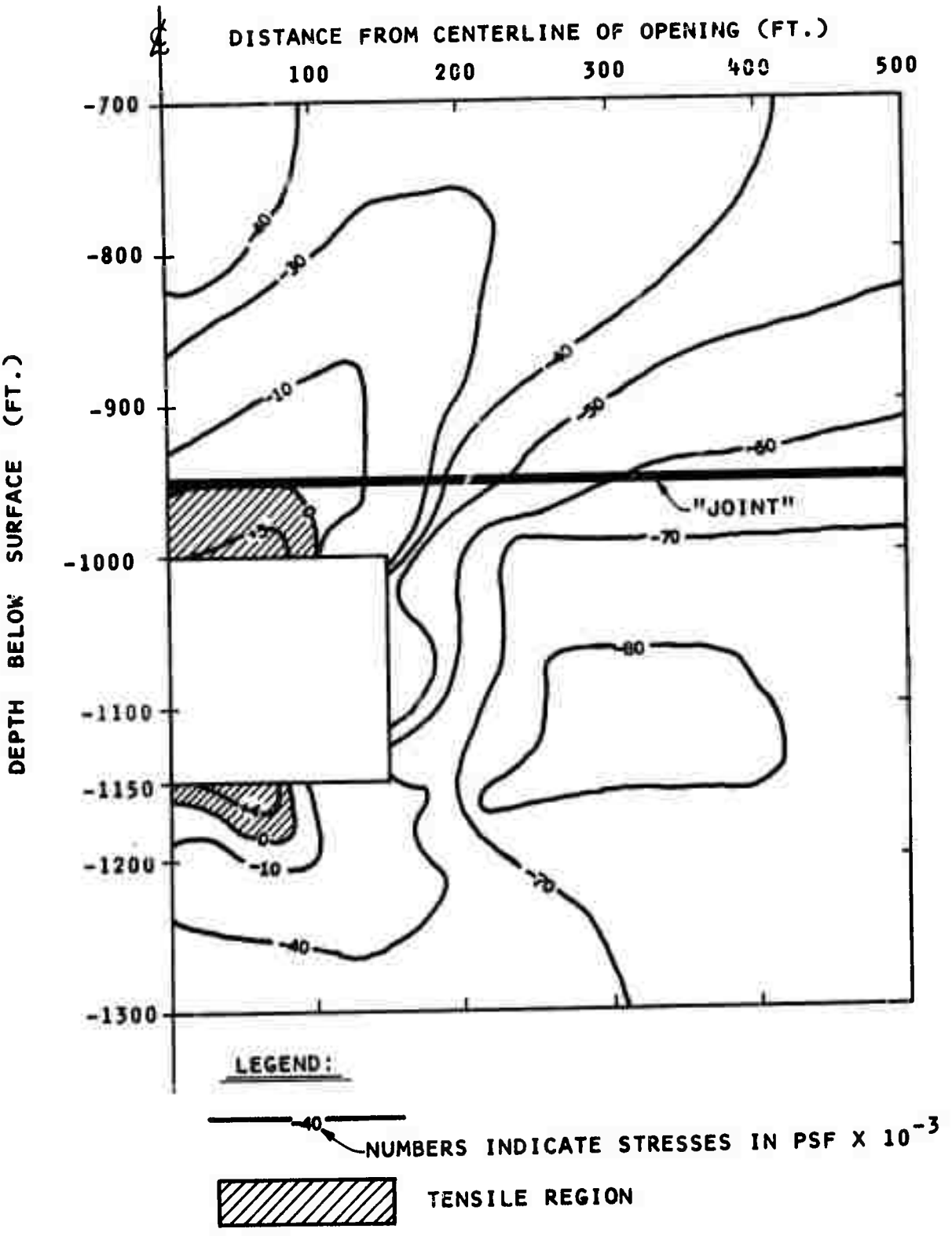

FIG. 22 - DISTRIBUTION OF MAJOR PRINCIPAL STRESS AROUND A RECTANGULAR OPENING (COMBINED FINITE ELEMENT SOLUTION)

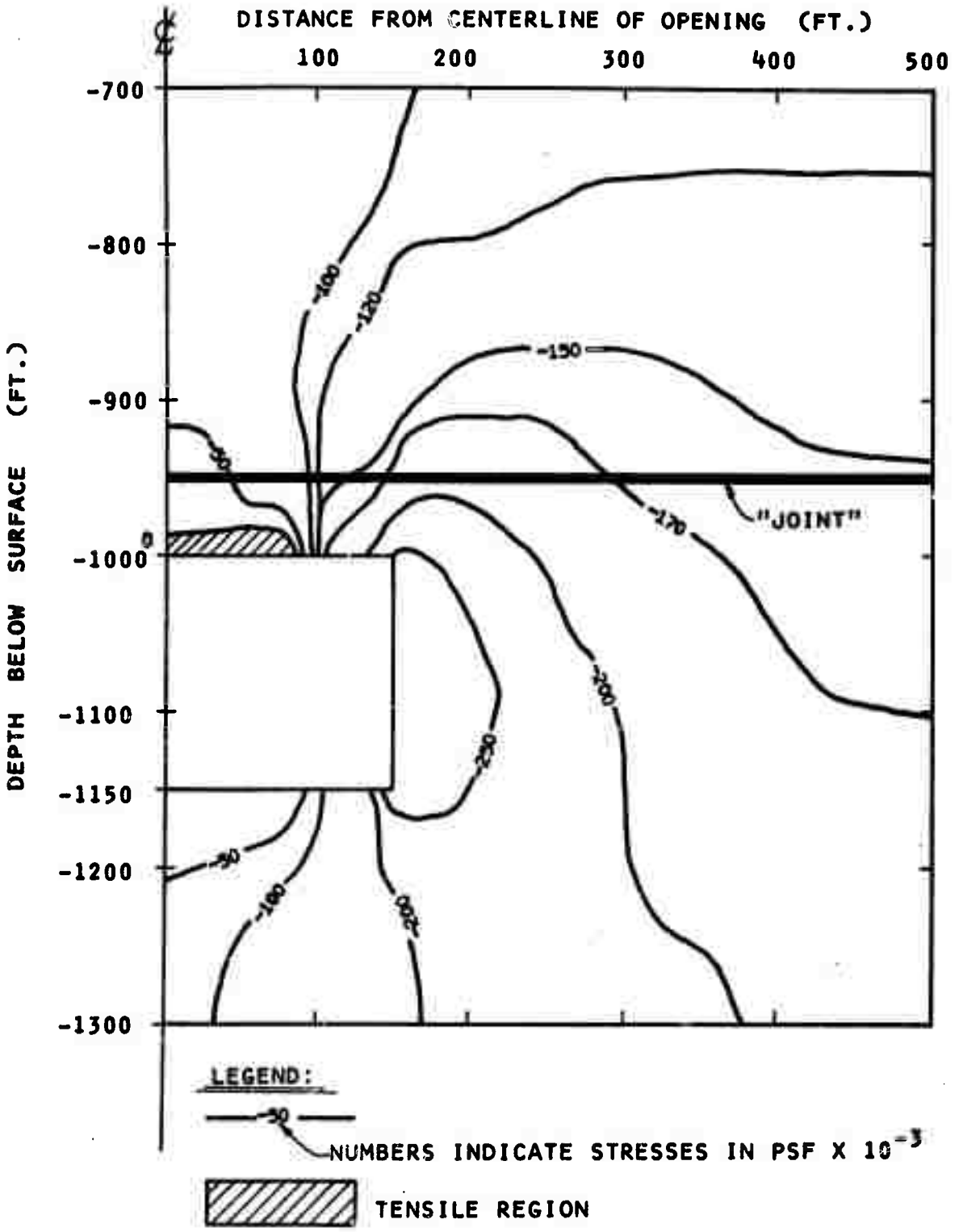

FIG. 23 - DISTRIBUTION OF MINOR PRINCIPAL STRESS AROUND A RECTANGULAR OPENING (ELASTIC CASE)

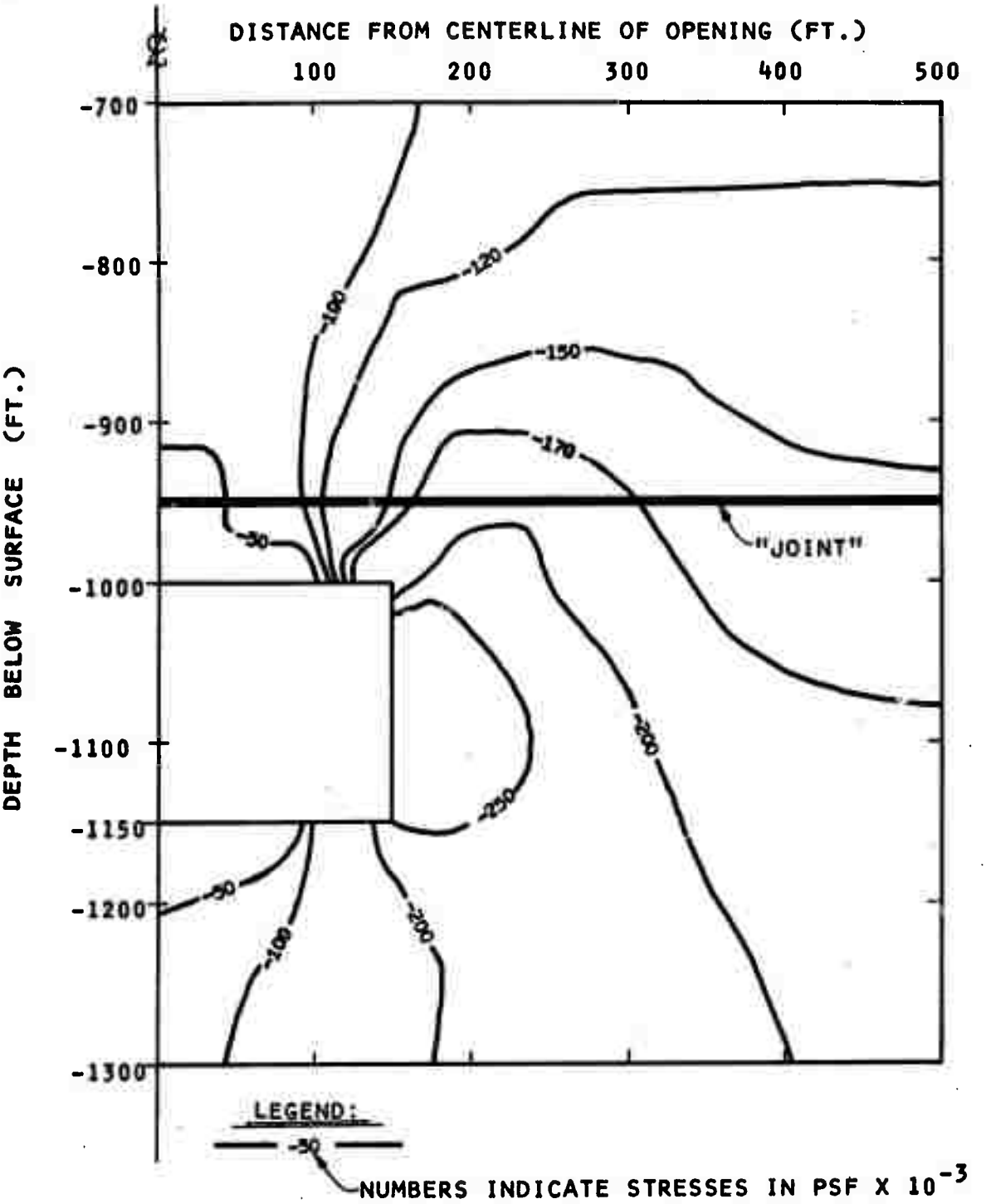

FIG. 24 - DISTRIBUTION OF MINOR PRINCIPAL STRESS AROUND A RECTANGULAR OPENING (COMBINED FINITE ELEMENT SOLUTION)

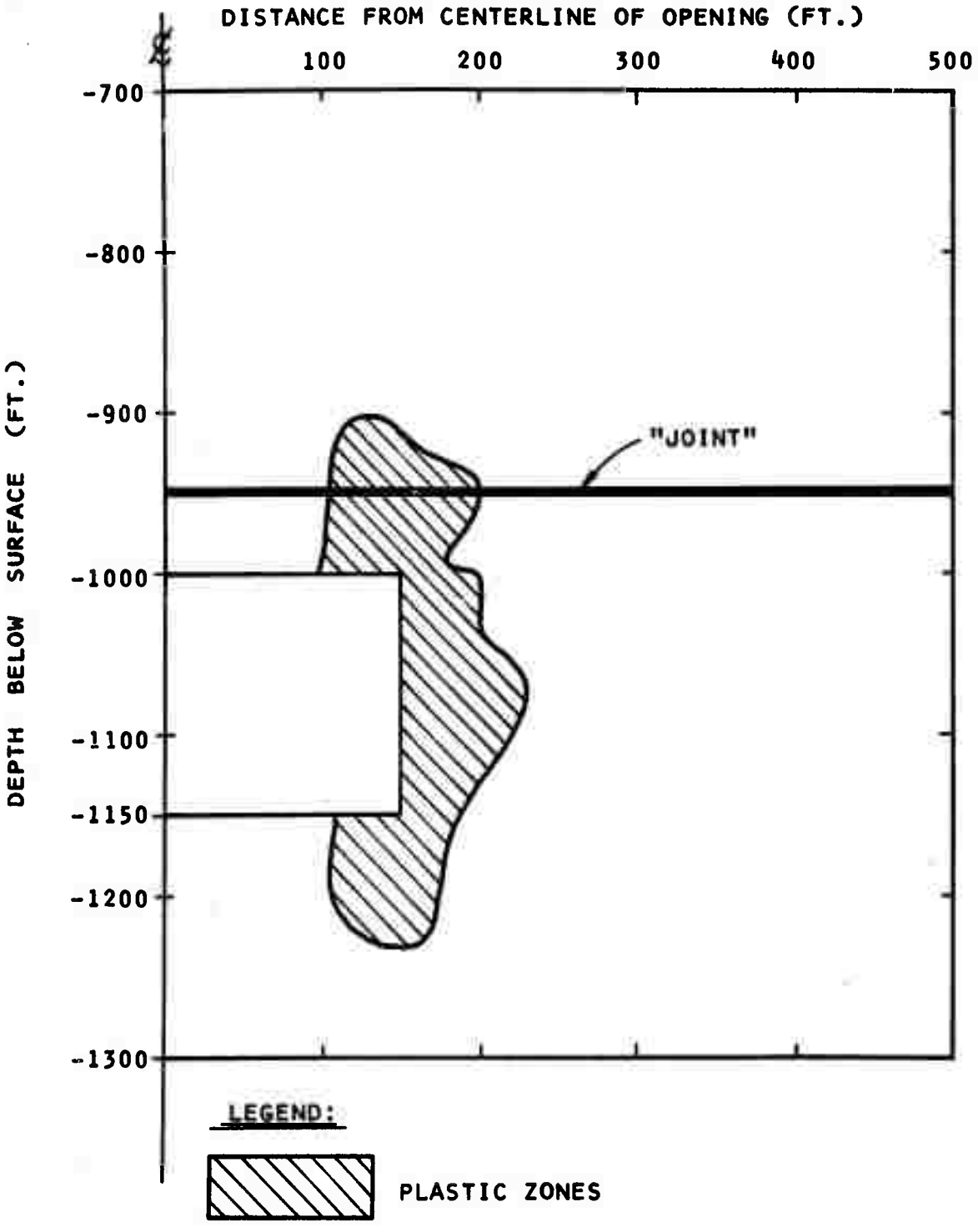

FIG. 25 - DEVELOPMENT OF PLASTIC ZONES AROUND A RECTANGULAR OPENING (COMBINED FINITE ELEMENT SOLUTION)

ANALYSES OF LABORATORY MODELS AND CASE HISTORIES (Phase 2)

The Phase 2 work consists of the analyses of a laboratory model study and a case history study using the combined computer program developed in Phase 1. The results of these analyses were compared with observed performance. Selection of case histories and laboratory models was made on the basis of availability of adequate information on material properties, geological conditions and performance to satisfactorily model the problem.

The possibility of utilizing the results of tests on well-instrumented laboratory models of unlined openings in rock-like materials e.g., Heuer and Hendron (1971), Haas and Clark (1970), and Rosenblad (1971) for evaluating the ability of the program developed in Phase 1 to predict performance was also studied. The geologic conditions and performance of the Morrow Point Underground Powerplant and Straight Creek Tunnel Pilot Bore were studied to determine their suitability for analysis.

Preliminary studies indicated that the Morrow Point Underground Powerplant and model tests reported by Heuer and Hendron (1971) were suitable for evaluating the ability of the computational techniques developed in Phase 1 to predict stresses, strains, and deformations in a rock mass surrounding an excavation.

Analysis of Laboratory Model

Description of Model Study

Heuer and Hendron (1971) conducted a series of model tests on unlined openings in a rock-like material. The geometry of the

model block tested is shown in Fig. 26. The model was constructed to represent a segment of a long tunnel. The test was conducted under plane strain conditions which were achieved by adjusting the axial stress in the longitudinal direction during the test to null any longitudinal displacement. The model block consisted of two halves assembled as shown in Fig. 26. The behavior of the model was monitored by internal foil strain gage rosettes installed on the block interface at various radii. Circumferential strain gages were also installed on the tunnel wall. Two sets of diametrical extensometers were also used to measure the closure of the opening. The loads applied to the model consisted of horizontal and vertical stresses applied at the boundary as shown in Fig. 26. Tests were conducted under three ratios of horizontal to vertical stress, (σ_h/σ_v), 1.0, .75 and .25. Only the tests with σ_h/σ_v = .25 are analyzed in this study.

The material used for construction of the model blocks was a water/plaster/sand mixture in the ratio of 1.2/1/9. The sand was a fine Sangamon sand. A summary of the test results obtained from triaxial tests on the material is presented in Figs. 27 to 29. From Fig. 27, the material constants used in Equation (5) for the yield function were calculated to be α = 0.262 and k = 189 psi respectively. The tensile strength of the material was determined to be 35 psi as compared with the unconfined compressive strength of 600 psi. Fig. 28 indicates the nonlinear nature of the axial stress-strain curves at different confining pressures. The stress-strain curves show that the linear approximation is valid only up

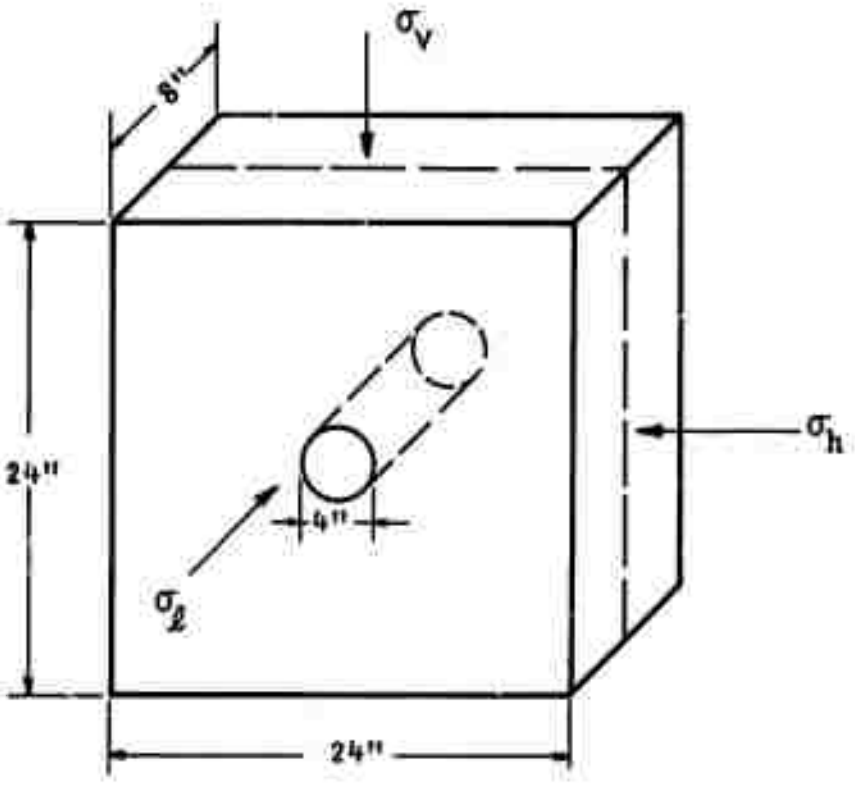

FIG. 26 - GEOMETRY OF MODEL BLOCK
(AFTER HEUER AND HENDRON, 1971)

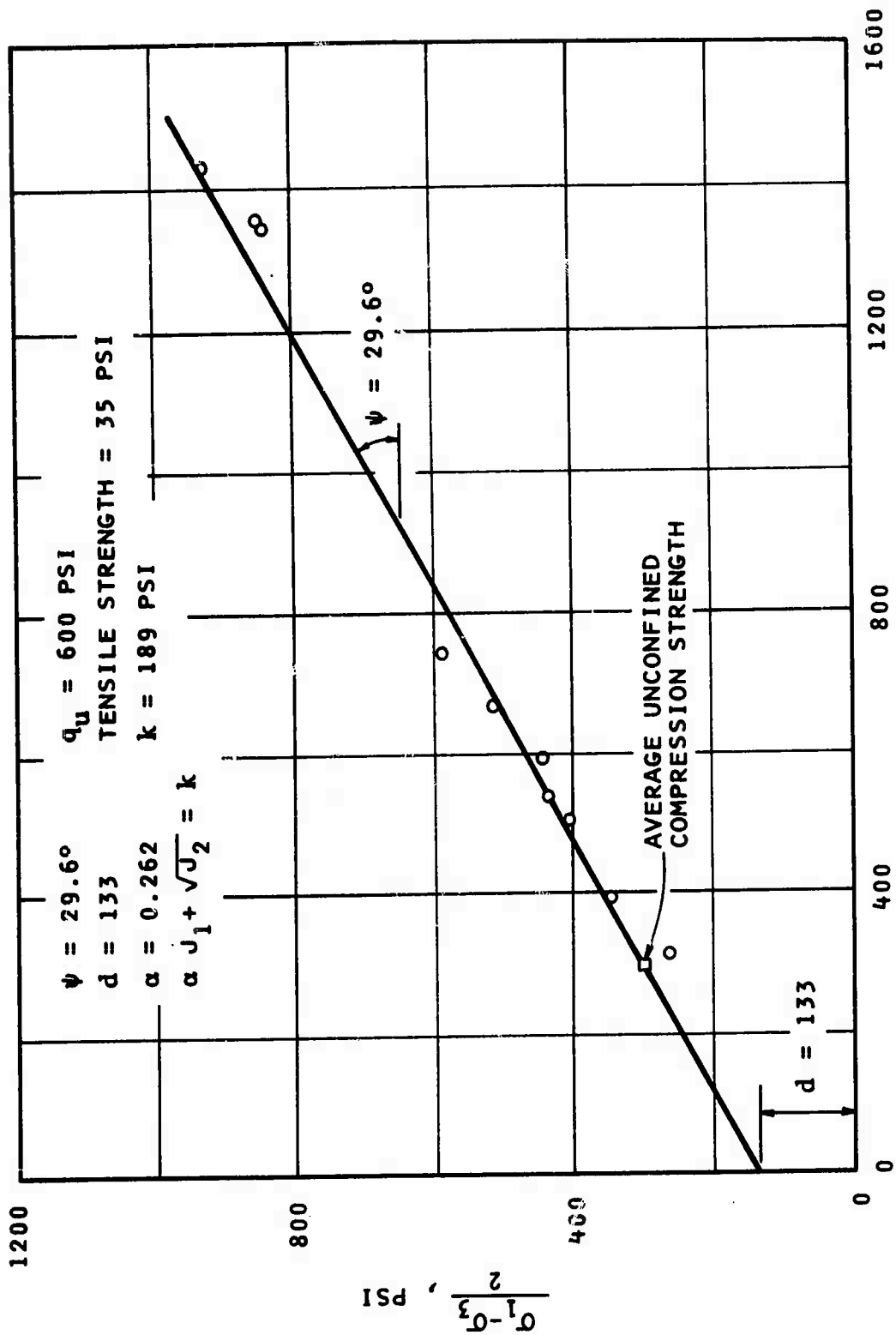

FIG. 27 - SUMMARY OF TRIAXIAL COMPRESSION TEST ON ROCK-LIKE MATERIAL (AFTER HEUER AND HENDRON, 1971)

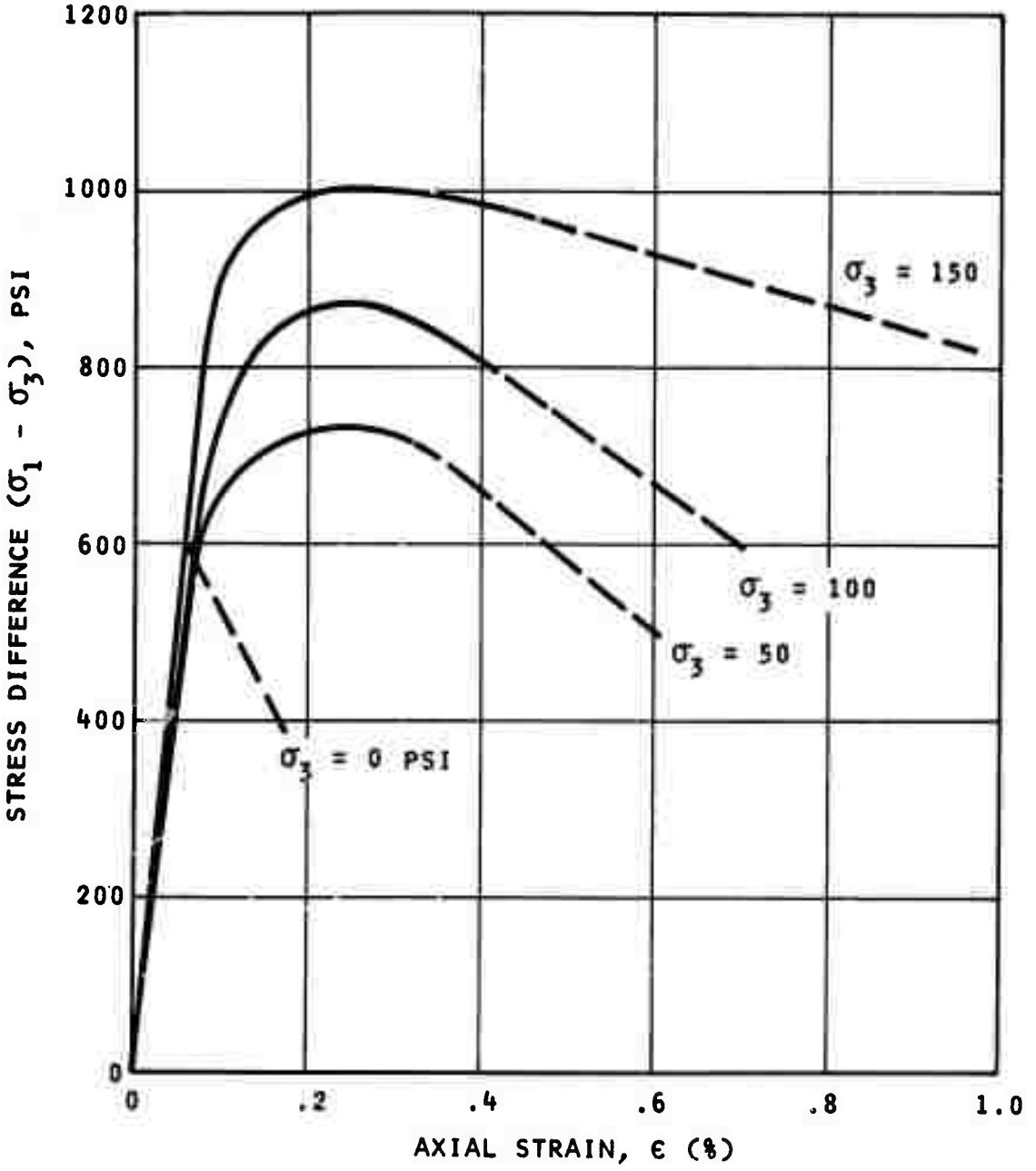

FIG. 28 - AVERAGE STRESS-STRAIN CURVES AT DIFFERENT CONFINING PRESSURES - TRIAXIAL COMPRESSION SPECIMENS (AFTER HEUER AND HENDRON, 1971)

to the principal stress difference ($\sigma_1 - \sigma_3$) of 600 to 800 psi depending on the confining pressure. Fig. 29 shows the variation of the Poisson's ratio with the principal stress difference. It may be noted that the Poisson's ratio increases with an increase in the principal stress difference, the increase depending on the confining pressure. This behavior indicates that the material dilates during shearing. The value of the Poisson's ratio as measured from the test varied from 0.14 to 0.67. Values above 0.5 indicate that the material is not an ideal linear isotropic elastic material.

Behavior of the Model

The behavior of the model during loading for the case analyzed (σ_h/σ_v = 1/4) is described in a later section in which the computed and observed behavior is compared. Only the development of fractures is discussed here. Fig. 30 shows the pattern of fractures developed at σ_v = 800 psi. During testing, the fractured wedges at the springlines shown in Fig. 30 became visible when the applied load was incremented from σ_v = 690 psi to σ_v = 765 psi. As the stress level was increased, more fractures formed and the wedges moved into the opening. Another significant set of fractures is seen in Fig. 30 extending away from the opening back into the model. These fractures appear to be extensions of the fractures which formed the wedges at the springline. At the crown and invert, high tensile circumferential strains were measured at applied stress levels above σ_v = 400 psi. Heuer and Hendron (1971) hypothesized that tension cracks might have formed

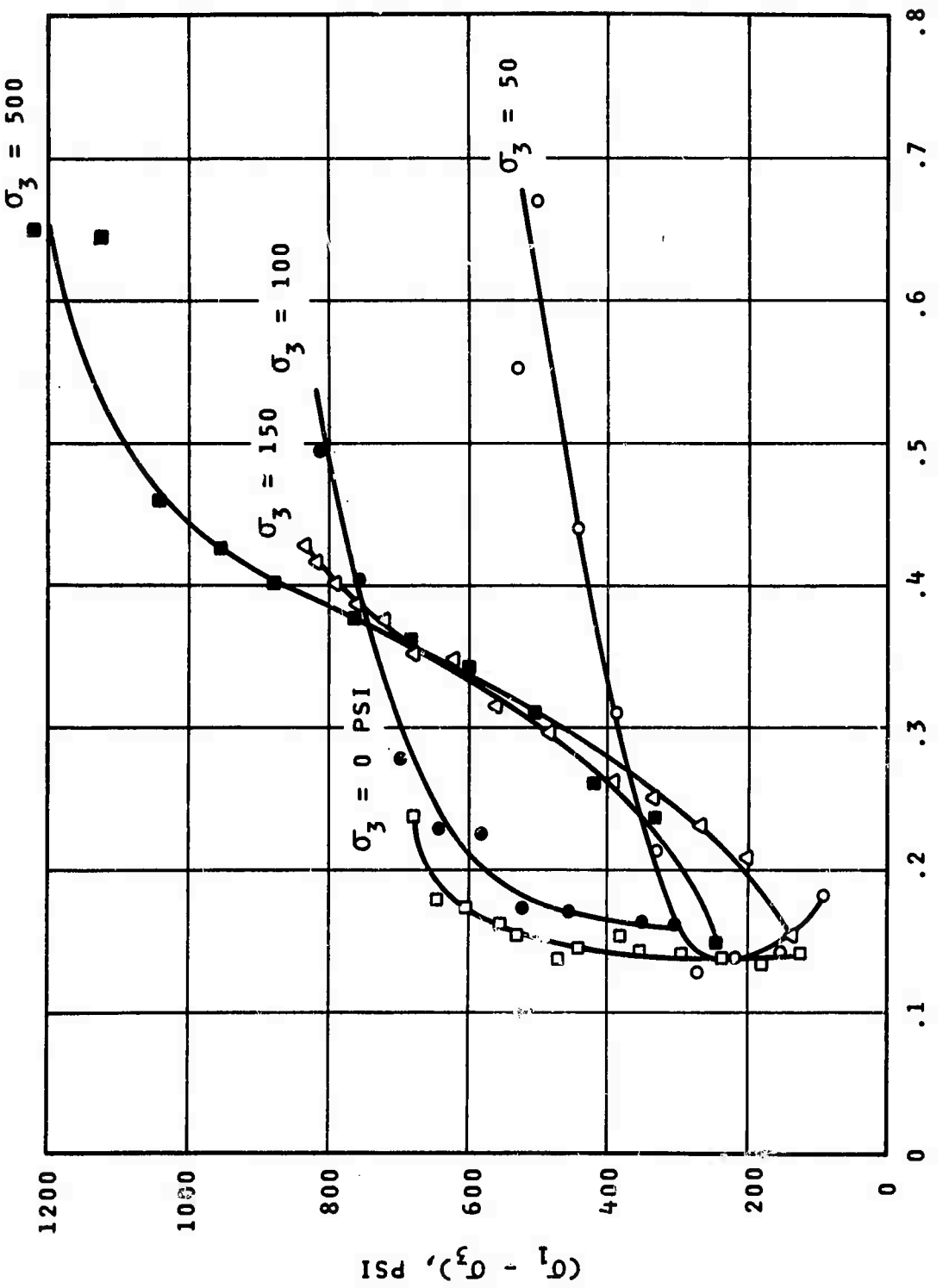

FIG. 29 - VARIATION OF POISSON'S RATIO WITH PRINCIPAL STRESS DIFFERENCE, TRIAXIAL COMPRESSION TESTS (AFTER HEUER AND HENDRON, 1971)

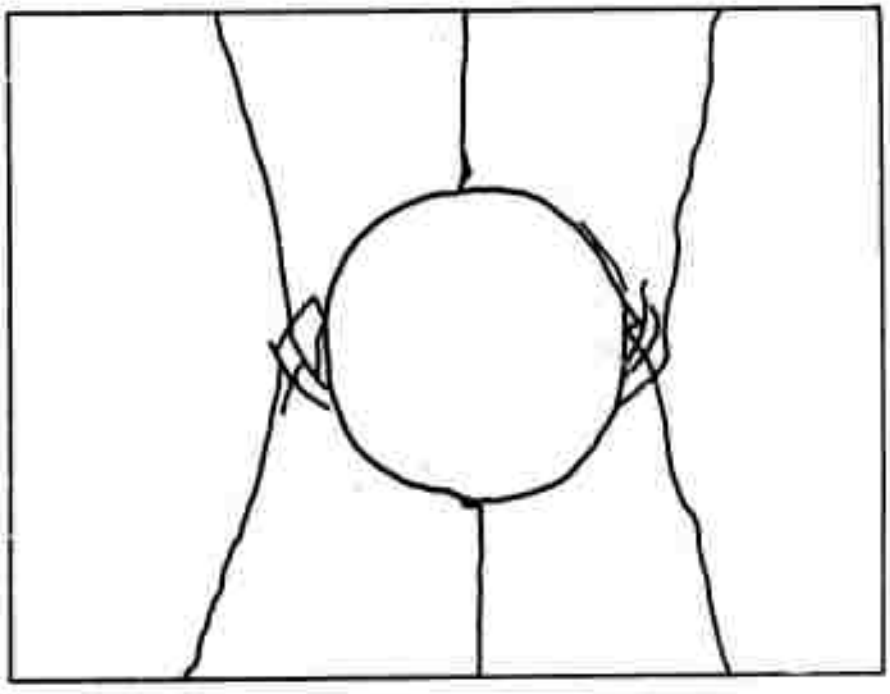

FIG. 30 - FRACTURES DEVELOPED IN MODEL TEST (σ_h/σ_v = 1/4) (AFTER HEUER AND HENDRON, 1971)

during testing. However, no cracks were visible after testing. It was assumed that the cracks were open during the test and then closed upon removal of load.

Analysis of Model Study

Idealization of the Model - Because of the symmetry of the model with respect to its axes, as shown in Fig. 26, it is only necessary to analyze a quadrant of the cross-section. Fig. 31 shows the finite element idealization of the model.

Material Properties Used in the Analysis - As described previously, the material tested shows some nonlinear stress-strain behavior with respect to the elastic modulus and the Poisson's ratio. For the purpose of analysis, it was necessary to use a single value of the modulus and the Poisson's ratio. The value of the modulus was determined from Fig. 36 to be 833,000 psi. The Poisson's ratio of 0.14 was used in the analysis.

The incremental analysis was performed to simulate the actual loading path (σ_h/σ_v = 1/4). The incremental loads applied are shown in Fig. 31. Two cases were analyzed under the assumption that the material behaved as an elasto-plastic material and had a limited tensile strength of 35 psi. The first case (Case 1) assumed that there was no fractured wedge formed during testing. The second case (Case 2) assumed that a fractured wedge formed at the springline during testing and separated from the main body of the model. The details of these cases are described in the following sections.

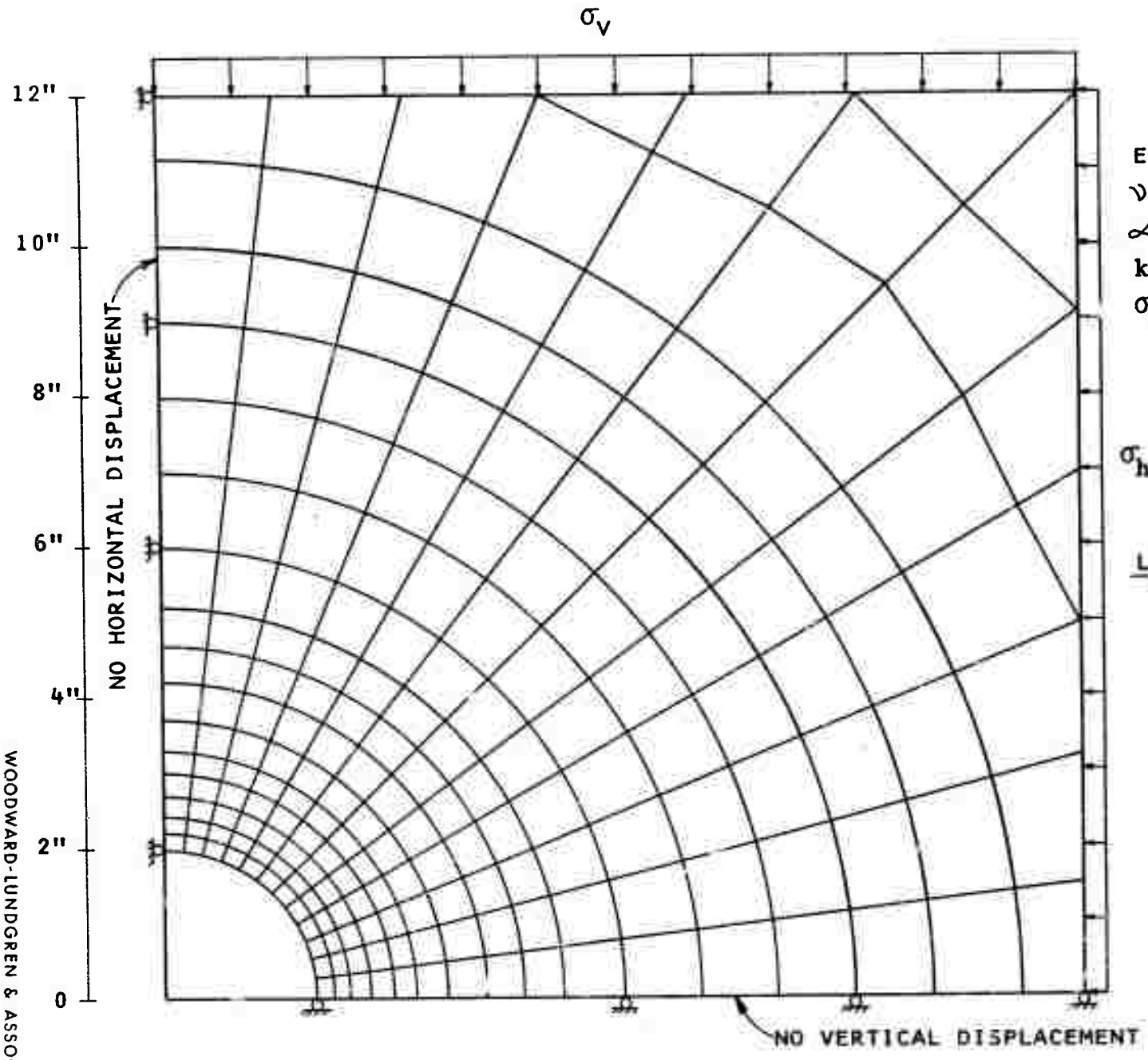

E = 833,000 PSI

ν = 0.14

α = 0.262

k = 189 PSI

σ_h/σ_v = 1/4

LOAD INCREMENT NO.	$\Delta\sigma_v$ PSI	$\Delta\sigma_h$ PSI
1	200	50
2	100	25
3	100	25
4	100	25
5	100	25
6	100	25
8	100	25

FIG. 31 FINITE ELEMENT IDEALIZATION OF MODEL BLOCK

WOODWARD-LUNDGREN & ASSOCIATES

Presentation and Discussion of Results

The results of analysis together with some of the measured behavior are shown in Figs. 32 to 38. Figs. 32 and 33 illustrate the development of plastic and tensile regions at three levels of the axial stress 400, 600, and 800 psi. The observed fractures are also shown in Figs. 32 and 33. On comparing Figs. 30 and 32, it may be noted that the development of the plastic region in Fig. 32 is similar to the shear-fractured wedges developed at the springline as shown in Fig. 30. At σ_v = 800 psi, a large plastic region developed back into the model, Fig. 32. The location of the actual shear fracture, also shown in Fig. 32, is along the edge of the plastic region. It was observed in the model test that a region of tensile stress developed at the crown and invert. However, there was little failure in this zone indicating that the tensile stresses were below the tensile strength of the material. An elastic analysis indicates that a large tensile region developed with a tensile stress higher than the tensile strength at the crown and invert (Fig. 34). An elasto-plastic analysis indicates that a much smaller zone of tension cracks would develop if the material exhibits elasto-plastic behavior. The results of the elasto-plastic analysis appears to agree with observed behavior.

In order to simulate the propagation of fractures and their effects on the behavior of the model, an analysis was performed (Case 2) after removing the wedge that formed under a vertical stress of 600 psi as indicated by the results of the analysis

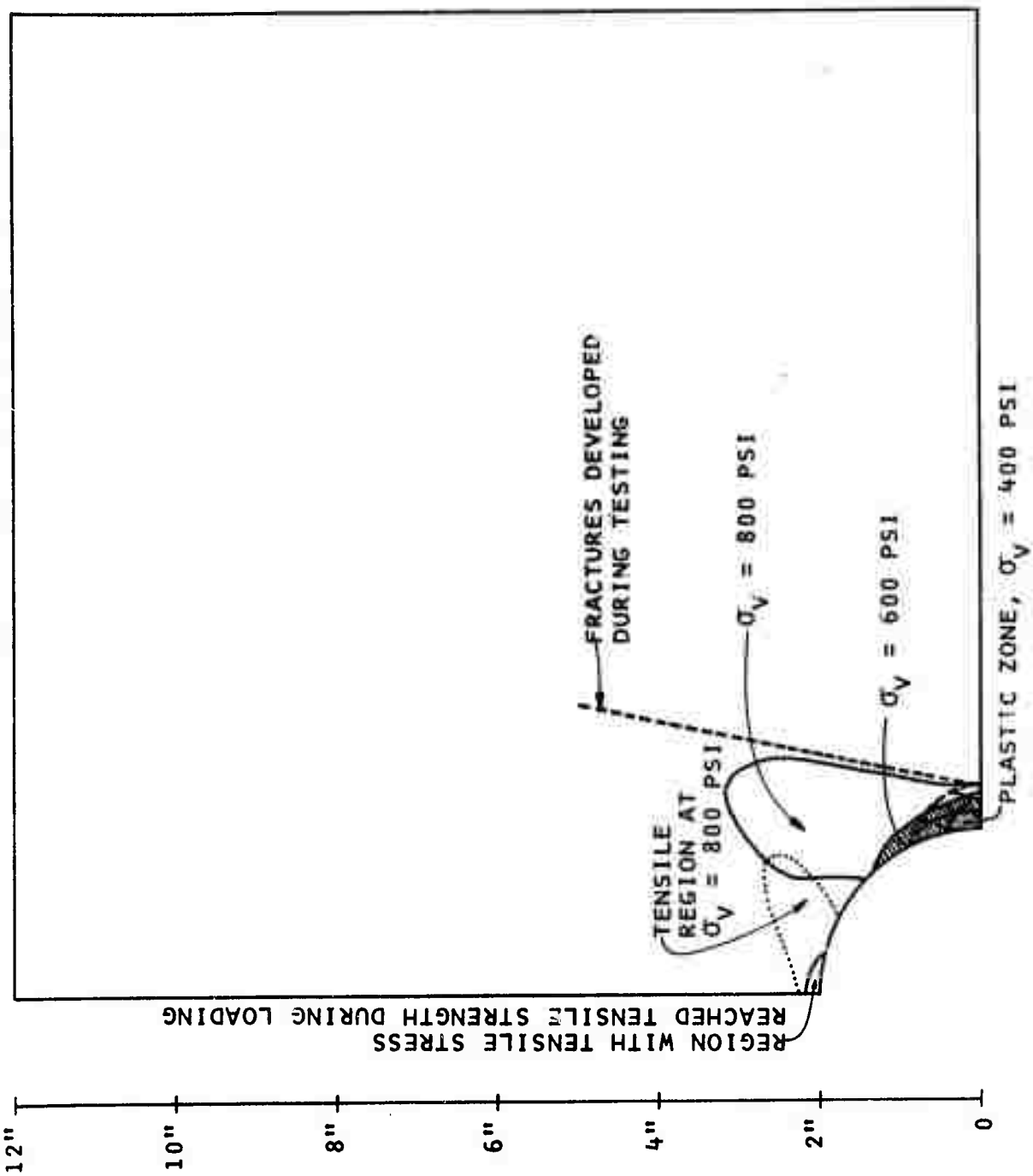

FIG. 32 - RESULTS OF ANALYSIS OF MODEL TESTS, σ_h/σ_v = 1/4, SHOWING DEVELOPMENT OF PLASTIC AND TENSILE REGIONS, CASE 1

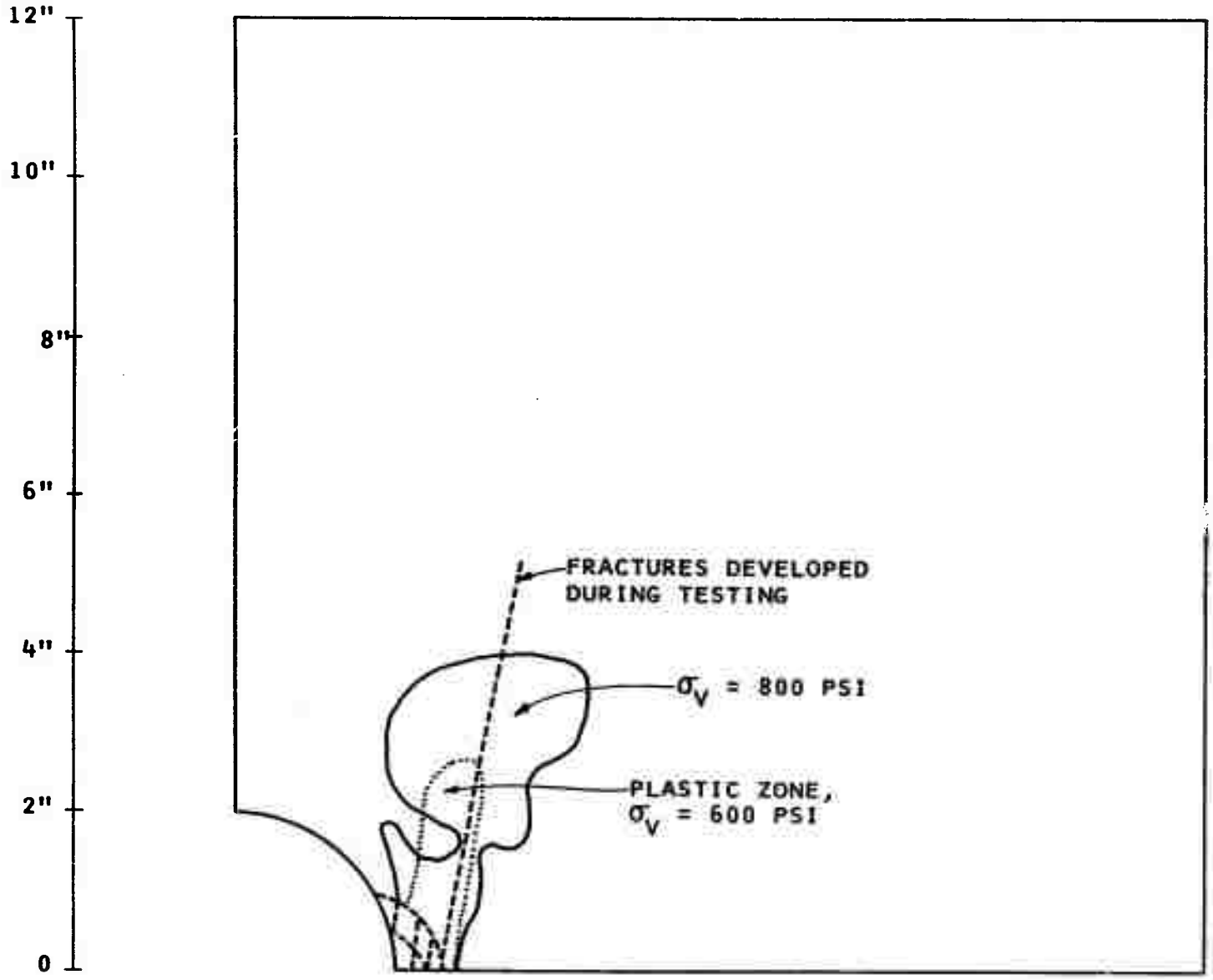

FIG. 33 - RESULTS OF ANALYSIS OF MODEL TEST, σ_h/σ_v = 1/4, SHOWING DEVELOPMENT OF PLASTIC REGIONS, CASE 2

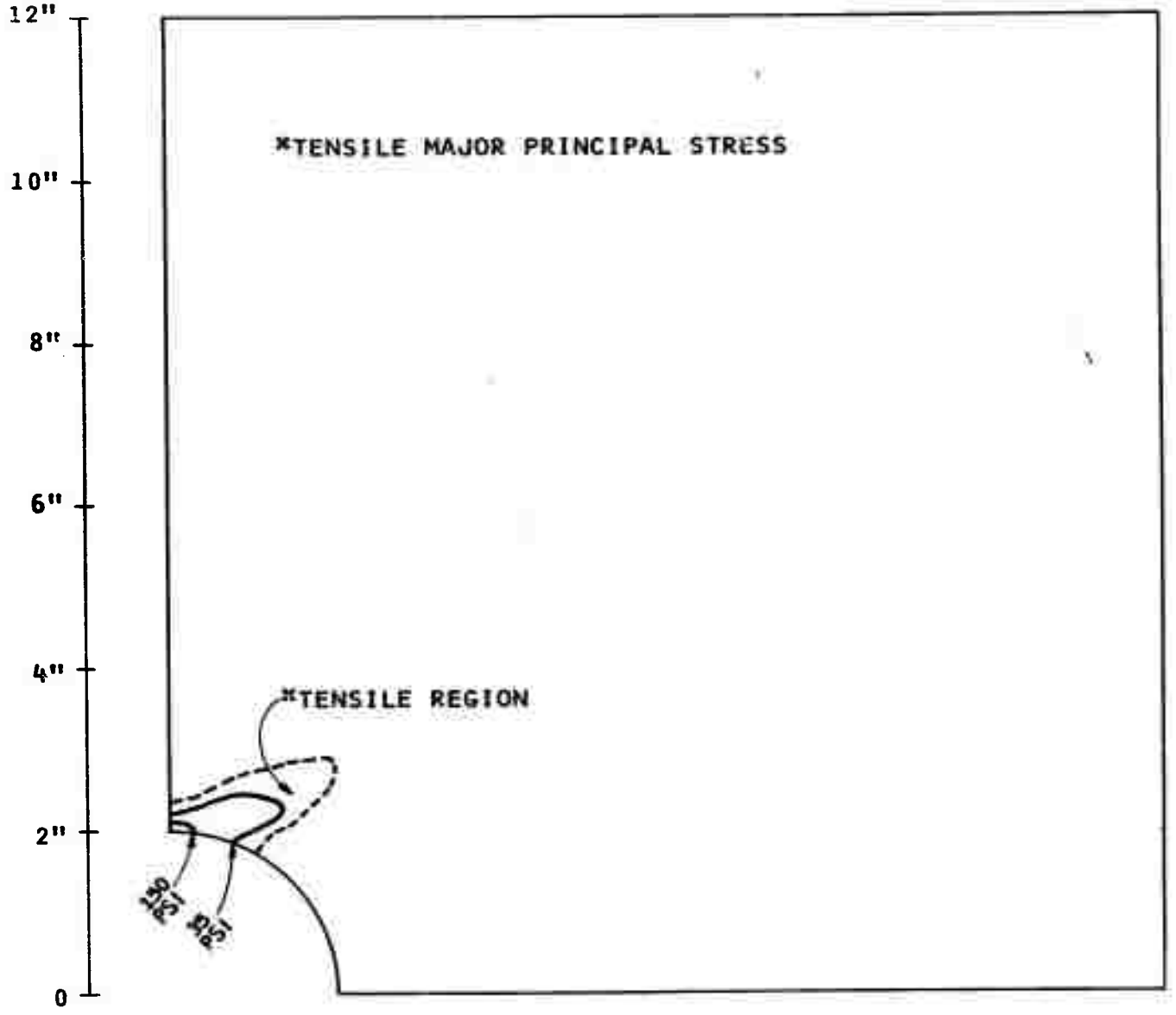

FIG. 34 - ELASTIC ANALYSIS OF MODEL TEST σ_h/σ_v = 1/4, SHOWING TENSILE REGION σ_3 = 800 PSI

WOODWARD-LUNDGREN & ASSOCIATES

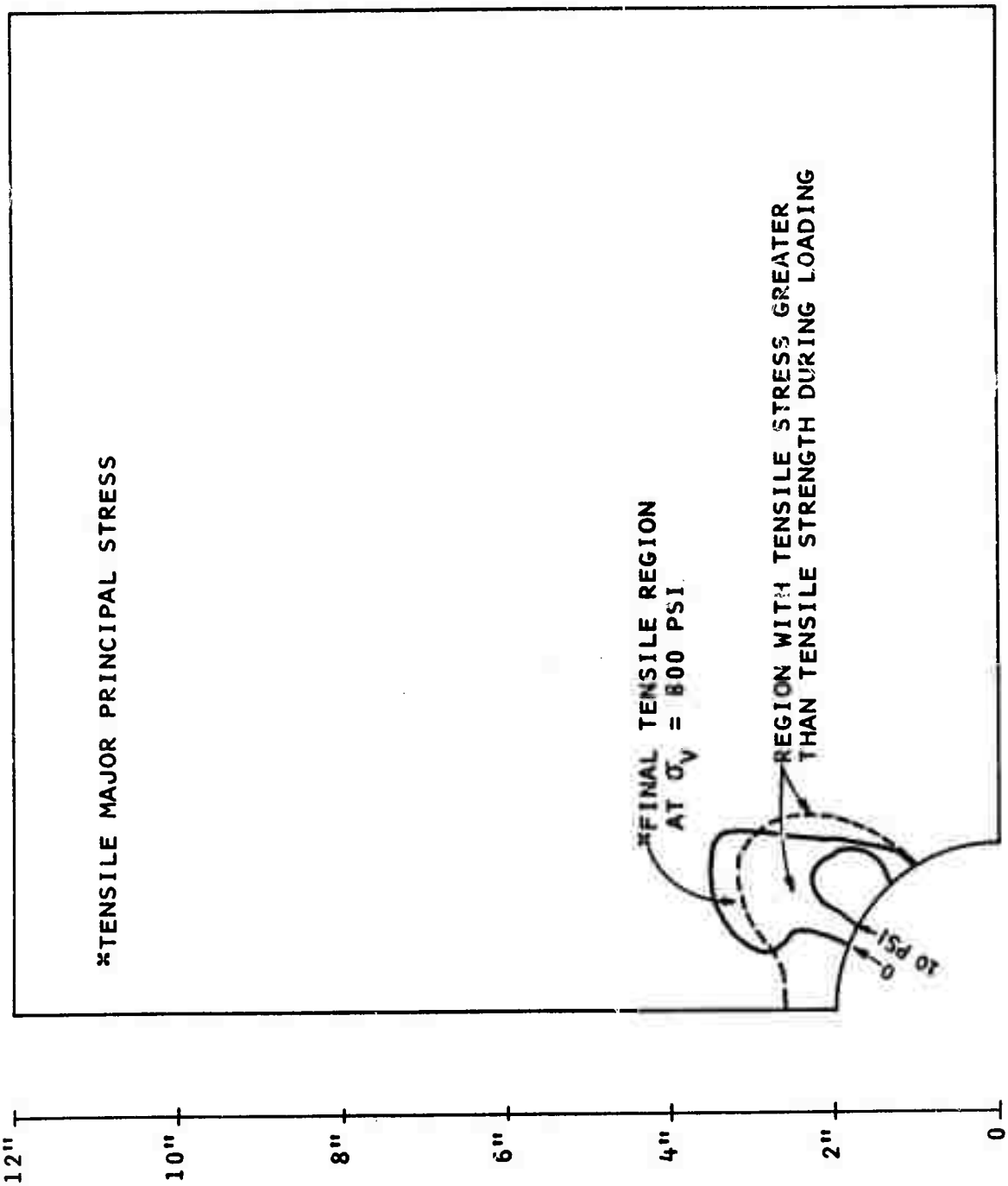

FIG. 35 - RESULTS OF ANALYSIS OF MODEL TESTS, σ_h/σ_v = 1/4
SHOWING TENSILE REGION, CASE 2

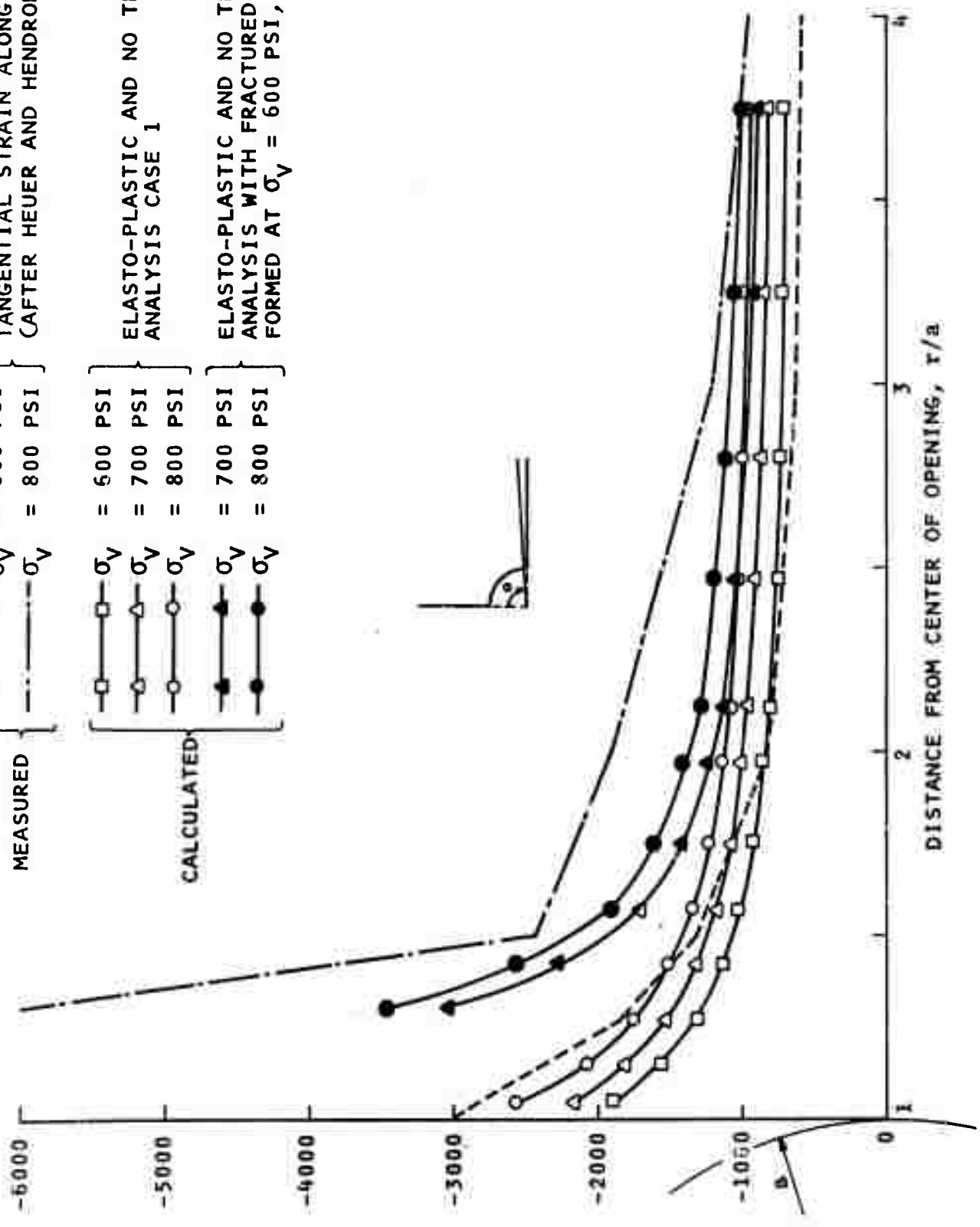

FIG. 36 - DISTRIBUTION OF VERTICAL STRAINS ALONG $\theta = 86.25^{\circ}$, $\sigma_h/\sigma_v = 1/4$, ANALYSIS OF MODEL TESTS

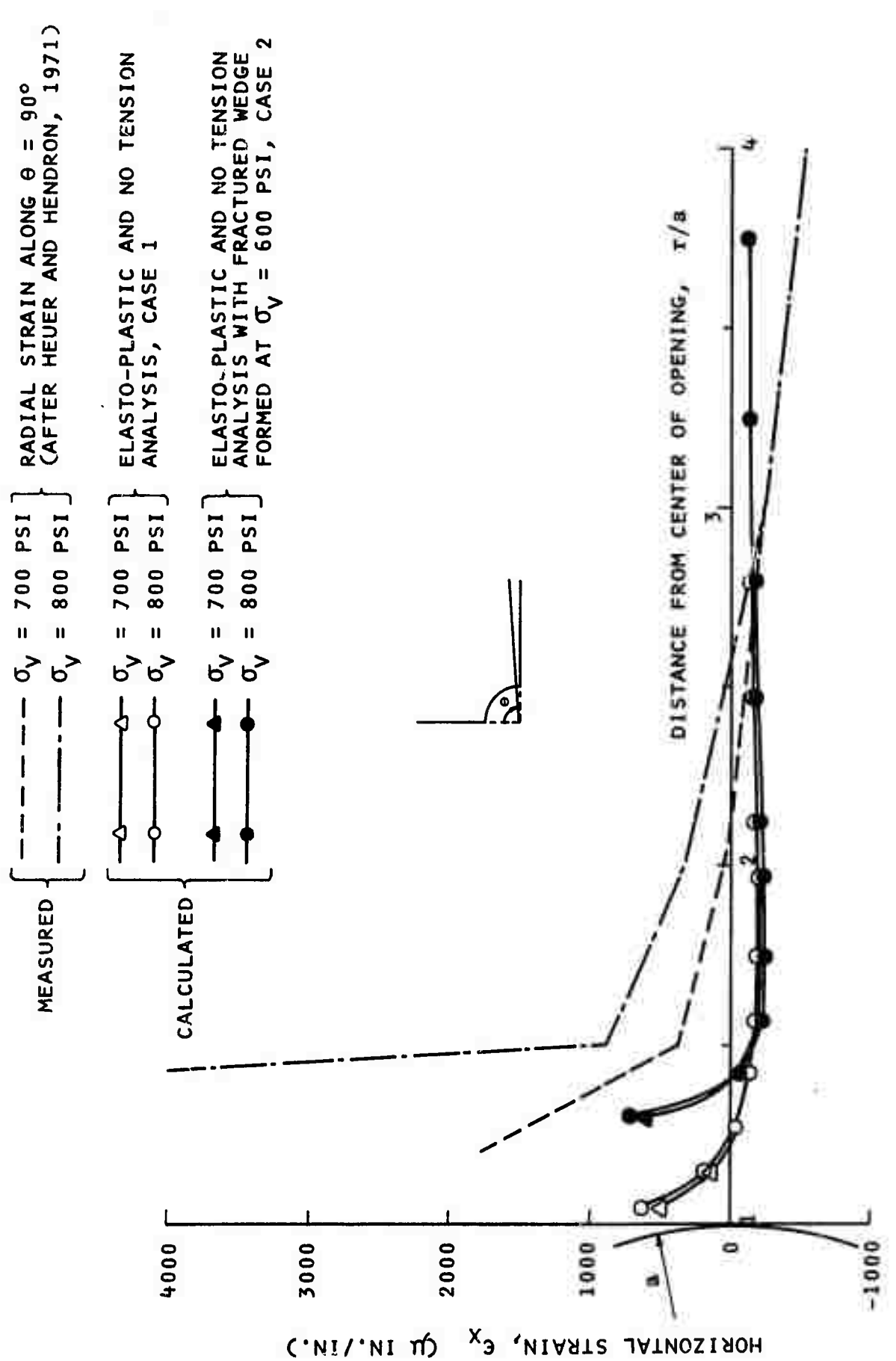

FIG. 37 - DISTRIBUTION OF HORIZONTAL STRAINS ALONG $\theta = 86.25^{\circ}$, $\sigma_h/\sigma_v = 1/4$, ANALYSIS OF MODEL TESTS

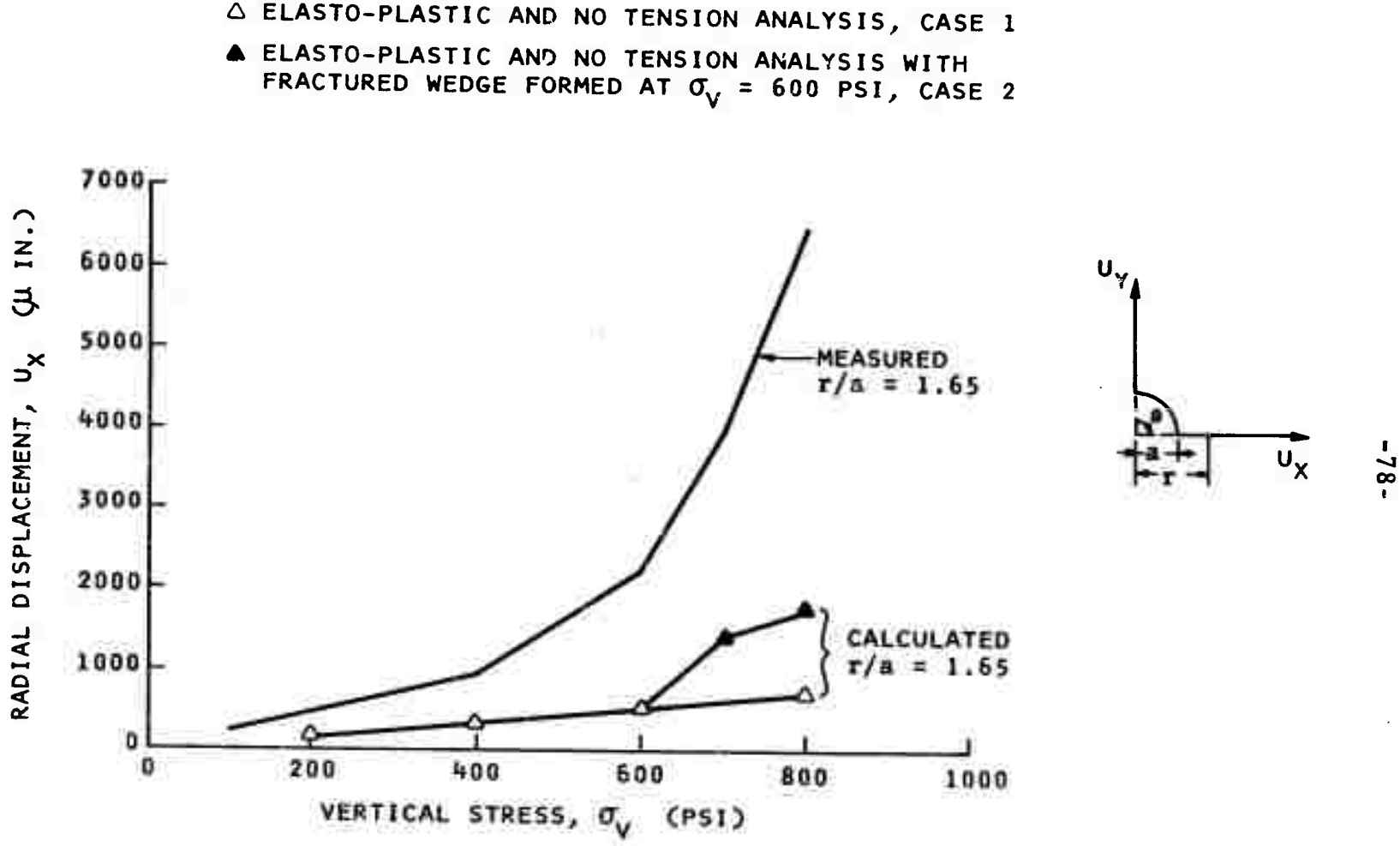

FIG. 38 - VARIATION OF RADIAL DISPLACEMENT WITH APPLIED STRESS, σ_h/σ_v = 1/4, θ = 90°, ANALYSIS OF MODEL TESTS

shown in Fig. 32. Under these conditions, the plastic zone extended behind the wedge and propagated into the model block as shown in Fig. 33. The direction in which the plastic zone developed as the loads increased was similar to the observed propagation of fractures. Fig. 33 shows the extend of the plastic zone as the loads were increased to the vertical stress of 800 psi. It may be noted that the observed shear fracture lies in the middle of the plastic zone indicating that the elastic-analysis can provide a good indication with respect to the development of the critical zone in the vicinity of the opening.

The tensile stress region in the final stress distribution and the zone where the major principal tensile stress was greater than the tensile strength during the entire loading process is shown in Fig. 35. Comparisons of tensile regions and the regions with values of tensile stress greater than tensile strength during loading for Cases 1, 2 and the elastic analysis (Figs. 32, 33 and 34, respectively), indicate the following features: (i) The Case 2 analysis shows that a larger region with a tensile stress greater than the tensile strength (35 psi) developed during loading. (ii) The "no tension" analysis indicates that upon subsequent loading the tensile region near the crown and invert was recompressed. (iii) The tensile region was shifted from the crown and invert to the region closer to the fractures at the springline indicating that the development of fractures at the springline caused a redistribution of stresses in the rock surrounding the opening.

In order to compare with the strains measured in the model tests, element strains were computed from the nodal point displacements. These strains were assumed to occur at the centroid of the element. The computed vertical and horizontal strains along the line ($\theta = 86.25^{o}$) close to the horizontal axis ($\theta = 90^{o}$) for Cases 1 and 2 are shown in Figs. 36 and 37, respectively, for the stress levels between σ_v = 600 psi and σ_v = 800 psi. For the purpose of comparison, the measured tangential and radial strains along the horizontal axis are also plotted in Figs. 36 and 37. Because of the relatively large scatter in the measurements obtained from the electrical strain gages, Heuer and Hendron (1971) concluded that the strain measurements would only give a qualitative indication of the response of the model. Comparison of the measured and calculated behavior shows that at the low stress levels, they are in good agreement, Figs. 36 and 37. However, as the stress level increased and the fractured wedges formed, the strains increased to a level much greater than that predicted from the Case 1 analysis in which the model block was assumed to act as continuum. The results of the Case 2 analysis indicated a strain pattern and magnitude in approximate agreement with measured values. This indicates that the formation of fractured wedges at the springline has a great effect on the behavior of the model block. Discrepancies between the measured strains and the strains computed by Case 2 analysis at the higher stress levels may in large part be attributed to the formation of the second set of fractures extending back into the model block away from the opening.

Fig. 38 shows the measured and computed radial displacements at a point on the horizontal axis ($\theta = 90^{o}$, $r/a = 1.65$). Both the measured and computed radial displacements indicate the point moved outward from the opening as the loads increased. The measured displacements are about three times larger than those computed from the elastic or elasto-plastic analysis from the low stress level up to $\sigma_v = 600$ psi. The large increase in displacements for $\sigma_v \geq 600$ psi may be attributed to the development of the fractured wedges and the fractures back into the model block. The Case 2 analysis showed a similar increase in radial displacement due to the formation of the fractured wedges at the springline. Discrepancies between the measured and calculated displacements at higher stress levels may also be attributed to the formation of the second set of fractures back into the model block.

Analysis of the model tests indicates that the elasto-plastic analysis provides valuable information for evaluating the critical zone in an intact rock surrounding an opening.

After significant fractures develop in the rock surrounding an opening, the rock becomes discontinuous along the fractures and strain displacement distributions within the rock could not be accurately determined by the elasto-plastic analysis. This is due to the inability of the analysis to simulate (1) the propagation of shear fractures in the rock, and (2) the nonlinear stress-strain behavior and dilatancy of the rock-like material during shearing.

Although the analysis cannot simulate accurately the behavior of the model after the formation of shear fractures surrounding the opening, some indication can be obtained with regard to propagation of fractured zones.

Morrow Point Underground Powerplant Excavation

Description

The Morrow Point Underground Powerplant was constructed by the U.S. Bureau of Reclamation on the Gunnison River some 20 miles east of Montrose, Colorado (Dodd, 1967 and Brown, et al. 1971). The powerplant chamber is 206 ft long and 57 ft wide with a height ranging from 65 to 134 ft and is located about 400 ft below the ground surface. The plan of the powerplant and other adjacent structures is shown in Fig. 39. A cross-section of the powerplant chamber along A-A'(line 4 + 12 ft) is shown in Fig. 40. It may be noted, from Figs. 39 and 40, that the powerplant chamber is situated behind a steep valley rock wall. The crown of the chamber on the river side (b line wall, Fig. 40) is about 200 ft behind the ground surface.

The powerplant is located entirely within the Pre-Cambrian metamorphic rocks. The composition of the metamorphic rock consists predominantly of mica schist and quartz-mica schist with some biotite schist and pegmatite. The bedding strikes nearly normal to the powerplant alignment and dips upstream at angles varying from 15° to 60°, averaging about 35°. There are two distinct shear zones intersecting the powerplant area. The lower zone (shear zone A) strikes N 40° W, dips 32° E, and

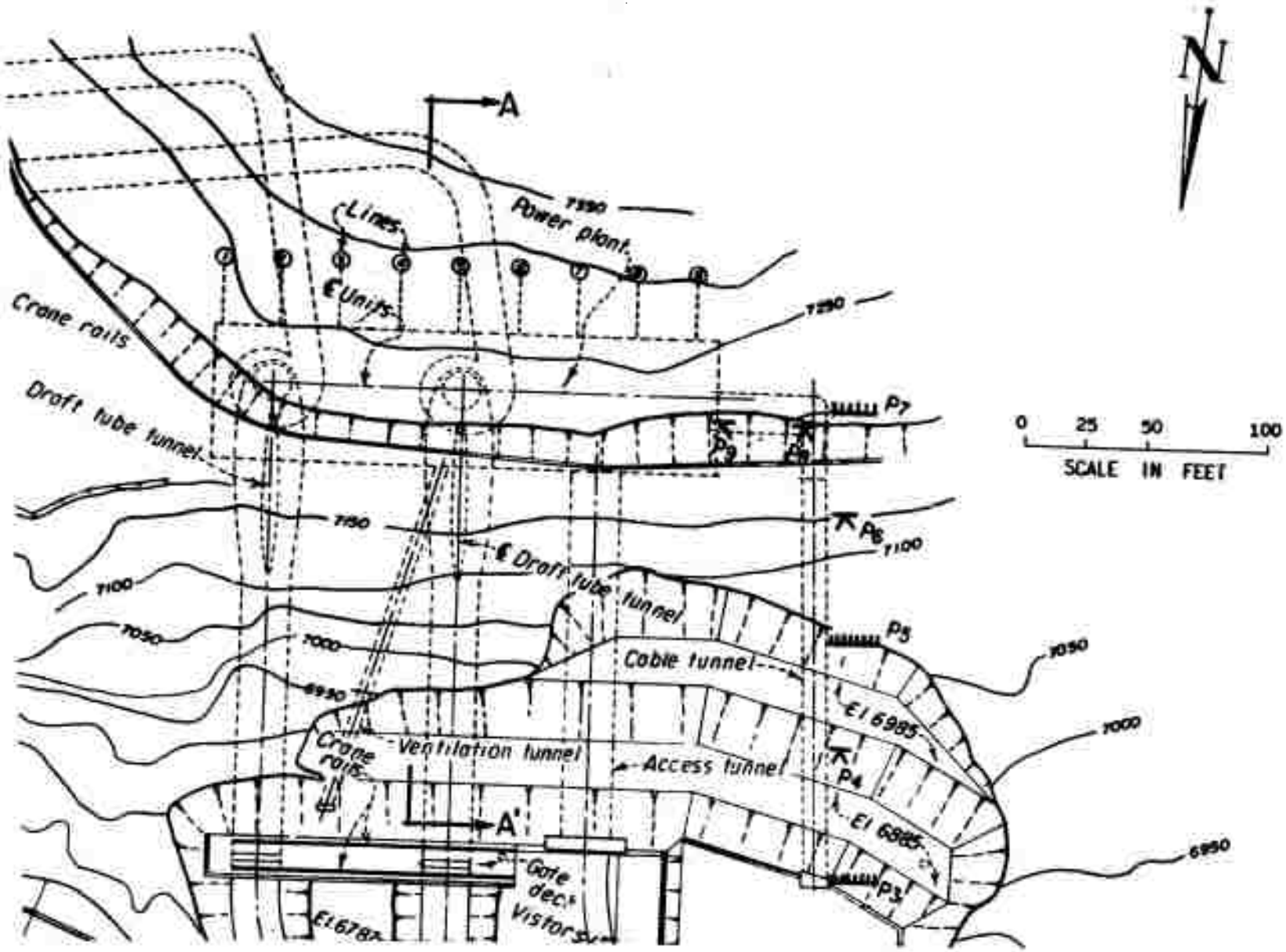

FIG. 39 - PLAN AND LOCATION OF MORROW POINT POWERPLANT (AFTER DODD, 1967)

WOODWARD-LUNDGREN & ASSOCIATES

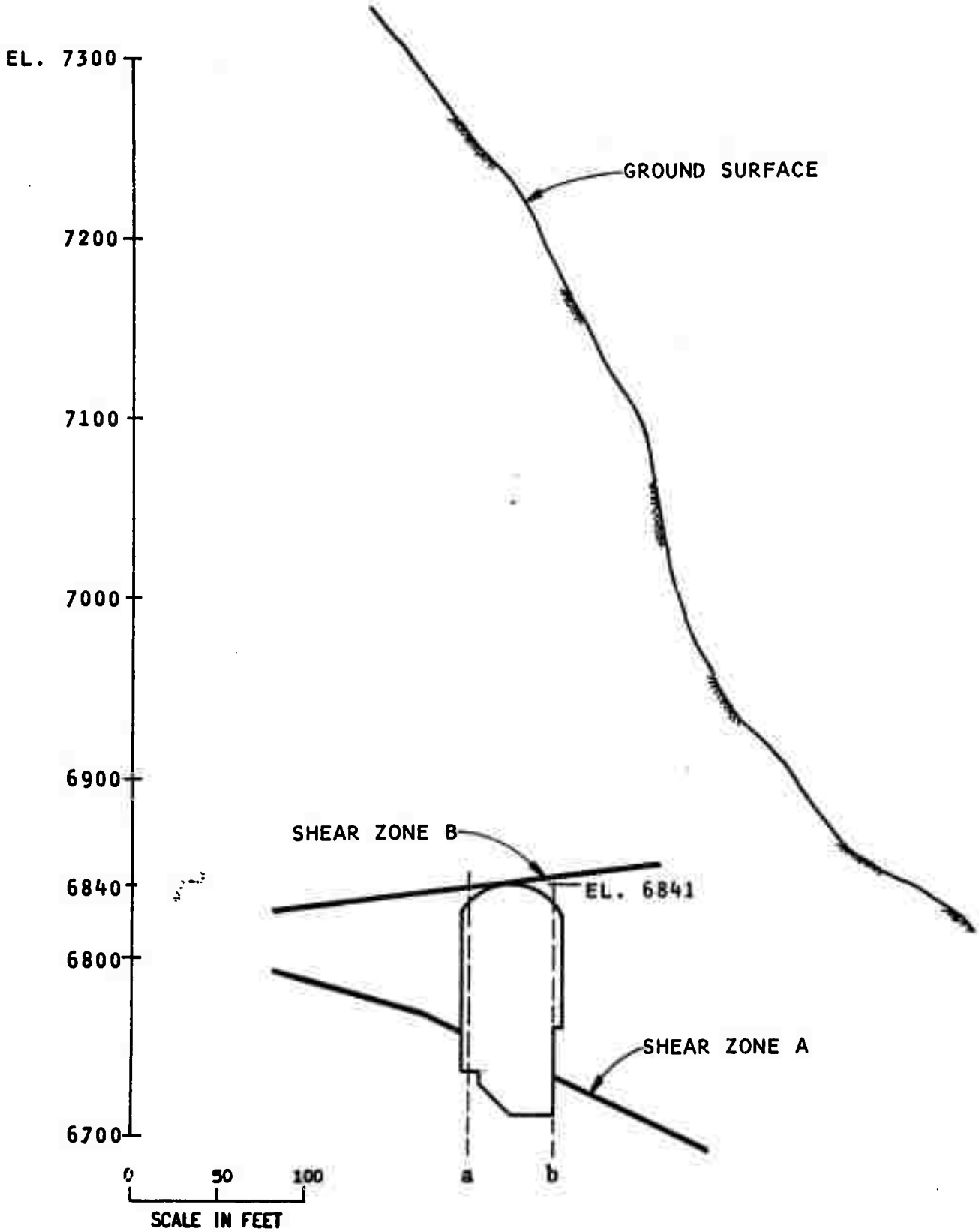

FIG. 40 - CROSS-SECTION A-A' (LINE 4 + 12 FT) OF THE POWERPLANT CHAMBER, MORROW POINT POWERPLANT

consists of a one to five ft zone of fault gouge and fractured rock. The upper zone (shear zone B) has a strike of N 20° E, a dip of 23° E and consists of a one to three ft zone of fault gouge and fractured rock. The orientations of the three major joint sets that intersect the chambers are: strike N 63° W and dip 82° SW; strike N 36° E, and dip 80° W; strike N-S and dip 43° E.

Five basic rock types are present in the chamber. Their percentages as exposed at the rock surface of the chamber are shown below:

Type I	Biotite Schist	15%
Type II	Mica Schist	20%
Type III	Quartz-Mica Schist or Micaceous Quartzite	40%
Type IV	Quartzite	20%
Type V	Pegmatite	5%

Significant Features of the Behavior of the Powerplant Excavation

The crown of the chamber was first excavated during a three month period from May 1965 through July 1965. The excavation of the remaining chamber continued from August 1965 through March 1966. When the excavation reached the El. 6793 bench, 48 ft below the crown, some initial movement of the a-line rock wall occurred. When the powerplant was excavated to El. 6748, 92 ft below the crown, an accelerated inward movement of 1.5 inches was measured at line 4 + 12 ft. As the excavation proceeded, the a-line rock

wall continuously moved inward but at a diminishing rate. Significant rock movement ceased by the end of March 1966 (Brown, Morgan and Dodd, 1971). The maximum observed inward movement of the a-line wall at line 4 + 12 ft was 2.5 inches. Fig. 41 shows the history of the observed rock movements at line 4 + 12 ft reported by Brown, et al. (1971).

Brown et al. (1971) hypothesized that the anomalous rock behavior along the a-line rock wall might involve a mass movement of a rock wedge shown in Figs. 42 and 43. It was hypothesized that shear zones A and B intersect at an average distance of 130 ft behind the a-line wall, forming a rock wedge. In addition, two planes of failure must exist for the wedge to move into the opening. One is the upper shear failure plane with an apparent dip of 17^{o} intersecting the chamber near the springline of the rock arch. The other is essentially vertical and intersects the chamber between line 2 + 15.5 ft and the east end wall of the chamber. A cross-section through the chamber at line 4 + 12 ft showing the rock wedge is illustrated in Fig. 43.

To stabilize rock movements along the a-line wall, the following four steps were taken (Brown, et al., 1971). (1) Installation of nine 1.69 inch diameter deformed reinforcement anchor bars in drill holes crossing shear zone A from the hanging wall to the foot wall. (2) Installation of 27 additional long rock bolts in the a-line wall between the 1-line and 3-line. The bolts were

- INDICATES MOVEMENT TOWARDS CENTERLINE OF CHAMBER

+ INDICATES MOVEMENT AWAY FROM CENTERLINE OF CHAMBER

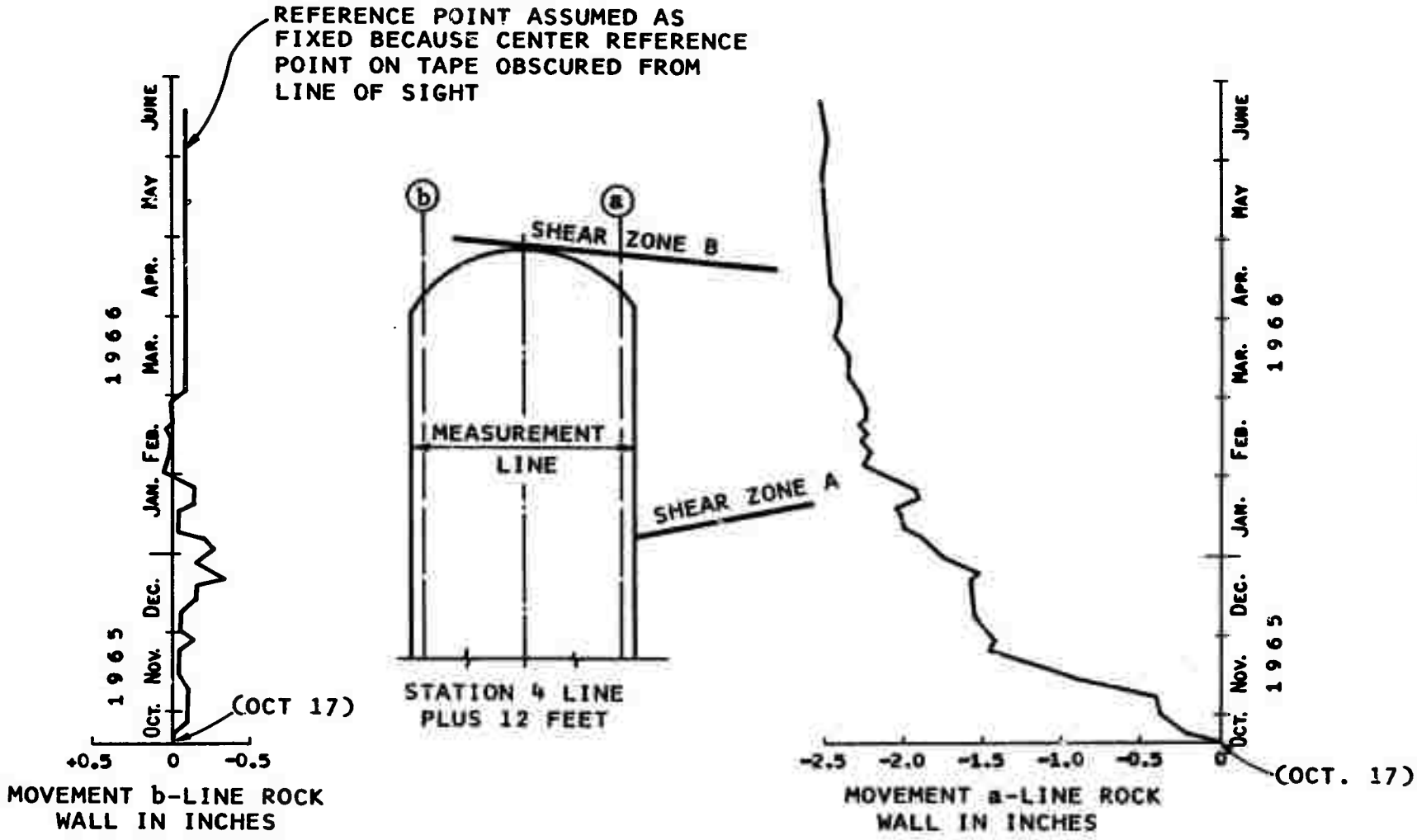

FIG. 41 - HISTORY OF ROCK MOVEMENT AT MORROW POINT POWERPLANT (AFTER BROWN, ET AL., 1971)

WOODWARD-LUNDGREN & ASSOCIATES

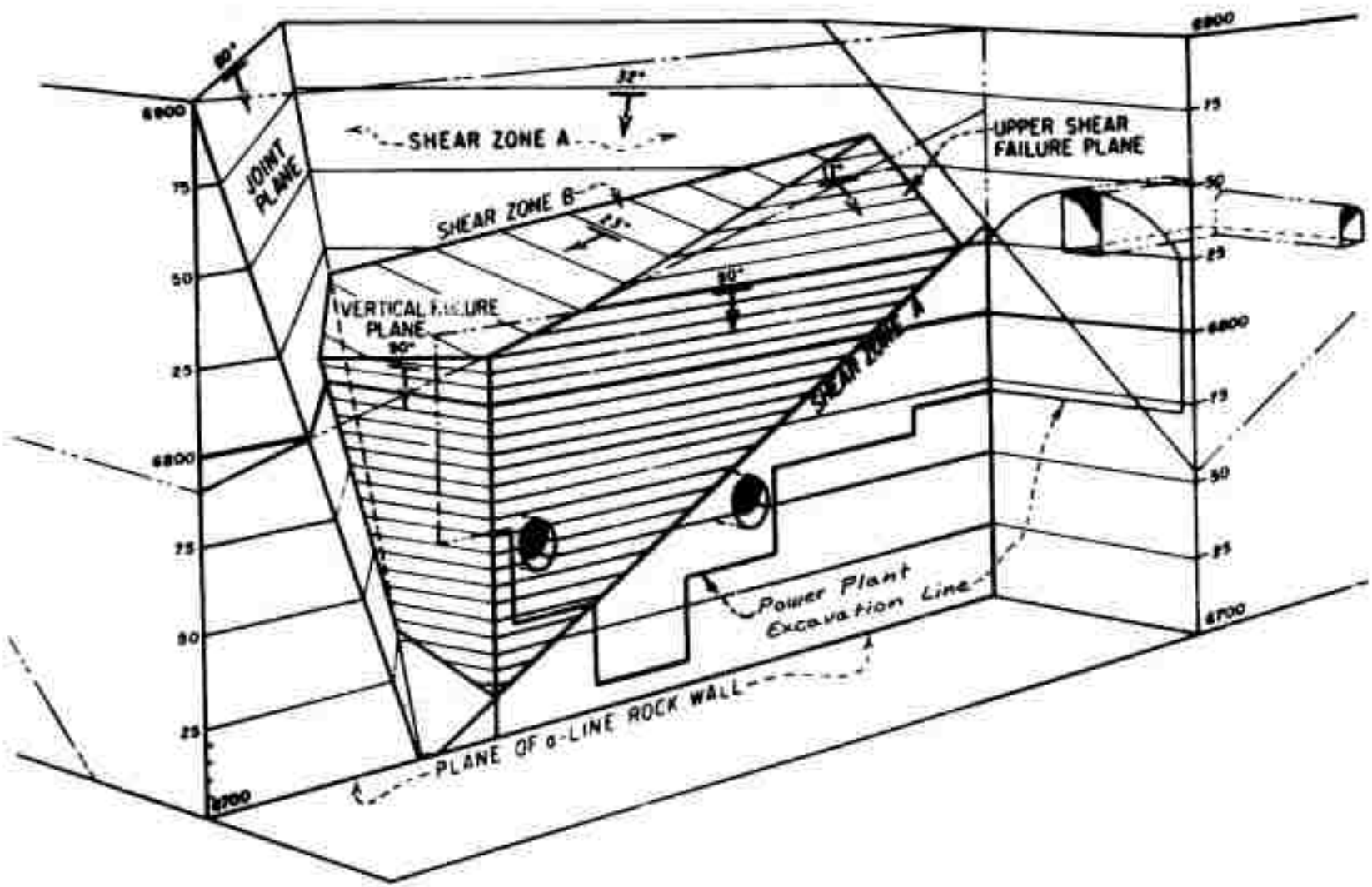

FIG. 42 - THREE-DIMENSION VIEW OF ROCK WEDGE, MORROW POINT POWERPLANT (AFTER BROWN, ET AL. 1971)

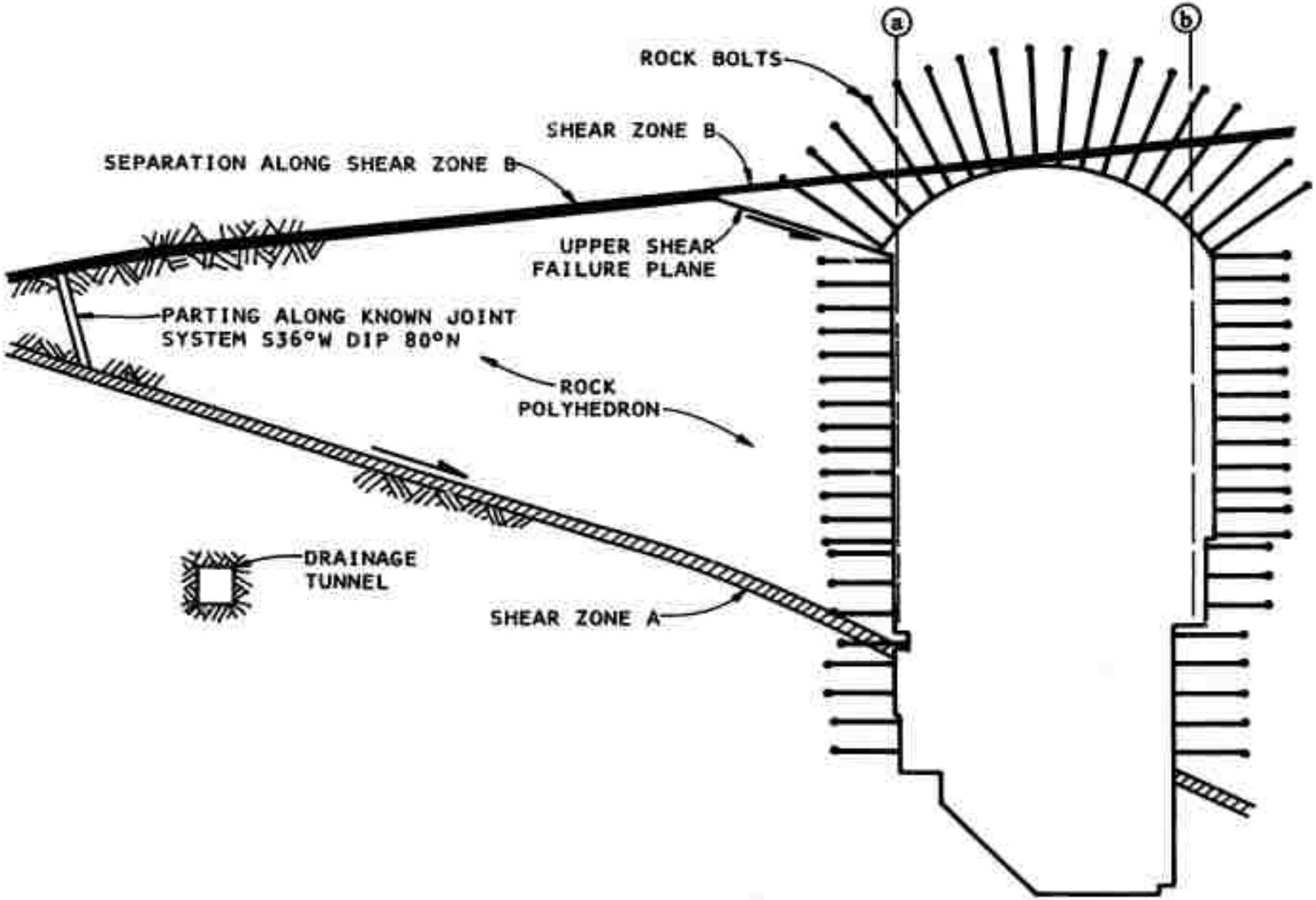

FIG. 43 - SCHEMATIC DIAGRAM OF A-LINE ROCK WEDGE MOVEMENT (AFTER BROWN, ET AL. 1971)

placed diagonally in plan across the vertical zone of incipient failure into sound rock. (3) Installation of 25 post-tensioned tendons from the a-line rock wall through shear zone A to the drainage tunnel. (4) Installation of 10 pairs of flat jacks in the first stage concrete opposite the exposed face of the rock wedge to provide a restraining force between the concrete structure and rock.

Idealization of the Powerplant Excavation

a. Finite Element Idealization - As discussed previously, the observed maximum rock movements occurred at line 4 + 12 ft. Therefore, a cross-section through the opening at this location (Fig. 43) was chosen for analysis. A finite element idealization of the section is shown in Fig. 44. The essential features in the idealization are the steep sloping valley ground surface, shear zones A and B and two other incipient failure planes. The steep sloping ground surface makes estimating the initial in-situ stresses difficult. As described previously, both the rock wedge and the movements associated with it are three-dimensional in nature. However, for the purposes of analysis, it was necessary to idealize it as a two-dimensional plane strain problem. Shear zones A, B and the other two incipient failure planes are shown in Fig. 43 as distinct discontinuities extending in the direction perpendicular to the cross-section. These discontinuities are idealized with Goodman's one-dimensional joints.

b. Material Properties - Extensive testing programs were conducted by the Bureau of Reclamation (1965) to determine rock

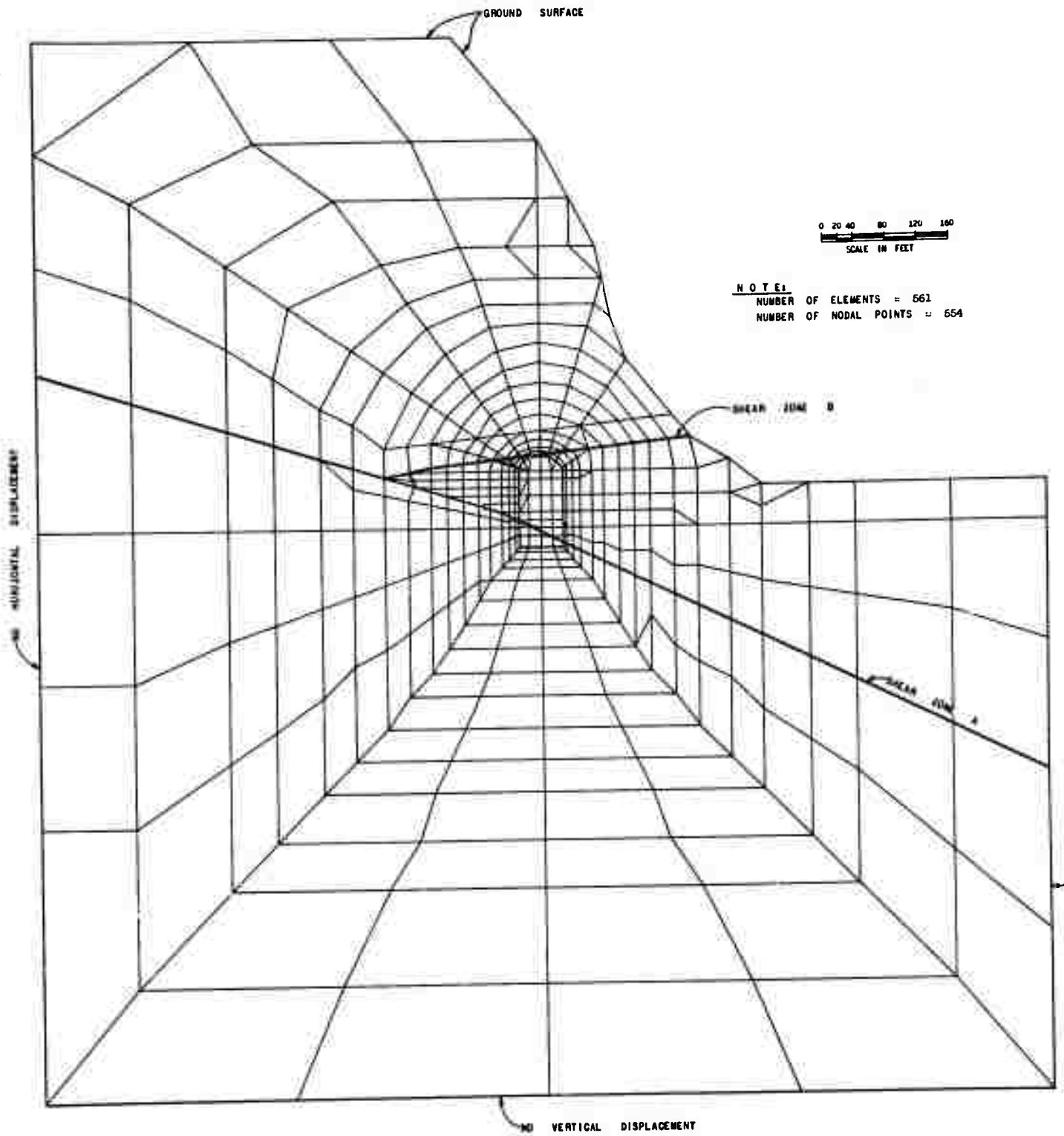

FIG. 44 - FINITE ELEMENT IDEALIZATION FOR MORROW POINT UNDERGROUND POWERPLANT EXCAVATION

properties at the Morrow Point Dam site. These included direct shearing and sliding friction both in the field and the laboratory, triaxial tests and field jacking tests of foundation rock. The strength and elastic properties of the rock above and below shear zone A used in the analysis are summarized in Table 1. As described previously, both shear zones A and B were idealized by one-dimensional joint elements. The properties of these shear zones are approximated by the normal and shear joint stiffnesses (Goodman, 1969) which are functions of normal and tangential deformability of the shear zones and their geometries. No data were available for the normal and shear stiffnesses of the shear zones. Therefore, two sets of joint stiffness were utilized to parametrically study the influence of the deformability of the shear zones on the behavior of the powerplant excavation. The strength parameters assumed for the shear zones are also presented in Table 1.

c. Initial State of Stress at the Powerplant - The initial state of stress in the rock mass influences the stability of the rock elements or discontinuities after the excavation and the magnitude of the forces which have to be applied to the excavated boundaries to simulate the creation of the opening. Therefore, the higher the initial stresses are, the greater the stress changes and movements are in the rock mass surrounding the excavation.

Two types of measurements using overcoring techniques were made at the Morrow Point Powerplant to determine the initial state of

TABLE 1 - SUMMARY OF MATERIAL PROPERTIES USED IN ANALYSES, MORROW POINT POWERPLANT

Case Material	1G Gravity Loading Without Opening	1 Simulation of Powerplant Excavation	2G Gravity Loading Without Opening	2 Simulation of Powerplant Excavation
1 Rock above Shear Zone A	$E = 1.8 \times 10^6$ psf $\nu = 0.49$ (assumed) $\gamma = 171$ pcf	$E = 1.8 \times 10^6$ psf $\nu = 0.02$ $c = 115{,}000$ psf $\phi = 36°$	$E = 1.8 \times 10^6$ psf $\nu = 0.49$ (assumed) $\gamma = 171$ pcf	$E = 1.8 \times 10^6$ psf $\nu = 0.05$ $c = 115{,}000$ psf $\phi = 36°$
2 Rock below Shear Zone A	$E = 2.52 \times 10^6$ psf $\nu = 0.49$ (assumed $\gamma = 171$ pcf	$E = 2.52 \times 10^6$ psf $\nu = 0.05$ $c = 288{,}000$ psf $\phi = 55°$	$E = 2.52 \times 10^6$ psf $\nu = 0.49$ (assumed) $\gamma = 171$ pcf	$E = 2.52 \times 10^6$ psf $\nu = 0.10$ $c = 288{,}000$ psf $\phi = 55°$
3 Shear Zone A Shear Zone B Two Incipient Failure Planes	$K_N = 2 \times 10^6$ pcf $K_S = 1 \times 10^6$ pcf (assumed)	$K_N = 2 \times 10^6$ pcf $K_S = 1 \times 10^6$ pcf $c = 0$ $\phi = 25°$ (assumed)	$K_N = 1 \times 10^6$ pcf $K_S = 1 \times 10^5$ pcf	$K_N = 1 \times 10^6$ pcf $K_S = 1 \times 10^5$ pcf $c = 0$ $\phi = 25°$ (assumed)
4 Part of Shear Zone B Reinforced by Rock Bolts	-----	$K_N = 2 \times 10^6$ pcf $K_S = 1 \times 10^7$ pcf $c = 100{,}000$ psf $\phi = 45°$ (assumed)	-----	$K_N = 1 \times 10^6$ pcf $K_S = 1 \times 10^7$ pcf $c = 100{,}000$ psf $\phi = 45°$ (assumed)

WOODWARD-LUNDGREN & ASSOCIATES

stress (Bureau of Reclamation, 1965). The measurements were made before the excavation in the 6 ft diameter exploratory tunnel at distances varying from 4 ft to 10 ft behind the excavated surface of the tunnel. Test results showed that the in-situ stresses along the exploratory tunnel at the powerplant varied from 1400 psi to 600 psi for vertical stress and 2700 psi to 170 psi for horizontal stress indicating that (1) the in-situ stresses varied with location, (2) the vertical stress may be greater than the gravity stress, and (3) the horizontal stress may be greater than the vertical stress. Because of the limited data with regard to the magnitude of the in-situ stresses and the difficulties associated with estimating their values in the rock mass, the initial state of stress used in the analysis was obtained by a gravity turn-on analysis of the rock mass without the opening. These analyses were conducted to account for the effects of the steep valley wall located in the vicinity of the powerplant excavation. For these analyses, the higher values of the Poisson's ratio (= 0.49) was assumed for the rock to simulate the likelihood of a high horizontal stress.

The values of the initial stresses which have to be applied at excavated boundary to simulate the excavation were obtained by a method similar to that suggested by Clough and Duncan (1969). The nodal point stresses on the excavated boundary were estimated from the stresses in the surrounding elements. The procedure is described in Appendix A.

Analysis Procedures

As indicated previously, two cases using high and low normal and shear joint stiffnesses for the shear zones were analyzed utilizing the computer program developed in Phase 1. For each case, the initial stresses for each element were first obtained by performing a gravity turn-on analysis. The nodal stresses were then determined along the excavated surface in accordance with the procedure described in Appendix A and applied at the excavated boundary. Very small values of the elastic constants were assigned to those elements in the opening to simulate the cavity. Material properties utilized in the analysis are presented on Table 1.

Presentation and Discussion of Results

The results of the analyses are presented in Figs. 45 and 46 and Table 2. Fig. 45 illustrates the horizontal displacements for points along the face of the powerplant chamber, and Fig. 46 shows the vertical displacements. The observed movements on the a- and b-line walls are also shown in Figs. 45 and 46. For the case with high joint stiffnesses, the horizontal inward movement at El. 6793 was calculated to be 0.44 inch on the a-line wall and 0.41 inch on the b-line wall. The observed inward movements at the corresponding points are 2.5 inches on the a-line and 0.1 inch on the b-line wall. When the low joint stiffnesses were used, the calculated inward movements increased to 1.35 inches on the a-line wall and 0.62 inch on the b-line wall.

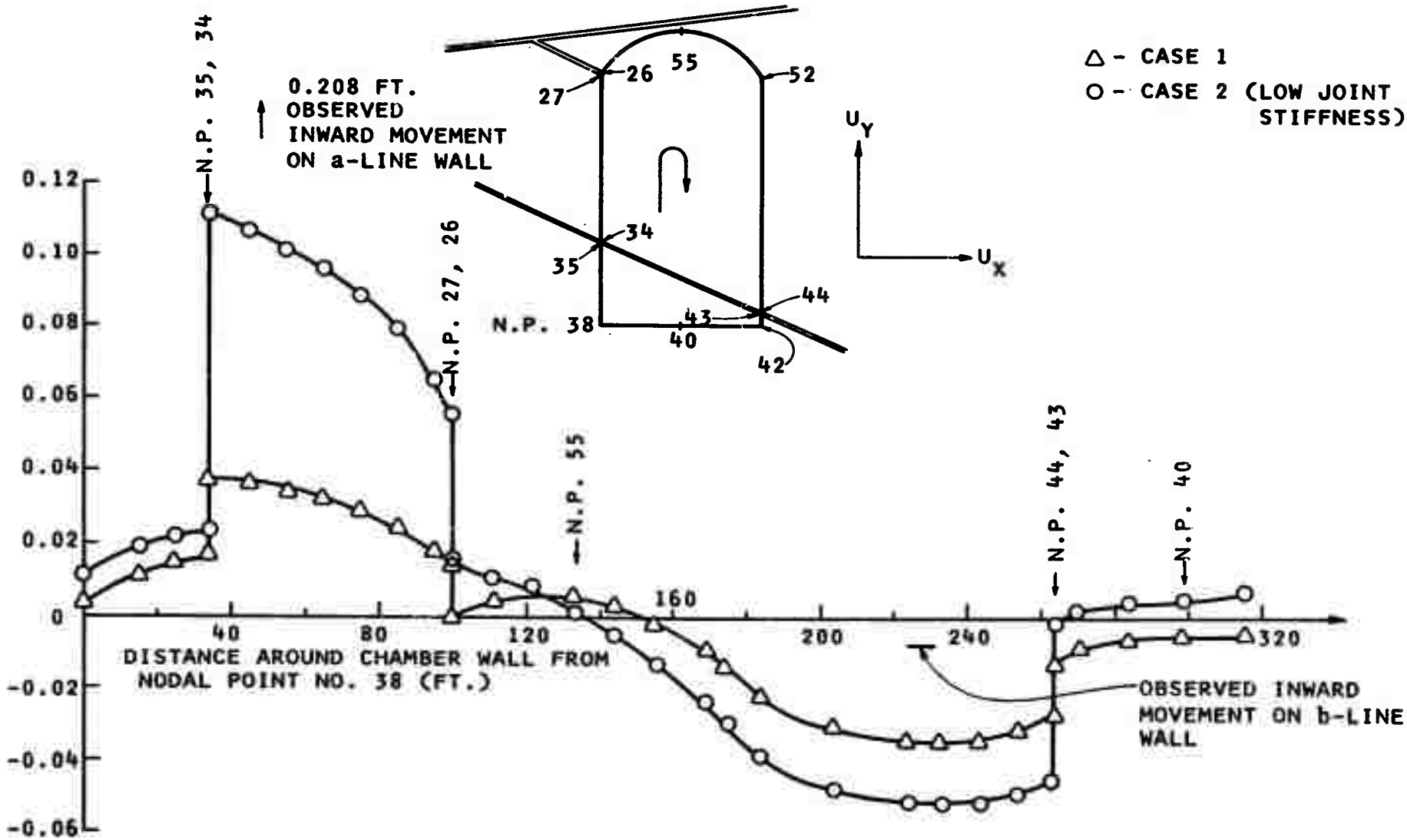

FIG. 45 - HORIZONTAL DISPLACEMENTS ALONG FACE OF POWERPLANT CHAMBER, MORROW POINT POWERPLANT

WOODWARD-LUNDGREN & ASSOCIATES

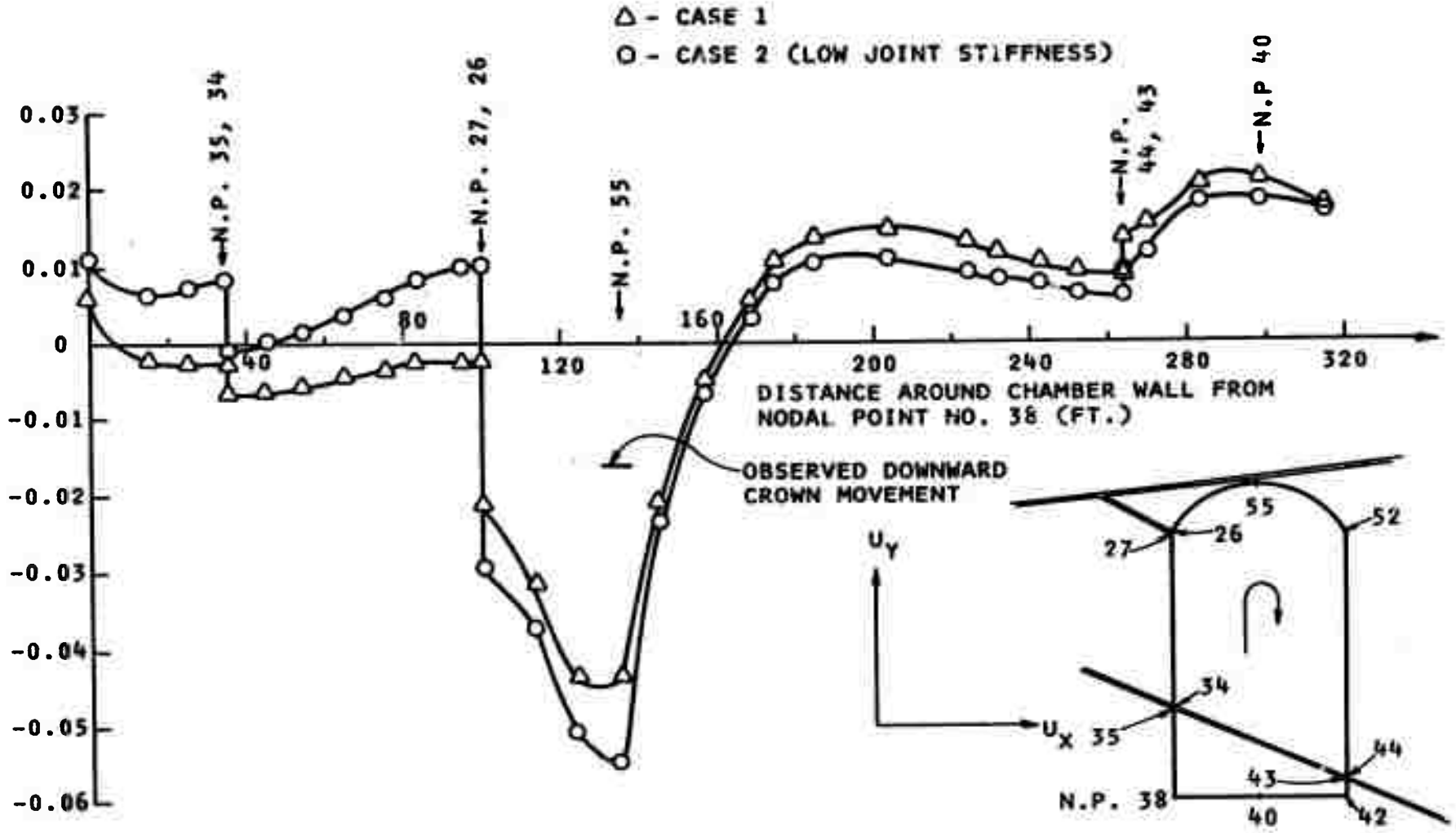

FIG. 46 - VERTICAL DISPLACEMENTS ALONG FACE OF POWERPLANT CHAMBER, MORROW POINT POWERPLANT

TABLE 2 - OBSERVED AND CALCULATED ROCK MOVEMENTS ON a- AND b-WALLS IN THE POWERPLANT CHAMBER

	Observed* (in.)	Calculated* (in.)	
		Case 1 With High Joint Stiffness	Case 2 With Low Joint Stiffness
a-line wall at El. 6793	-2.5	-0.44	-1.35
a-line wall at El. 6823	-2.1	-0.21	-0.92
b-line wall at El. 6793	-0.1	-0.41	-0.62
b-line wall at El. 6823	+0.2	-0.18	-0.37

* Only horizontal movements are indicated.

"-" indicates movements towards centerline of chamber.

"+" indicates movements away from centerline of chamber.

The results indicate that the analysis provided a qualitative estimate of rock movements at the Morrow Point Powerplant excavation. The computed deformations are of the same order of magnitude as those observed. The difference between the computed and observed deformation is significant in terms of percentages but is considered satisfactory in terms of numerical values when it is recognized that the following approximations were made in the analysis. (1) The rock wedge and the movements associated with it are three-dimensional in nature, Fig. 42. A two-dimensional plane strain analyses would tend to underestimate the movements. (2) The initial state of stress was estimated in the analyses. It is quite possible that a higher initial state of stress, especially higher horizontal stresses might exist in the rock mass which would cause higher induced stresses and movements. (3) No data were available on the properties of the shear zones present in the rock mass. It was necessary to assume their values in the analysis.

It should also be recognized that the powerplant was excavated in stages, whereas the analysis assumed that the excavation was created instantaneously. For an ideal elastic material, the assumption would not result in any error. However, in those cases where the loading path has an influence on the results, the effect of the above stated assumption can be significant. High stress concentrations during the excavation process could cause displacements which would be larger than those computed on the assumption of an instantaneous creation of the opening.

Summary of the Achievement for Phase 2

A number of laboratory studies and field case histories were evaluated to determine their suitability for analysis utilizing the computer program developed in Phase 1. A laboratory model study of an opening in a rock-like material, reported by Heuer and Hendron (1971), and the excavation for the Morrow Point Powerplant were analyzed. The results of the analyses were compared with observed behavior. It was found that the results of the analysis could be utilized to predict zones of potential failure.

CONCLUSIONS AND RECOMMENDATIONS

The puspose of this study was to evaluate the ability of the available finite element techniques for the solution of plane problems to predict the stresses, strains, and deformations in a rock mass surrounding an excavation. In the course of this investigation, a general computer program, which incorporates no tension, joint perturbation and elasto-plastic analysis, was developed. This general computer program was employed to analyze the Morrow Point Powerplant excavation and a laboratory model study of an opening in a rock-like material conducted by Heuer and Hendron (1971). The results of the analysis were compared with actual performance.

The analysis of the model study indicated that the combined computer program could identify the likely failure zones that will occur around an opening in an intact rock. However, the

techniques developed are not adequate to simulate accurately the propagation of fractures and the resulting deformation that might occur.

The analyses of the Morrow Point Underground Powerplant excavation indicated that the developed computer program could be utilized to analyze and assist in predicting the performance of excavations in a rock mass. The results of the analyses of the Morrow Point Powerplant excavation provided a qualitative estimate of the movements that occurred at the excavation. The accuracy of the prediction would be improved if better information was available on (1) the initial state of stress in rock, (2) the geologic discontinuities such as joints, shear zones, foliations, and bedding planes, and (3) in-situ properties of the rock.

It was found that the effort necessary to idealize problems for analysis was far greater than anticipated. If accurate results are desired, great care has to be taken in the idealization. Since real problems, in general, include certain factors which cannot be modelled accurately, it may be necessary to utilize more than one idealization to obtain bounds on the possible behavior of the excavation.

Computational techniques which have the capability of including realistic idealizations of in-situ rock conditions can provide a qualitative estimate of the behavior of a rock mass in the vicinity of an excavation. Considering the idealizations used

and the accuracy of the available input information, the ability of the computational techniques to predict quantitative behavior is considered acceptable.

Recommendations for Future Research

It is recommended that a major effort should be directed towards the study of case histories for the purpose of establishing the reliability of various analytical methods to predict performance and to provide a basis for improvements. Such studies should emphasize the requirements for idealization and field input information. Without such studies, analytical techniques will not gain acceptance in the design profession.

This study has provided the basis for recommending that the following additional features be incorporated into this computer program:

(i) Theoretical concepts and computational techniques for predicting the development and propagation of fractures in a rock mass.

(ii) Computational techniques to analyze the influence of support systems and construction procedures.

In some cases, new techniques will have to be developed; in others, it will be necessary to incorporate work already done into the computer program.

Operational programs for conducting a linear elastic analysis of three-dimensional structures are available. Efforts should be directed towards modifying these programs to include the capability of modelling and analyzing realistic in-situ rock conditions e.g., joints, no tension, etc. Case history studies should be analyzed to determine the applicability of these techniques to practical problems.

REFERENCES

1. Aiyer, A. K., "An Analytical Study of the Time-dependent Behavior of Underground Openings," thesis presented to the University of Illinois, Urbana, in 1969, in partial fulfillment of the requirements for the degree of Doctor of Philosophy.

2. Baker, L. E., Sandhu, R. S., and Shieh, W. Y., "Application of Elasto-plastic Analysis in Rock Mechanics by Finite Element Method," Proc. of Eleventh Symposium on Rock Mechanics, Berkeley, California, June, 1969.

3. Boresi, A. P. and Deere, D. U., "Creep Closure of a Spherical Cavity in an Infinite Medium (with Special Application to Project Dribble, Tatum Salt Dome, Mississippi)", for Holmes and Narver, Inc., Las Vegas Division, 1963.

4. Brown, Gilbert L., Morgan, Ernest D., and Dodd, Jerry S. "Rock Stabilization at Morrow Point Powerplant," Journal of the SM and FD, ASCE, Vol. 97, No. SM1, Proc. Paper 7820, January 1971.

5. Bureau of Reclamation, "A Technical Representation of Morrow Point Dam and Powerplant Foundation Investigation, Colorado River Storage Project," Denver, Colorado, 1965.

6. Chang, C-Y and Duncan, J. M., "Analysis of Soil Movement Around a Deep Excavation," Journal of the SM and FD, ASCE, Vol. 96, No. SM5, Proc. Paper 7512, September 1970.

7. Clough, G. W. and Duncan, J. M., "Finite Element Analyses of Port Allen and Old River Locks," College of Engineering, Office of Research Services, University of California, Berkeley, California 1969.

8. Clough, R. W., "The Finite Element Method in Plane Stress Analysis," Proceedings, Second ASCE Conf. on Electronics Computation, Pittsburgh, Pennsylvania, Sept. 1960.

9. Dodd, Jerry S., "Morrow Point Underground Powerplant Rock Mechanics Investigations," U. S. Bureau of Reclamation Report, March 1967.

10. Drucker, P. C. and Prager, W., "Soil Mechanics and Plastic Analysis or Limit Design," Q. Appl. Math., Vol. 10, 1952, pp. 157-165.

11. Dunlop, P., Duncan, J. M., and Seed, H. B., "Finite Element Analyses of Slopes in Soil," Report No. TE 68-3, Office of Research Services, University of California, 1968.

12. Goodman, R., Taylor, R., and Brekke, T., "A Model for the Mechanics of Jointed Rock," Proceedings, American Society of Civil Engineers, Vol. 94, No. SM3, May, 1968, pp. 637-660.

13. Goodman, R., "The Deformability of Joints," ASTM Special Technical Publication 477, 1970.

14. Greenbaum, G. A., "Creep Analysis of Axisymmetric Bodies," thesis presented to the University of California, Los Angeles, in 1966, in partial fulfillment of the requirements for the degree of Doctor of Philosophy.

15. Heuer, R. E. and Hendron, A. J., Jr., "Geomechanical Model Study of the Behavior of Underground Openings in Rock Subjected to Static Loads, Report 1, Development of Modeling Techniques, Oct. 1969, Report 2, Tests on Unlined Openings in Intact Rock, Feb. 1971," Dept. of Civ. Engineering, University of Illinois, Urbana, Illinois.

16. Heuze, F. E., Goodman, R. E. and Bornstein, A., "Numerical Analyses of Deformability Tests in Jointed Rock, Joint Perturbation and No Tension Finite Element Solutions," Rock Mechanics - Felsmechanik, V. 3, No. 4, Springer Verlag ed.

17. Judd, W. R. and Perloff, W. H., "Strain Distribution Around Underground Openings - Tech. Report No. 5, Comparison Between Predicted and Measured Displacements," Purdue University, Sch. of Civ. Engrg., Lafayette, Indiana, March 1971.

18. Nair, K., "Stability Studies for Project Payette," final report submitted to Fenix & Scisson, Inc., Tulsa, Oklahoma by Woodward-Clyde-Sherard & Associates and Material Research and Development, Inc., Oakland, California, Oct. 1967.

19. Nair, K. and Boresi, A. P., "Stress Analysis for Time-dependent Problems in Rock Mechanics," Procs, 2nd Congress of the International Society for Rock Mechanics, Belgrade, September 1970.

20. Nair, K., and Chang, C-Y, "Analytical Methods for Predicting Subsidence," Report submitted to Solution Mining Research Institute, Chicago, Illinois, 1971.

21. Patton, F. D., "Multiple Modes of Shear Failure in Rock," Proc 1st Congress of the International Society of Rock Mechanics, Lisbon, Vol. I, pp. 509-513, 1966.

22. Prager, W., and Hodge, P. G., "Theory of Perfectly Plastic Solids," Published by John Wiley & Sons, Inc. 1951.

23. Reyes, S. F., "Elastic-Plastic Analysis of Underground Openings by the Finite Element Method," thesis presented to the University of Illinois, Urbana, in 1966, in partial fulfillment of the requirements for the degree of Doctor of Philosophy.

24. Reyes, S. F., and Deere, D. U., "Elastic-Plastic Analysis of Underground Openings by the Finite Element Method," Proceedings, First Congress of the International Society of Rock Mechanics, Lisbon, Portugal, 1966.

25. Sandu, R. S., Hooper, J. R. and Wu, T. H., "Stresses, Deformations and Progressive Failure of Non-Homogeneous Fissured Rock," First semiannual report, project RF 3177A1, Department of Civil Engineering, The Ohio State University, 1971.

26. Wilson, Edward L., "Finite Element Analysis of Two-Dimensional Structures," SESM Report No. 63-2, University of California, Berkeley, 1963.

27. Wilson, Edward L., "Structural Analysis of Axisymmetric Solids," AIAA Journal, Vol. 3, No. 12, December 1965.

28. Zienkiewicz, O. C., The Finite Element Method in Structural and Continuum Mechanics, McGraw-Hill, London (1967).

29. Zienkiewicz, O. C., Valliappan, S., and King, I. P., "Stress Analysis of Rock as a 'No Tension' Material," Geotechnique, Vol. 18, March 1968.

30. Zienkiewicz, O. C., Valliappan, S., and King, I. P., "Elasto-Plastic Solutions of Engineering Problems: 'Initial Stress' Finite Element Approach," Inter. Journal for Numerical Methods in Engineering (1969) Vol. 1, No. 1, 75-100.

31. Zienkiewicz, O. C., Best B., Dullage, C. and Stagg, K. G. "Analysis of Nonlinear Problems in Rock Mechanics with Particular Reference to Jointed Rock Systems," Procs. 2nd Congress of the International Society of Rock Mechanics, Vol. 3, No. 8-14, Belgrade, Yugoslavia, 1970.

APPENDIX A

EVALUATION OF NODAL STRESSES FROM STRESSES IN THE SURROUNDING ELEMENTS

APPENDIX A

EVALUATION OF NODAL STRESSES FROM STRESSES IN THE SURROUNDING ELEMENTS

Dunlop, Duncan and Seed (1968), Chang and Duncan (1970), and Clough and Duncan (1969) have shown that excavation may be simulated in the finite element method by applying stresses to the boundary exposed by excavation. This technique was employed in the present study. In the finite element method, stresses are generally determined only at the element centroids. To simulate excavation, it is necessary to determine the stresses on the surface to be exposed by excavation. A technique similar to that used by Clough and Duncan (1969) was employed to evaluate nodal stresses on the excavated boundary from the stresses in the surrounding elements.

The relationship between the known stresses at the element centroids and the unknown stresses at the nodal points on the excavated boundary may be developed using an interpolation function expressed in the following form:

$$\sigma = a_1 + a_2 x + a_3 y + a_4 xy \qquad \text{(A-1)}$$

in which σ is the nodal stress to be interpolated, x and y are the coordinates of the nodal point and a_1, a_2, a_3, and a_4 are interpolation coefficients. In order to use equation (A-1) to determine the stresses at the nodes of an element to be excavated, three

sets of the interpolation coefficients are calculated (one each for σ_x, σ_y, and σ_{xy}) using the known stresses in the element to be excavated and the stresses in three adjacent elements. For a given stress component, σ, the unknown interpolation coefficients are expressed as:

$$\begin{aligned}
\sigma(1) &= a_1 + a_2 x_1 + a_3 y_1 + a_4 x_1 y_1 \\
\sigma(2) &= a_1 + a_2 x_2 + a_3 y_2 + a_4 x_2 y_2 \\
\sigma(3) &= a_1 + a_2 x_3 + a_3 y_3 + a_4 x_3 y_3 \\
\sigma(4) &= a_1 + a_2 x_4 + a_3 y_4 + a_4 x_4 y_4
\end{aligned} \tag{A-2}$$

in which σ (1) is the stress in element 1, σ (2) is the stress in element 2, etc. Equation (A-2) may be expressed in matrix form as:

$$\{\sigma\}_e = [M]\ \{a\} \tag{A-3}$$

in which $\{\sigma\}_e$ is the stresses for elements 1, 2, 3 and 4, [M] is the coordinate matrix for elements 1, 2, 3 and 4, and {a} is the unknown interpolation coefficients. {a} may be expressed by:

$$\{a\} = [M]^{-1}\ \{\sigma\}_e \tag{A-4}$$

The interpolation coefficients may then be used to solve for the stresses, $\{\sigma\}_n$, at each node of the element to be excavated.

$$\{\sigma\}_n = [N]\ \{a\} \tag{A-5}$$

in which [N] is the coordinate matrix for nodes I, J, K, and L. Equations (A-4) and (A-5) may be combined, as follows:

$$\{\sigma\}_n = [N]\ [M]^{-1}\ \{\sigma\}_e \tag{A-6}$$

Thus the values of stresses at the nodes of an element to be excavated may be defined in terms of the center point stresses of that element and three adjacent elements. Evaluation of equation (A-6) is performed in Subroutine NPSTRS.

APPENDIX B

A Combined Computer Program Using Finite Element Techniques for Elasto-plastic, Joint Perturbation, and No Tension Analysis of Underground Openings in Rock

A COMBINED COMPUTER PROGRAM USING FINITE ELEMENT TECHNIQUES FOR ELASTO-PLASTIC, JOINT PERTURBATION, AND NO TENSION ANALYSIS OF UNDERGROUND OPENINGS IN ROCK

Identification

The program which consists of a main program and 13 subroutines (STIFF, MODIFY, QUAD, TRISTF, JTSTIF, BANSOL, STRESS, REDO, JTSTR, EPLAST, INITST, PRINST, NPSTRS), was developed by Chin-Yung Chang using a computer program written by E. Wilson and modified by Goodman, Taylor and Brekke (1968).

Purpose

The combined computer program was developed on the basis of three concepts: elasto-plastic, joint perturbation and no tension analysis for calculating stresses and displacements for plane strain conditions in a rock mass surrounding underground openings. The rock mass may consist of joints, faults, bedding planes and other geologic discontinuities, and exhibit elasto-plastic and "no tension" behavior.

Sequence of Operation

(a) The main program handles the initial input and monitors the calling of the subroutines in a specified order as shown in Fig. A1. If specified, for the last iteration of the last increment in an analysis, stresses and excess stresses to be redistributed for two-dimensional elements, normal and tangential stresses for joint elements, nodal point displacements and yield functions for two-dimensional elements are punched onto cards to be used for restarting computation.

(b) Subroutine STIFF assembles the general stiffness matrix for the entire structure, adds in concentrated loads at the nodal points, adds in loads due to boundary pressures and modifies the stiffness matrix for the boundary conditions.

(c) In Subroutine QUAD the constitutive equations are formulated.

(d) Subroutine TRISTF forms the stiffness matrix for triangular subelements and if specified, element loadings due to gravity are generated.

(e) Subroutine JTSTIF forms the stiffness matrix for each joint element.

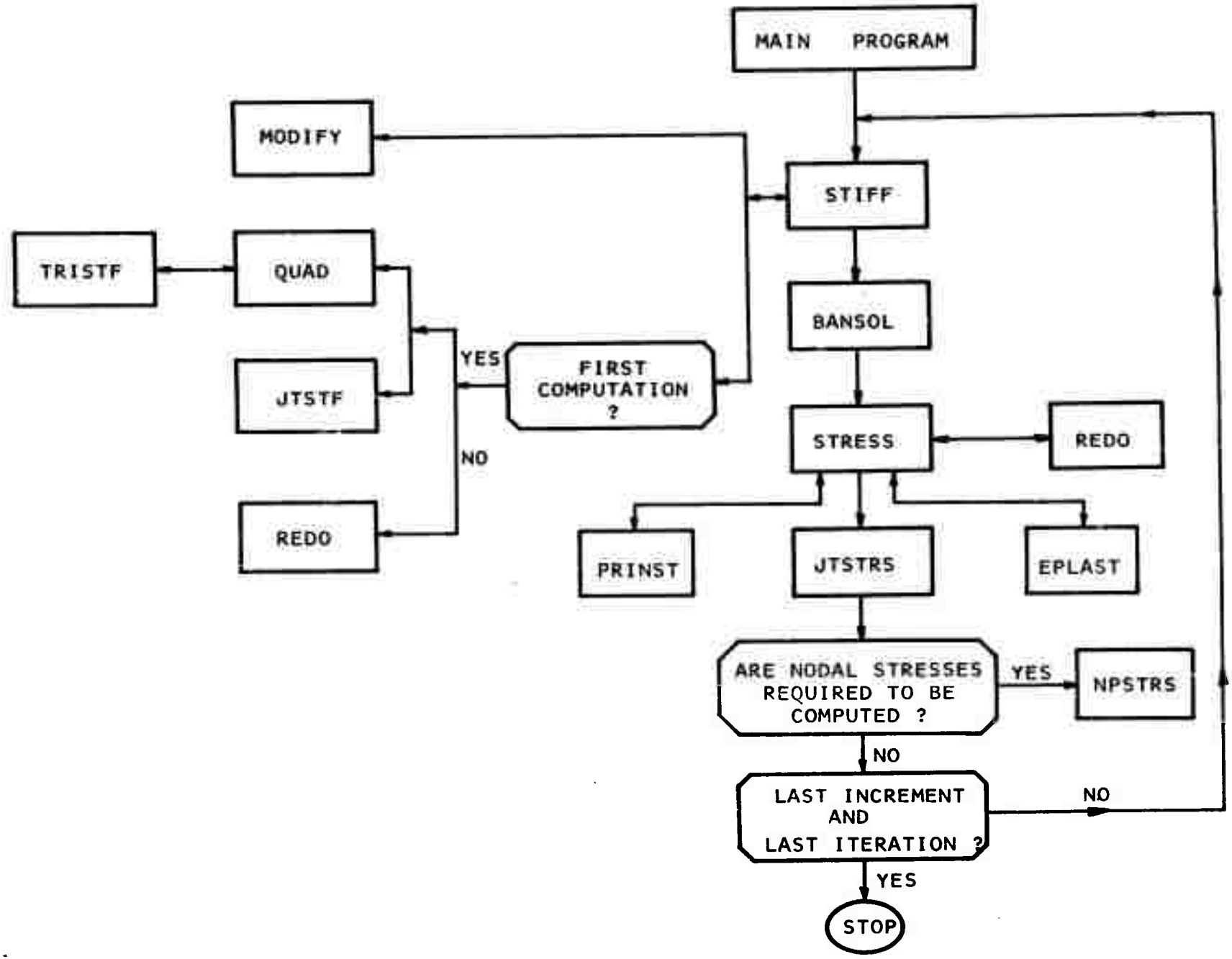

FIG. B1 - SIMPLIFIED FLOW DIAGRAM SHOWING SEQUENCE OF OPERATION OF ALL SUBROUTINES

WOODWARD-LUNDGREN & ASSOCIATES

(f) Subroutine MODIFY modifies the stiffness matrix for the boundary conditions.

(g) Subroutine REDO calculates equilibrating nodal point forces due to gravity if specified, and for excess stresses if the elements are subjected to tensile stresses greater than that allowable.

(h) Subroutine BANSOL solves the simultaneous equations representing the structural stiffness matrix and the structural load vector for nodal point displacements.

(i) Subroutine STRESS calculates incremental stresses and strains, cumulates stresses, and prints stresses and strains for two-dimensional elements.

(j) Subroutine JTSTRS calculates and prints normal and tangential stresses, normal and tangential displacements (cumulative and incremental) and excess normal and tangential stresses to be redistributed by comparing stress with strength for joint elements. The equilibrating nodal point forces are also computed from the excess stresses and stored for the next iteration.

(k) Subroutine EPLAST calculates yield functions and elasto-plastic stress-strain relation for those two-dimensional elements in yield. The excess stresses to be redistributed are computed as a difference between changes in stress calculated from the elastic stress-strain relation and those calculated from the elasto-plastic stress-strain relation.

(l) Subroutine INITST generates initial stresses under free-field conditions.

(m) Subroutine PRINST calculates magnitudes and directions of the principal stresses and strains.

(n) Subroutine NPSTRS computes stresses at nodes on the excavated boundary from stresses in surrounding elements.

Output

The data describing the finite element configuration, the material properties and pressures applied to the excavated face to simulate excavation for the opening are printed after being read. Nodal point displacements (incremental and cumulative), stresses, strains and yield functions for two-dimensional elements; normal and tangential stresses, normal and tangential displacements (incremental and cumulative) for joint elements, are printed after each increment or iteration. If specified, for the last iteration of the last increment in an analysis, stresses, strains and excess stresses to be redistributed for two-dimensional elements, normal and tangential stresses for joint elements, nodal point displacements and yield functions for two-dimensional elements are punched onto cards to be used for restarting computation.

Input Data Procedure

1st CARD TYPE: FORMAT (8A10) (One Card)

Cols 2-80 Identifying information to be printed with results.

2nd CARD TYPE: FORMAT (4I5, 2F10.2, 2I5, 3F10.5) (One Card)

Cols.		
1-5	NUMNP	- Number of nodal points (maximum 900)
6-10	NUMEL	- Number of elements (maximum 800)
11-15	NUMMAT	- Number of different materials (maximum 12)
16-20	NUMPC	- Number of pressure cards
21-30	ACELX	- Acceleration in X-direction
31-40	ACELY	- Acceleration in Y-direction
41-45	NP	- Number of approximations (increments)
46-50	NRES*	- = -1, Residual stresses generated from which residual load is calculated.

*If NREAD = 1, NRES should not be greater than zero.
If NRES = -1 or 1, gravity turn-on analysis is performed.
If NRES = -1, stresses at nodes on the excavated boundary are to be calculated and punched out onto cards, i.e. 21th and 22nd card types are needed.

= 0, Residual stresses generated but residual load is zero.

= 1, Residual stresses read as input from which residual load is generated.

= 2, Residual stresses read as input, but residual load is zero.

Cols. 51-60 FRAC - Percentage of maximum tensile stress considered as cracked zone, read in zero.

61-70 REFPR - Vertical stress at the reference point.

71-80 DEPTH - Y - ordinate at the reference point.

3rd CARD TYPE: FORMAT (16I5) (One Card)

Cols. 1-5 NPRSNT - Present loading increment number.

6-10 NREAD - = 0, no data from previous computation will be read as input.

= 1, data from last increment are read as input.

11-15 NPUNCH - = 0, data will not be punched out at the last iteration.

= 1, data will be punched out at the last iteration of the last increment.

16-20 NSTSRT - = 1, stresses in R-θ directions will be printed. For this case, the center of the circular opening has to be located at the origin of the coordinate system.

4th CARD TYPE: FORMAT (I5, F10.5)

Cols. 1-5 ITN(N) - Number of iterations for N^{th} increment.

6-15 PRATIO(N) - Percentage of total pressure applied for N^{th} increment.

Repeat for each loading increment.

5th CARD TYPE: FORMAT (16I5) (One Card)

Cols 1-5 MJØINT - Total number of material types for joints (maximum 12)

6-10 MTENS - Total number of material types that can sustain tension.

6th CARD TYPE: FORMAT (16I5) (Omit this card if MJOINT=0 on 5th card type)

Cols. 1-5 MJNT(I) - Material type number for joint elements.
6-10 Same
11-15 ----

7th CARD TYPE: FORMAT (16I5) (Omit this card if MTENS=0 on 5th card type)

Cols. 1-5 MNTEN(I) - Material type number which can sustain tension.
6-10 Same
11-15 ----

8th CARD TYPE: FORMAT (I5, 2F10.5) (One Card)

Cols. 1-5 MTYPE - Material type number.
6-15 RO(MTYPE)- Mass density of this material type.
16-20 AKO(MTYPE) - Ratio of horizontal to vertical stress.

9th CARD TYPE: FORMAT (8F10.5)

Cols. 1-10 E(1, MTYPE)- Tensile strength for normal materials or normal stiffness for joint materials
11-20 E(2, MTYPE)- Modulus in compression for normal mtls. or shear stiffness for joint materials
21-30 E(3, MTYPE)- Poisson's ratio for normal materials or cohesion for joint materials
31-40 E(4, MTYPE)- Modulus in tension for normal materials angle of friction for joint mtls.(degree
41-50 E(5, MTYPE)- Cohesion for normal materials or maximum allowable closure (input as negative) for joint materials
51-60 E(6, MTYPE)- Angle of friction for normal mtls. (degrees)

Repeat 8th and 9th card types for all material types.

10th CARD TYPE: FORMAT (I5, F5.0, 4F10.0) (One card for each nodal point)

Cols. 1-5 N - Nodal point number
6-10 CODE (N)- Number which indicates if displacements or forces are to be specified
= 0 UR is the specified X-load and UZ is the specified Y-load

= 1 UR is the specified X-displacement and UZ is the specified Y-load

= 2 UR is the specified X-load and UZ is the specified Y-displacement

= 3 UR is the specified X-displacement and UZ is the specified Y-displacement

Cols. 11-20 R(N) - X-ordinate
21-30 Z(N) - Y-ordinate
31-40 UR(N) - X-load or displacement
41-50 UZ(N) - Y-load or displacement

Nodal points must be numbered in sequence. If nodal point numbers are omitted, those omitted are generated automatically at equal spacings, between those specified and CODE(N) is assigned zero. The first and last must be specified.

11th CARD TYPE: FORMAT (16I5) (One card for each element)

Cols. 1-5 M - Element number
6-10 IX(M,1)- Nodal point I
11-15 IX(M,2)- Nodal point J
16-20 IX(M,3)- Nodal point K
21-25 IX(M,4)- Nodal point L
26-30 IX(M,5)- Material number

The nodal point numbers must be numbered consecutively proceeding counterclockwise around the elements. The nodal point numbers for any element must not differ by more than 39. If element numbers are omitted, those missing will be generated by incrementing the element number and each nodal point number (I, J, K and L) by one, and assigning the same material number as the last element specified. The first and last elements must be specified.

Triangular elements are also permissable, and are identified by repeating the last nodal point number (i.e., I, J, K, K). For joint elements, nodal points must be numbered I, J, K, L counterclockwise proceeding along length of joint from I to J and along length from K to L. Nodal points I and L (J and K) have different numbers but identical coordinates.

One-dimensional elements are also permissable and are identified by the node number sequence (I, J, J, I).

12th CARD TYPE: FORMAT (16I5)

Cols. 1-5 I - Nodal point number I along the boundary IJ where the boundary pressure is applied.

6-10 J - Nodal point number J along the boundary IJ.

11-15, 16-20 Same as above; two nodal point numbers for each boundary where the boundary pressure is applied.

21-25, 26-30 ----

As shown in Figure B2, nodal points I and J must be ordered in counterclockwise order about centroid of element on which the pressure is applied.

13th CARD TYPE: FORMAT (16I5)

Cols. 1-5 NPCAV - Number of nodal points along the boundary where the boundary pressures are applied.

14th CARD TYPE: FORMAT (I5, 3F10.0)

Cols. 1-5 NPCA(M) - Nodal point number where the boundary pressure is applied.

6-15 PSCA(M,1) - X normal stress at nodal point NPCA(M)

16-25 PSCA(M,2) - Y normal stress at nodal point NPCA(M)

26-35 PSCA(M,3) - XY shear stress at nodal point NPCA(M)

Stresses (σ_x, σ_y, and τ_{xy}) are shown positive in Figure B2.

As shown in Figure B2, stresses (σ_x, σ_y, τ_{xy}) at the nodal point are converted to normal and shear stress on the boundary. Then the nodal point forces are calculated from the normal and shear stress along the boundary assuming linear stress distribution along the boundary. The normal and shear stress along the boundary are shown positive in Figure B2.

12th, 13th and 14th card types are neglected if NUMPC = 0 on the 2nd card type.

15 CARD TYPE: FORMAT (I5, 3E15.5) (One card for each element)

Cols. 1-5 N - Element number

6-20 STRS(N,1) - Initial stress σ_x

21-35 STRS(N,2) - Initial stress σ_y

36-50 STRS(N,3) - Initial stress τ_{xy}

This card type is neglected if NRES $\leq$ 0.

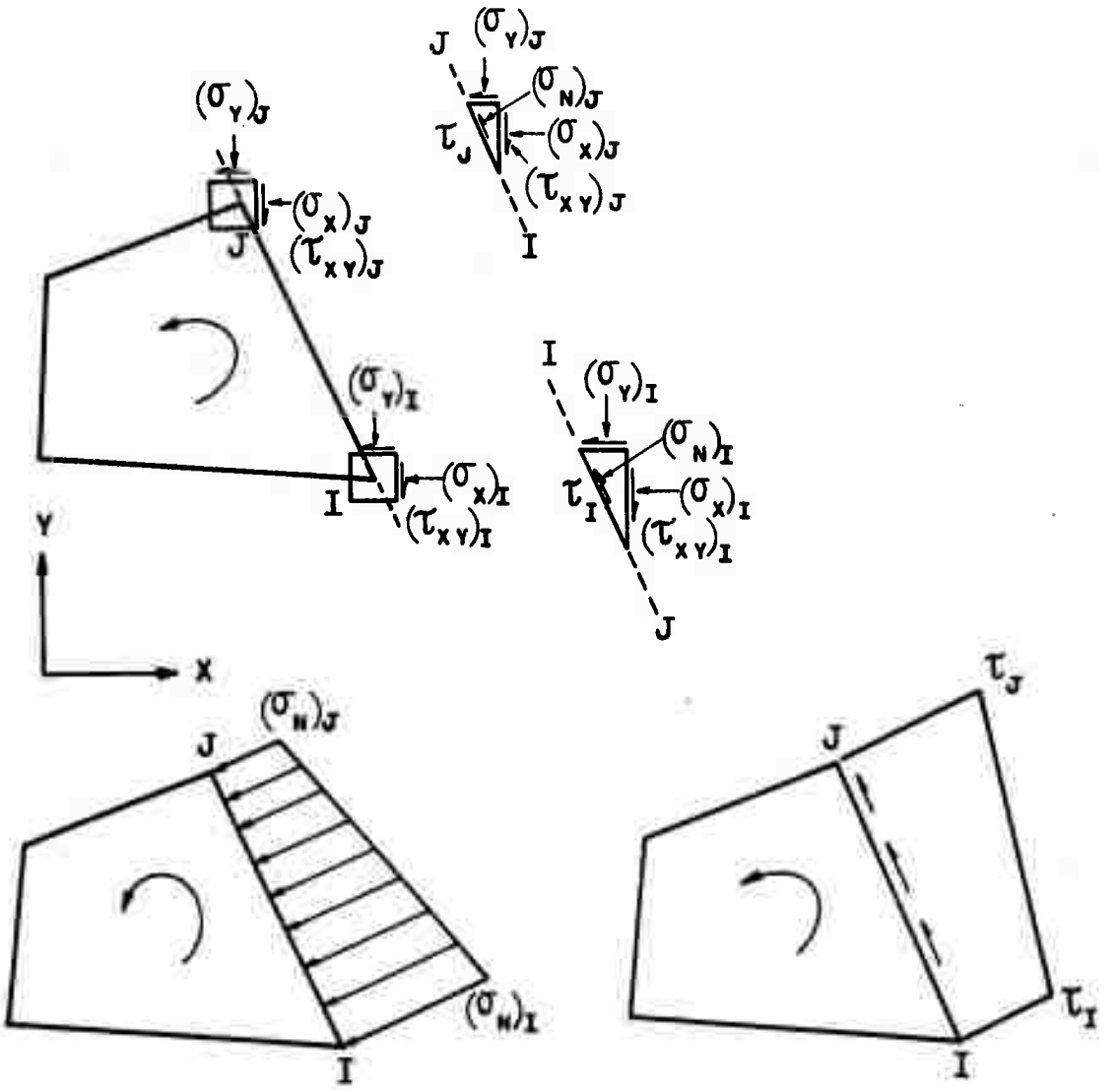

FIG. B2 - SIGN CONVENTION FOR BOUNDARY PRESSURE

16th CARD TYPE: FORMAT (I5)

Cols. 1-5 NJT - Total number of joint elements.

17th CARD TYPE: FORMAT (2F20.5, I5)

Cols. 1-20 FN(I) - Normal stress across joint element NEJT(I)
21-40 FT(I) - Tangential stress across joint element NEJT(I)
41-45 NEJT(I)- Element number for joint element

Repeat 17th card type for all joint elements

16th and 17th card types are neglected if NRES $\leq$ 0 on the 2nd card type.

18th CARD TYPE: Binary data cards for all elements

STRS(N,1) - σ_x
STRS(N,2) - σ_y
STRS(N,3) - τ_{xy}

SEP(N,1) - Excess stress σ_x'
SEP(N,2) - Excess stress σ_y'
SEP(N,3) - Excess stress $\tau_{x'y}$

MTAG(N) - An index indicating if the element has failed in tension.
If MTAG(N) = 1, the element has not failed in tension.
MTAG(N) = 2, the element has failed in tension in one direction only
MTAG(N) = 3, the element has failed in tension in two orthogonal directions.

19th CARD TYPE: Binary data cards for all joint elements, neglected if MJOINT = 0.

NJT - Total number of joint elements
FN(N) - Normal stress across joint element
FT(N) - Tangential stress across joint element

18th and 19th card types are ngelected if NREAD = 0 on the 3rd card type, i.e., these cards are need to restart the computation.

20th CARD TYPE: Binary data cards for all nodal point displacements, yield function, axial stress, and all strain components for all elements.

DISP(N,1) - x - displacement for node N
DISP(N,2) - y - displacement for node N

FY(N) - Yield function for element N

SIGZ(N) - axial stress for element N

STRN(N,1) - strain component, ε_x, for element N
STRN(N,2) - strain component, ε_y, for element N
STRN(N,3) - strain component, ε_{xy}, for element N

20th card type is neglected if NREAD = 0 on the 3rd card type, i.e., these cards are needed to restart the computation.

21th CARD TYPE: FORMAT (I5)

Cols. 1-5 NPST - Number of nodal points at which nodal stresses are to be computed.

22nd CARD TYPE: FORMAT (16I5)

Cols.		
1-5	NS(I)	- Nodal point number at which nodal stresses are to be computed.
6-10	NSEL(I,1)	- First interpolation element number
11-15	NSEL(I,2)	- Second interpolation element number
16-20	NSEL(I,3)	- Third interpolation element number
21-25	NSEL(I,4)	- Fourth interpolation element number
26-30		
31-35		
36-40	same as above	
41-45		
46-50		
.....		
.....		

Repeat for all nodal points at which nodal stresses are to be computed.

The mid-points of no three of the four interpolation elements may lie on a horizontal or vertical line. These elements should be read in a criss-crossed fashion as shown in Fig. B3. The centroids of the first and second elements should not lie on a vertical line.

21th and 22nd card types are required if NRES = -1 on the 2nd card type.

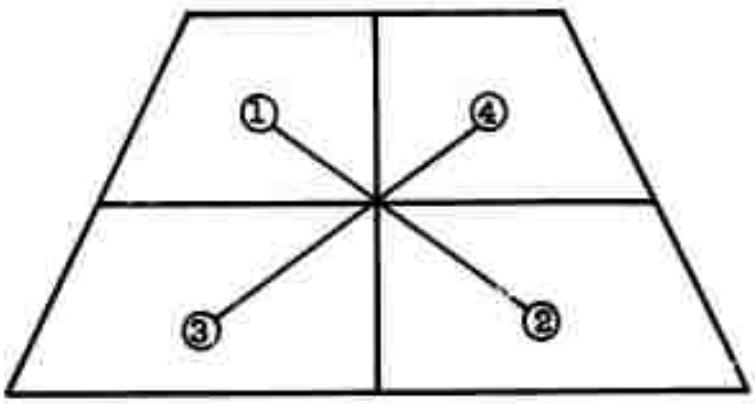

FIG. B3 - SEQUENCE FOR READING IN INTERPOLATION ELEMENTS

APPENDIX C

CAPABILITIES OF OPERATIONAL THREE-DIMENSIONAL FINITE ELEMENT PROGRAMS FOR THE ANALYSIS OF PROBLEMS IN ROCK MECHANICS

CAPABILITIES OF OPERATIONAL THREE-DIMENSIONAL FINITE ELEMENT PROGRAMS FOR THE ANALYSIS OF PROBLEMS IN ROCK MECHANICS

Introduction

With very few exceptions, all the work done in the application of finite element methods to problems in rock mechanics has been concerned with axisymmetric and plane problems. In general, an actual field situation is three-dimensional and, in some cases, an axisymmetric or plane formulation of the problem may not be satisfactory. Therefore, the development of finite element programs for the three-dimensional analysis of boundary value problems is of interest in design of excavations in rock.

The purpose of this brief discussion is not to elaborate on the theory or the details of the development of three-dimensional finite element programs, but to evaluate what is available in terms of operational programs in their ability to assist in the design of excavations in rock.

Capabilities of Operational Programs

When the original proposal was written, there was very little available in documentation on operational programs. Since that time, some information has become available on existing programs. The most significant piece of information has been a recent report by Professor E. L. Wilson*, which provides detailed information on an operational program for the analysis of three-dimensional solid structures. Since this is the most recent reference available, it is utilized as a basis for considering the available capabilities for analyzing excavations in rock.

It is important to recognize that, as in the historical development of plane finite element programs for use in practical problems in rock mechanics, the first step is the development of the program to analyze linear elastic problems. From a fundamental standpoint, this is the most difficult step. The attainment of this is therefore of considerable significance. It is now a question of adapting this basic program as was done for the plane case to include the various features that are significant in rock mechanics problems. This is no trivial task, but the most important step has been taken.

For examining the capabilities of the available program, it is most convenient to consider the factors that have to be modelled in evaluating the stability of openings in rock and examine the

---

*"SOLID SAP, A Static Analysis Program for Three-Dimensional Solid Structures, UC SESM 71-19" by Edward L. Wilson. Report to Denver Mining Research Center, U.S. Department of Interior, Structural Engineering Laboratory, University of California, Berkeley, California. September 1971. There was an earlier version which was not as suitable for rock mechanics problems as the above report.

ability of the available finite element program to model these factors.

Geometry - In general, the geometry of the problem is three-dimensional. The most significant capability of the program is its ability to model this aspect of the problem.

Material Properties - At the present time, the computer program only considers linear elastic materials. The three-dimensional elements also have the further limitation of isotropy. There are no provisions for conducting a "no tension" or "elasto-plastic" analysis or considering any other nonlinear material behavior.

Geologic Conditions - The two major considerations are non-homogeneity as evidenced by layered deposits and the existence of joints and other discontinuities. The non-homogeneity of the rock can be readily modelled. However, there are no provisions for considering joints and discontinuities.

An earlier published paper by Mahtab and Goodman* discusses the three-dimensional finite element analysis of jointed rock slopes. This paper is based on a doctoral dissertation by Mahtab.** The use of the program was demonstrated by solving a special case of a symmetric rock wedge on two joint planes which had linear stress-deformation characteristics. The general capability of the program is not clear. It does appear that the program developed by Mahtab does not have the computational refinements, the number of element types, the superior element characteristics and documentation, but it does have the capability of modelling joints.

Construction Sequence - Since the capabilities of the program are confined to linear elastic systems, the construction sequence has no significance; hence, there are no provisions for considering this factor.

Support Schemes - The program has the capability for analyzing various support schemes. The different element types e.g., plate, shell, truss, beam, etc., can be used to model a variety of support schemes. However, as far as we are aware, this feature of the program has not been exploited.

Except for the example solved by Professor Wilson and presented in the above-mentioned report, there does not appear to be any significant information on the computer time and time required to

---

* Mahtab, M. A. and Goodman, R. E., "Three-Dimensional Finite Element Analysis of Jointed Rock Slopes," Procs. 2nd Congress of the International Society of Rock Mechanics. Vol 3, No. 7-12, Belgrade, Yugoslavia, 1970.

** Mahtab, M. A., "Three Dimensional Finite Element Analysis of Jointed Rock Slopes," Ph.D. Thesis, University of California, Berkeley, 1970.

prepare the data. The problem solved was a quarter of a pillar and room in a mine of a homogeneous medium. It was a relatively simple problem. It took two man days to prepare the input data. The actual computer cost on CDC 6400 was $50.00 at commercial rates.

Idealizations would take considerably more time and the computational costs would be far greater when there are joints and different materials located in geometrically irregular patterns. Furthermore, if the materials and joints have nonlinear characteristics and the program is modified to model this effect, the computational time would be further increased. Once iteration and convergence questions become included, the time and cost in solving practical problems increases. It is necessary to evaluate if the additional cost and effort in idealizing the problem and conducting the analysis is justified in terms of a better prediction of performance. This can only be done on the basis of comparing predictions and observed performance for actual field problems.

Final Remarks

It would appear that two significant steps have been taken (i) a general linear elastic program has been developed and (ii) the formulation of three-dimensional joint elements has been completed. The next step is to extend the capabilities of the linear elastic program to include factors that are necessary to realistically model actual field problems. Initially, the joint elements that have been developed could be incorporated into the program. As a further refinement, nonlinear joint behavior which is controlled by the friction and cohesion along the joint should be included. Once this is done, problems of practical interest could be analyzed.

It is also necessary to gain experience in the modelling, analyses and interpretation of the results on the basis of case history studies. Some of this information should be obtained in an actual design environment where the constraints of time, money and available input information are always present.

APPENDIX D

TANGENTIAL STRESS DISTRIBUTIONS AND DISPLACEMENTS IN ELASTO-PLASTIC ANALYSIS OF A CIRCULAR OPENING

TANGENTIAL STRESS DISTRIBUTIONS AND DISPLACEMENTS IN ELASTO-PLASTIC ANALYSIS OF A CIRCULAR OPENING

In the semi-annual technical report, a comparison of the distribution of tangential stresses obtained from an elasto-plastic analysis of the problem, presented in Figure D1, conducted by Reyes (1966), Baker et al. (1969), and the study under Contract HO210046 was presented. The results of this comparison are shown in Figures D2 and D3. It can be observed that there are significant differences in the tangential stress distribution and displacements. The differences could have occurred from three sources: (i) the different loading paths used, (ii) variations in the method of computing the axial stress, and (iii) the degree of convergence obtained.

The problem was reanalyzed following a loading path consistent with that used by Baker, et al. (1969), and similar to that used by Reyes (1966), by applying the pressures on the outer boundary. The results of the analysis are shown in the body of the report, Figures 16 and 17. The stress distiribution and the peak tangential stress obtained are in satisfactory agreement with the results of Baker et al. and Reyes, differences being of the order of ±15%, and the displacements are almost identical. The results presented in the semi-annual technical report were obtained by assigning initial stresses to elements surrounding the opening and applying the boundary pressure to the excavated boundary to simulate the creation of the opening. The difference in the results, when compared with those obtained in the reanalyses, indicates the effect of the loading or unloading path on the stress distribution in an elasto-plastic material. This points out the importance of modelling the loading sequence.

Some difference in the tangential stress distribution may also be attributed to the degree of convergence obtained by each method of analysis and the different methods used in calculating the axial stress. This has been discussed in the report.

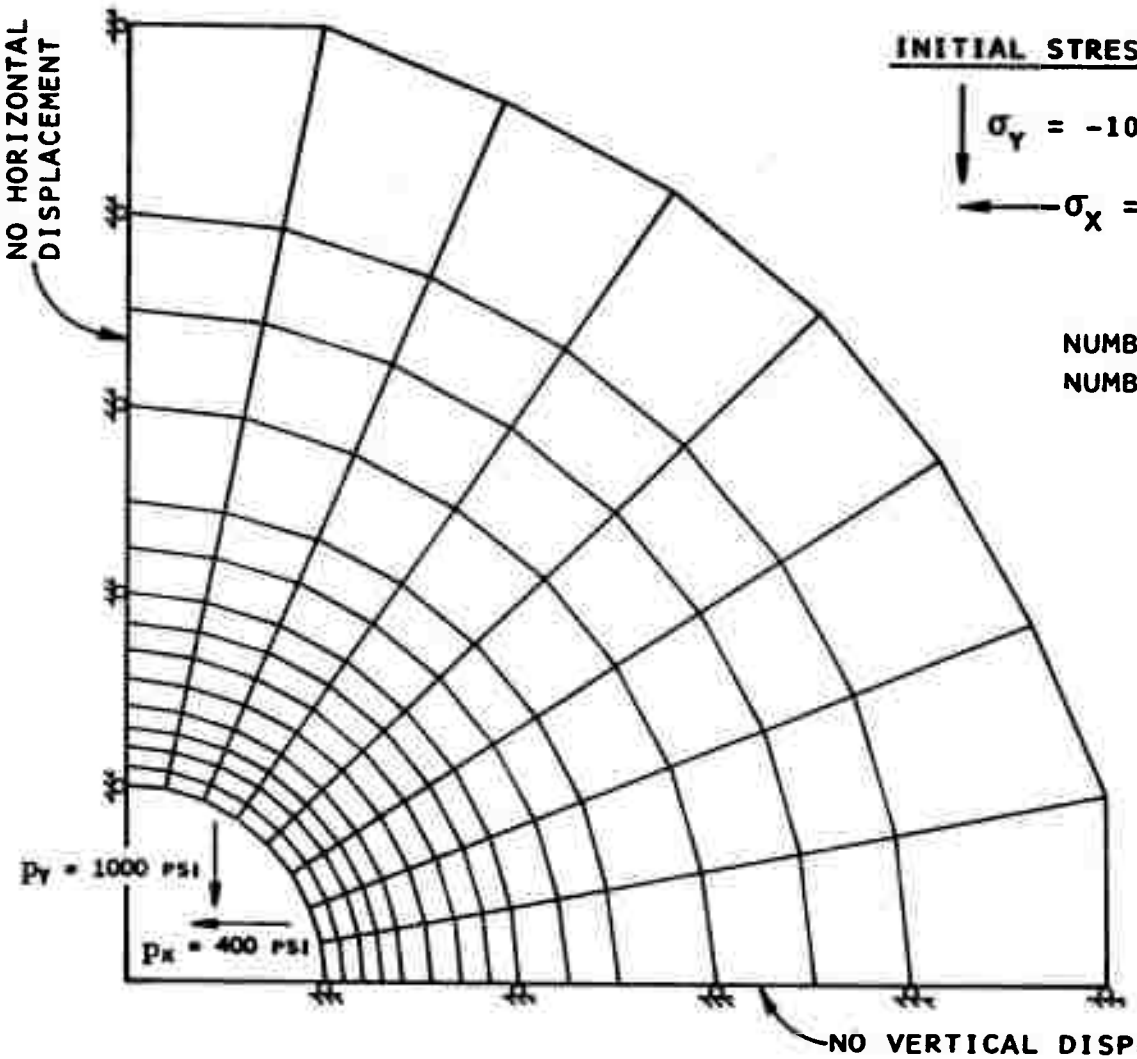

INCREMENT NO.	PERCENTAGE OF TOTAL BOUNDARY PRESSURE
1	0.370
2	0.256
3	0.105
4	0.089
5	0.073
6	0.058
7	0.049

FIG. D1 - FINITE ELEMENT MESH FOR AN ELASTO-PLASTIC ANALYSIS OF A CIRCULAR OPENING

WOODWARD-LUNDGREN & ASSOCIATES

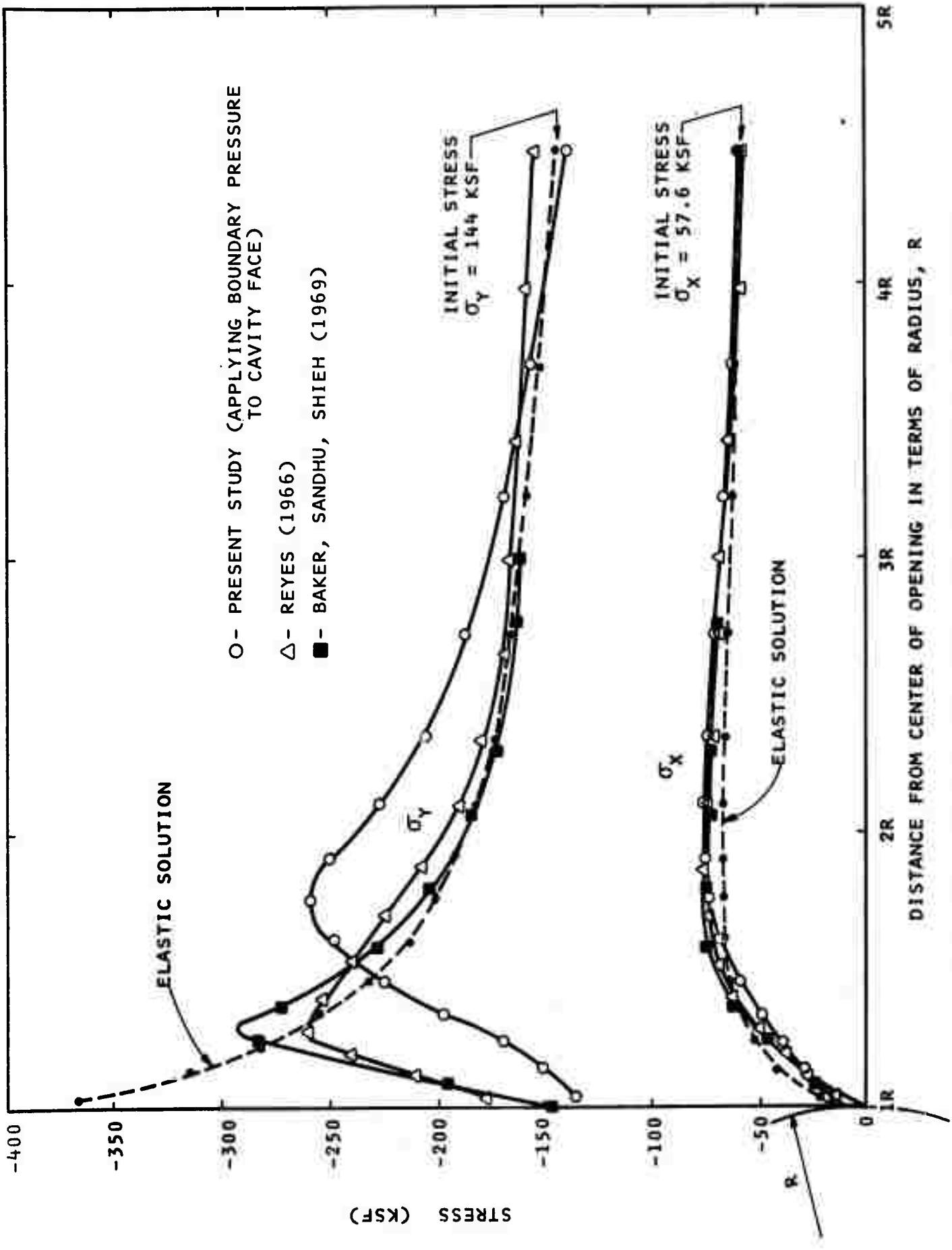

FIG. D2 - VERTICAL AND HORIZONTAL STRESSES ALONG HORIZONTAL SECTION OF A CIRCULAR OPENING

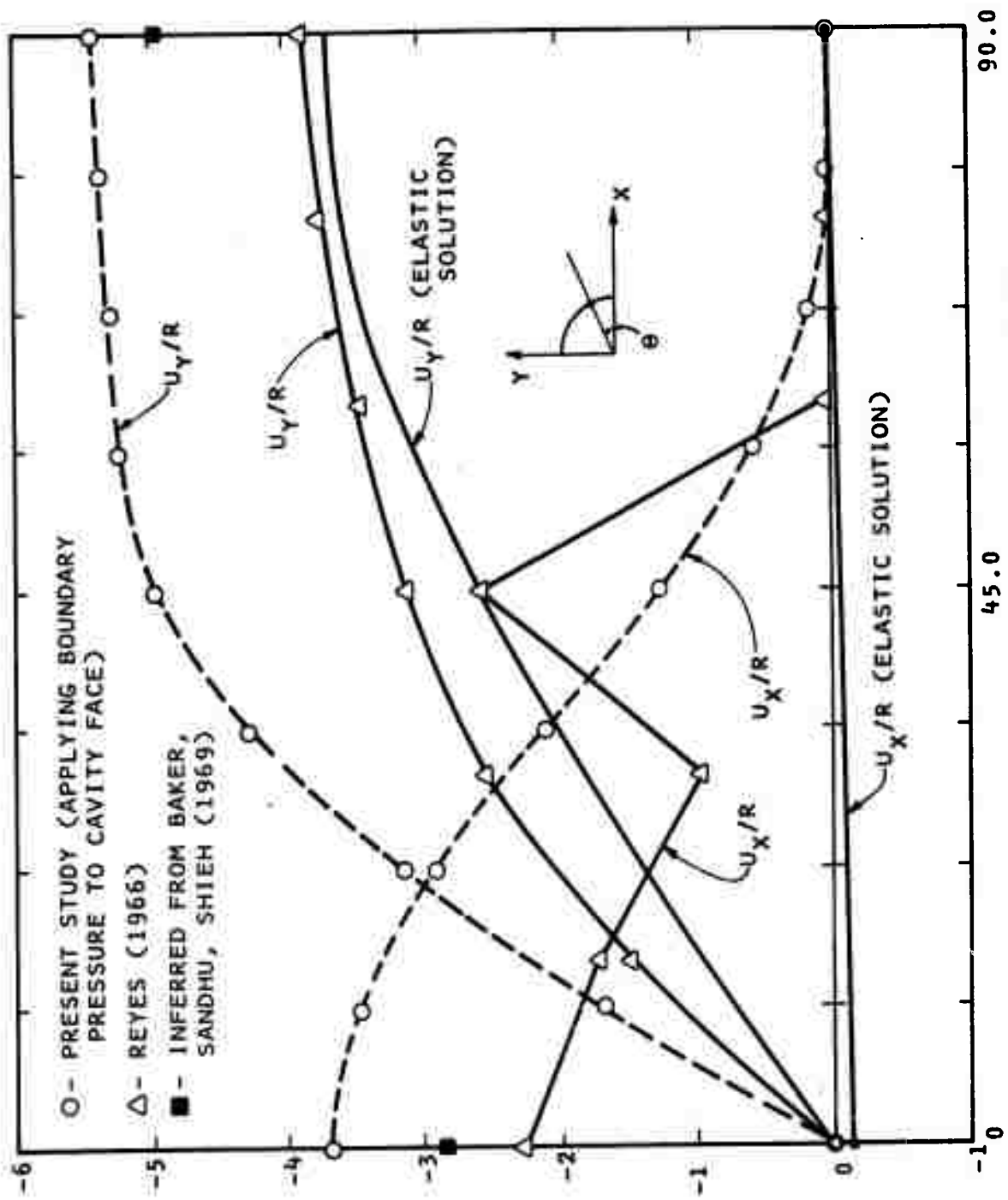

FIG. D3 - DEFORMATION ALONG CAVITY FACE OF A CIRCULAR OPENING AS COMPUTED BY ELASTIC AND ELASTIC-PLASTIC ANALYSIS